

## Mathematics of 2-dimensional lattices

### Continuously parameterised spaces of all 2-dimensional lattices classified up to similarity, isometry, or rigid motion

Vitaliy Kurlin

Received: date / Accepted: date

**Abstract** A periodic lattice in Euclidean space is the infinite set of all integer linear combinations of basis vectors. Any lattice can be generated by infinitely many different bases. This ambiguity was partially resolved but standard reductions remain discontinuous under perturbations modelling crystal vibrations.

This paper completes a continuous classification of 2-dimensional lattices up to Euclidean isometry (or congruence), rigid motion (without reflections), and similarity (with uniform scaling). The new homogeneous invariants allow easily computable metrics on lattices considered up to the equivalences above. The metrics up to rigid motion are especially non-trivial and settle all remaining questions on (dis)continuity of lattice bases. These metrics lead to real-valued chiral distances that continuously measure lattice deviations from higher-symmetry neighbours. The geometric methods extend the past work of Delone, Conway, and Sloane.

**Keywords** Lattice · rigid motion · isometry · invariant · metric · continuity

**Mathematics Subject Classification (2020)** 52C05 · 52C25 · 54H12 · 11H06  
Communicated by Peter Bubenik

#### 1 Motivations for a continuous classification of lattices and crystals

A *lattice*  $\Lambda \subset \mathbb{R}^n$  consists of all integer linear combinations of basis vectors  $v_1, \dots, v_n$ . This basis spans a parallelepiped called a *unit cell*  $U \subset \mathbb{R}^n$ . A *periodic point set* is obtained as a union of translated copies  $\Lambda + p_i$  for finitely many  $p_1, \dots, p_m \in U$ . Any periodic crystal can be modelled as a periodic set whose points represent atomic centers. For example, graphene is a hexagonal periodic set of carbon atoms, see Fig. 1. The book [32] reviews non-periodic quasicrystals.

Since crystal structures are determined in a rigid form, the most fundamental equivalence of their underlying lattices is a rigid motion. Any *rigid motion* in  $\mathbb{R}^2$  is a composition of translations and rotations. A more general *isometry* includes mirror reflections and is sometimes called a *congruence* in Euclidean geometry.

---

V.Kurlin

Computer Science, University of Liverpool, UK E-mail: vitaliy.kurlin@liverpool.ac.uk

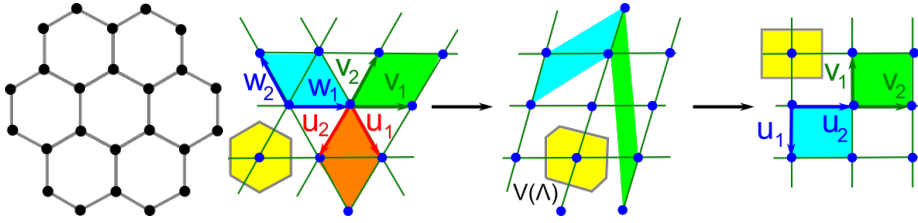


**Fig. 1** **Left:** a 2-dimensional layer of graphene is formed by carbon atoms. **Right:** one can generate a hexagonal lattice (as any other) by infinitely many bases and continuously deform into a rectangular lattice (far right) whose bases  $\{v_1, v_2\}$  and  $\{u_1, u_2\}$  are related by an orientation-reversing map. The yellow Voronoi domain  $V(A)$  of any point  $p$  in a lattice  $A$  consists of all points  $q \in \mathbb{R}^2$  that are non-strictly closer to  $p$  than to other points of  $A - p$ .

In the language of Computer Science, the classification of lattices up to isometry is a binary classification problem deciding if lattices  $A, A'$  are isometric, which can be denoted as  $A \cong A'$ . If a descriptor takes different values on distinct representations of isometric lattices  $A \cong A'$ , this pair of representations is called a *false negative*. Many descriptors of crystals and their lattices allow false negatives by a simple comparison of lattice bases. Any lattice can be represented by a reduced cell [19], see Definition 2.3 in section 2, which is unique up to isometry but this cell still has different bases as in Fig. 1. A descriptor without false negatives takes the same value on all isometric lattices and can be called an *isometry invariant*.

For example, the area of the unit cell  $U$  spanned by any basis of a lattice  $A$  is an isometry invariant because a change of basis is realised by a  $2 \times 2$  matrix with determinant  $\pm 1$ , which preserves the absolute value of the area. Such an invariant  $I$  may allow *false positives*  $A \not\cong A'$  with  $I(A) = I(A')$ . All lattices in Fig. 1 have unit cells of the same area. The area and many other invariants allow infinitely many false positives. An invariant  $I$  without false positives is called *complete* and distinguishes all non-isometric lattices so that if  $I(A) = I(A')$  then  $A \cong A'$ .

The traditional approach to deciding if lattices are isometric is to compare their conventional or reduced cells up to isometry. Though this comparison theoretically gives a complete invariant, in practice all real crystal lattices are non-isometric because of inevitable noise in measurements. All atoms vibrate above the absolute zero temperature, hence any real lattice basis is always slightly perturbed. The discontinuity of reduced bases under perturbations was experimentally known since 1980 [3], highlighted in [17, section 1] and formally proved in [41, Theorem 15].

A more practical goal is to find a complete invariant that is continuous under any perturbations of (bases of) lattices. Such a continuous and complete invariant will unambiguously parameterise the *Lattice Isometry Space*  $\text{LIS}(\mathbb{R}^n)$  consisting of infinitely many isometry classes of lattices in  $\mathbb{R}^n$ . For example, the latitude and longitude continuously parameterise the surface of Earth.

The space LIS of isometry classes is continuous and connected because any two lattices can be joined by a continuous deformation of their bases as in Fig. 1. Such deformation can be always visualised as a continuous path in the space  $\text{LIS}(\mathbb{R}^n)$ , whose full geometry remained unknown even for 2-dimensional lattices.

Lattices were previously represented by ambiguous or reduced bases, which are discontinuous under perturbations. Most discrete invariants such as symmetry groups are also discontinuous and cut the Lattice Isometry Space (LIS) into finitely many disjoint strata. Delone [9], later Conway and Sloane [13] reduced ambiguity of lattice representations by using obtuse superbases. Hence new continuous metrics and parameterisations on lattice spaces in Problem 1.1 are the next natural step.

The main contribution is a full solution to the mapping problem below.

**Problem 1.1 (lattice mapping)** *Find a bijective and continuous invariant  $I : \text{LIS}(\mathbb{R}^2) \rightarrow \text{Inv}$  mapping the Lattice Isometry Space to a simpler space of complete invariants. In detail, an invariant  $I$  should satisfy the following conditions.*

(1.1a) Invariance : *if  $\Lambda \cong \Lambda'$  then  $I(\Lambda) = I(\Lambda')$ , so  $I$  is preserved by isometry.*

(1.1b) Completeness (or injectivity) : *if  $I(\Lambda) = I(\Lambda')$ , then  $\Lambda \cong \Lambda'$  are isometric.*

(1.1c) Continuity : *the invariant map  $I$  is continuous in a suitable metric  $d$  satisfying all axioms: (1)  $d(I(\Lambda), I(\Lambda')) = 0$  if and only if  $\Lambda \cong \Lambda'$ , (2) symmetry  $d(I_1, I_2) = d(I_2, I_1)$ , (3) triangle inequality  $d(I_1, I_2) + d(I_2, I_3) \geq d(I_1, I_3)$ .*

(1.1d) Computability : *the metric  $d(I(\Lambda), I(\Lambda'))$  can be exactly computed in a constant time from reduced bases of  $\Lambda, \Lambda'$ , introduced Definition 2.3 in section 2.*

(1.1e) Inverse design : *a basis of  $\Lambda$  can be explicitly reconstructed from  $I(\Lambda)$ . ■*

Condition (1.1a) means that  $I$  has no false negatives: no pairs  $\Lambda \cong \Lambda'$  with  $I(\Lambda) \neq I(\Lambda')$ . Such a non-constant invariant  $I$  is a minimally useful descriptor because different values  $I(\Lambda) \neq I(\Lambda')$  guarantee that  $\Lambda \not\cong \Lambda'$ . Condition (1.1b) means that  $I$  has no false positives: no pairs  $\Lambda \not\cong \Lambda'$  with  $I(\Lambda) = I(\Lambda')$ . Combined conditions (1.1a,b) guarantee a bijection (or a 1-1 map)  $I : \text{LIS} \rightarrow \text{Inv} = I(\text{LIS})$ . Hence any lattice  $\Lambda$  is uniquely represented by its complete invariant  $I(\Lambda)$ .

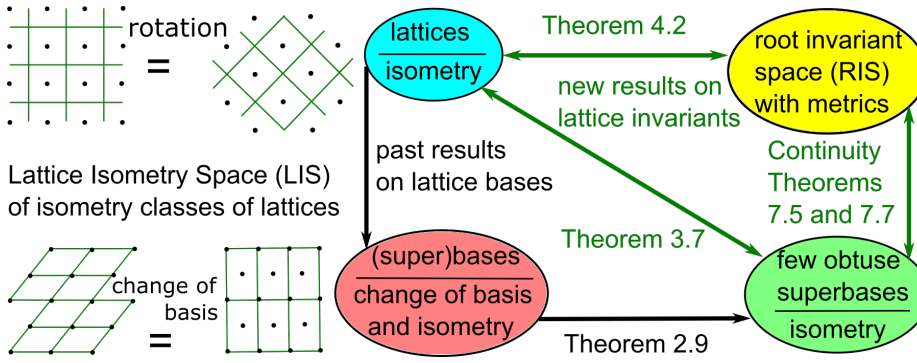
The metric axioms in (1.1c) imply positivity due to  $2d(I_1, I_2) = d(I_1, I_2) + d(I_2, I_1) \geq d(I_1, I_1) = 0$ . However, the identity of indiscernibles ( $d(I(\Lambda), I(\Lambda')) = 0 \Leftrightarrow \Lambda \cong \Lambda'$ ) cannot be missed, otherwise even the zero function  $d = 0$  satisfies all other axioms. A binary answer to the isometry problem provides only a discontinuous metric  $d(\Lambda, \Lambda')$  equal to 1 or another positive number for any non-isometric lattices  $\Lambda \not\cong \Lambda'$  even if  $\Lambda, \Lambda'$  are nearly identical. The new condition in (1.1c) makes Problem 1.1 harder than a classification, especially up to rigid motion.

Fig. 2 summarises the past obstacles and a full solution to Problem 1.1. The space  $\text{Inv}$  is the root invariant space  $\text{RIS}(\mathbb{R}^2)$  of ordered triples with continuous metrics. The related invariants will solve Problem 1.1 up to three other equivalence relations: rigid motion, similarity and orientation-preserving similarity.

The inverse design in (1.1e) will raise Problem 1.1 above metric geometry to define a richer structure of a vector space on LIS. It is easy to multiply any lattice by a fixed scalar, but a sum of any two lattices is harder to define in a meaningful way independent of lattice bases. We will overcome this obstacle due to a linear structure on the root invariant space (RIS) completely solving Problem 1.1.

## 2 Main definitions and an overview of past work and new results

This section defines the main concepts and reviews past work on lattice comparisons, see the definition of an isometry and orientation in the appendix. Any point



**Fig. 2**  $\text{LIS}(\mathbb{R}^2)$  is bijectively and continuously mapped to root invariants, which are ordered triples of square roots of scalar products of vectors of an obtuse superbase of a lattice  $A \subset \mathbb{R}^2$ .

$p$  in Euclidean space  $\mathbb{R}^n$  can be represented by the vector from the origin  $0 \in \mathbb{R}^n$  to  $p$ . This vector is also denoted by  $p$ . An equal vector  $p$  can be drawn at any initial point. The *Euclidean* distance between points  $p, q \in \mathbb{R}^n$  is  $|p - q|$ .

**Definition 2.1 (a lattice  $A$ , a primitive unit cell  $U(v_1, \dots, v_n)$ )** Let vectors  $v_1, \dots, v_n$  form a linear basis in  $\mathbb{R}^n$  so that any vector  $v \in \mathbb{R}^n$  can be written as  $v = \sum_{i=1}^n c_i v_i$  for some real  $c_i$ , and if  $\sum_{i=1}^n c_i v_i = 0$  then all  $c_i = 0$ . A lattice  $A$  in  $\mathbb{R}^n$  consists of  $\sum_{i=1}^n c_i v_i$  with integer coefficients  $c_i \in \mathbb{Z}$ . The parallelepiped  $U(v_1, \dots, v_n) = \left\{ \sum_{i=1}^n c_i v_i : c_i \in [0, 1] \right\}$  is called a primitive unit cell of  $A$ . ■

The conditions  $0 \leq c_i < 1$  on the coefficients  $c_i$  above guarantee that the copies of unit cells  $U(v_1, \dots, v_n)$  translated by all  $v \in A$  are disjoint and cover  $\mathbb{R}^n$ .

**Definition 2.2 (orientation, isometry, rigid motion, similarity)** For a basis  $v_1, \dots, v_n$  of  $\mathbb{R}^n$ , the signed volume of  $U(v_1, \dots, v_n)$  is the determinant of the  $n \times n$  matrix with columns  $v_1, \dots, v_n$ . The sign of this  $\det(v_1, \dots, v_n)$  can be called an orientation of the basis  $v_1, \dots, v_n$ . An isometry is any map  $f : \mathbb{R}^n \rightarrow \mathbb{R}^n$  such that  $|f(p) - f(q)| = |p - q|$  for any  $p, q \in \mathbb{R}^n$ . The unit cells  $U(v_1, \dots, v_n)$  and  $U(f(v_1), \dots, f(v_n))$  have non-zero volumes with equal absolute values. If these volumes have equal signs,  $f$  is orientation-preserving, otherwise  $f$  is orientation-reversing. Any orientation-preserving isometry  $f$  is a composition of translations and rotations, and can be included into a continuous family of isometries  $f_t$  (a rigid motion), where  $t \in [0, 1]$ ,  $f_0$  is the identity map and  $f_1 = f$ . A similarity is a composition of isometry and uniform scaling  $v \mapsto sv$  for a fixed scalar  $s > 0$ . ■

Any orientation-reversing isometry is a composition of a rigid motion and one mirror reflection in a linear subspace of dimension  $n - 1$  (a straight line in  $\mathbb{R}^2$ ).

The book [18] considered actions on lattices by groups with reflections. In  $\mathbb{R}^3$ , crystallography classifies symmetry groups into 219 classes up to affine transformations including orientation-reversing maps, more often into 230 classes when orientation is preserved as by rigid motion of real crystals. So the classification of lattices up to rigid motion is more practically important than up to isometry.

Any lattice  $\Lambda$  can be generated by infinitely many bases or unit cells, see Fig. 1. A standard approach to resolve this ambiguity is to consider a reduced basis below. In  $\mathbb{R}^3$ , there are several ways to define a reduced basis [19]. The most commonly used is Niggli's reduced cell [29], whose 2-dimensional version is defined below.

For vectors  $v_1 = (a_1, a_2)$  and  $v_2 = (b_1, b_2)$  in  $\mathbb{R}^2$ , let  $\det(v_1, v_2) = a_1 b_2 - a_2 b_1$  be the determinant of the matrix  $\begin{pmatrix} a_1 & b_1 \\ a_2 & b_2 \end{pmatrix}$  with the columns  $v_1, v_2$ .

**Definition 2.3 (reduced cell)** For a lattice  $\Lambda \subset \mathbb{R}^2$  up to isometry, a basis and its unit cell  $U(v_1, v_2)$  are reduced (non-acute) if  $|v_1| \leq |v_2|$  and  $-\frac{1}{2}v_1^2 \leq v_1 \cdot v_2 \leq 0$ . Up to rigid motion, the conditions are weaker:  $|v_1| \leq |v_2|$  and  $|v_1 \cdot v_2| \leq \frac{1}{2}v_1^2$ ,  $\det(v_1, v_2) > 0$ , and the new special condition : if  $|v_1| = |v_2|$  then  $v_1 \cdot v_2 \geq 0$ . ■

All bases in Fig. 1 are reduced up to rigid motion. The condition  $|v_1 \cdot v_2| \leq \frac{1}{2}v_1^2$  in Definition 2.3 geometrically means that  $v_1, v_2$  are close to being orthogonal: the projection of  $v_2$  to  $v_1$  is between  $\pm\frac{1}{2}|v_1|$ . The conditions  $|v_1| \leq |v_2|$  and  $-\frac{1}{2}v_1^2 \leq v_1 \cdot v_2 \leq 0$  in Definition 2.3 coincide with the conventional definition from [8, section 9.2.2] for type II (non-acute) cells in  $\mathbb{R}^3$  if we choose  $v_3$  to be very long and orthogonal to  $v_1, v_2$ . Alternative type I cells with non-obtuse angles have  $0 \leq v_1 \cdot v_2 \leq \frac{1}{2}v_1^2$ . Proposition 3.10(a) proves uniqueness of reduced bases.

Another well-known cell of a lattice is the Voronoi domain [37], also called the Wigner-Seitz cell, Brillouin zone or Dirichlet cell. We use the word domain to avoid a confusion with a unit cell in Definition 2.1. Though the Voronoi domain can be defined for any point of a lattice, it suffices to consider only the origin 0.

**Definition 2.4 (Voronoi domain  $V(\Lambda)$ )** The Voronoi domain of a lattice  $\Lambda$  is the neighbourhood  $V(\Lambda) = \{p \in \mathbb{R}^n : |p| \leq |p - v| \text{ for any } v \in \Lambda\}$  of the origin  $0 \in \Lambda$  consisting of all points  $p$  that are non-strictly closer to 0 than to other points  $v \in \Lambda$ . A vector  $v \in \Lambda$  is called a Voronoi vector if the bisector hyperspace  $H(0, v) = \{p \in \mathbb{R}^n : p \cdot v = \frac{1}{2}v^2\}$  between 0 and  $v$  intersects  $V(\Lambda)$ . If  $V(\Lambda) \cap H(0, v)$  is an  $(n - 1)$ -dimensional face of  $V(\Lambda)$ , then  $v$  is called a strict Voronoi vector. ■

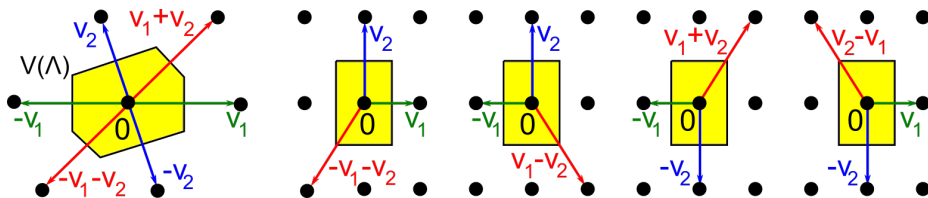


**Fig. 3** Left: a generic lattice  $\Lambda \subset \mathbb{R}^2$  has a hexagonal Voronoi domain with an obtuse superbase  $v_1, v_2, v_0 = -v_1 - v_2$ , which is unique up to permutations and central symmetry. **Other pictures:** two pairs of obtuse superbases (related by reflection) for a rectangular lattice.

Fig. 3 shows how the Voronoi domain  $V(\Lambda)$  can be obtained as the intersection of the closed half-spaces  $S(0, v) = \{p \in \mathbb{R}^n : p \cdot v \leq \frac{1}{2}v^2\}$  whose boundaries  $H(0, v)$  are bisectors between 0 and all strict Voronoi vectors  $v \in \Lambda$ . A generic lattice  $\Lambda \subset \mathbb{R}^2$  has a hexagonal Voronoi domain  $V(\Lambda)$  with six Voronoi vectors.

Any lattice is determined by its Voronoi domain by Lemma A.2 in the appendix. However, the combinatorial structure of  $V(\Lambda)$  is discontinuous under perturbations. Almost any perturbation of a rectangular basis in  $\mathbb{R}^2$  gives a non-rectangular basis generating a lattice whose Voronoi domain  $V(\Lambda)$  is hexagonal, not rectangular. Hence any integer-valued descriptors of  $V(\Lambda)$  such as the numbers of vertices or edges are always discontinuous and unsuitable for continuous quantification of similarities between arbitrary crystals or periodic point sets.

Optimal geometric matching of Voronoi domains with a shared centre led [27] to two continuous metrics (up to orientation-preserving isometry and similarity) on lattices. The minimisation over infinitely many rotations was implemented in [27] by sampling and gave approximate algorithms for these metrics. For any periodic point sets, the density functions [17] are generically complete in  $\mathbb{R}^3$  and have fast algorithms [34] in low dimensions  $n \leq 3$  but are incomplete even for periodic sequences in dimension  $n = 1$  [6, Example 10]. The complete invariant isoset [5] in  $\mathbb{R}^n$  has a continuous metric that can be approximated [4] with a factor  $O(n^2)$ .

Lemma 2.5 shows how to find all Voronoi vectors of any lattice  $\Lambda \subset \mathbb{R}^n$ . The doubled lattice is  $2\Lambda = \{2v : v \in \Lambda\}$ . Vectors  $u, v \in \Lambda$  are called  $2\Lambda$ -equivalent if  $u - v \in 2\Lambda$ . Then any vector  $v \in \Lambda$  generates its  $2\Lambda$ -class  $v + 2\Lambda = \{v + 2u : u \in \Lambda\}$ , which is  $2\Lambda$  translated by  $v$  and containing  $-v$ . All classes of  $2\Lambda$ -equivalent vectors form the quotient space  $\Lambda/2\Lambda$ . Any 1-dimensional lattice  $\Lambda$  generated by a vector  $v$  has the quotient  $\Lambda/2\Lambda$  consisting of only two classes  $\Lambda$  and  $v + \Lambda$ .

**Lemma 2.5 (criterion for Voronoi vectors [26], [13, Theorem 2])** *For any lattice  $\Lambda \subset \mathbb{R}^n$ , a non-zero vector  $v \in \Lambda$  is a Voronoi vector of  $\Lambda$  if and only if  $v$  is a shortest vector in its  $2\Lambda$ -class  $v + 2\Lambda$ . Also,  $v$  is a strict Voronoi vector if and only if  $\pm v$  are the only shortest vectors in the  $2\Lambda$ -class  $v + 2\Lambda$ . ▲*

Appendix A includes detailed proofs of key past results such as Lemma 2.5. Any lattice  $\Lambda \subset \mathbb{R}^2$  generated by  $v_1, v_2$  has  $\Lambda/2\Lambda = \{v_1, v_2, v_1 + v_2\} + \Lambda$ . Notice that the vectors  $v_1 \pm v_2$  belong to the same  $2\Lambda$ -class. Assume that  $v_1, v_2$  are not longer than  $v_1 + v_2$ , which holds if  $\angle(v_1, v_2) \in [60^\circ, 120^\circ]$ . If  $v_1 + v_2$  is shorter than  $v_1 - v_2$  as in Fig. 3 (left), then  $\Lambda$  has three pairs of strict Voronoi vectors  $\pm v_1, \pm v_2, \pm(v_1 + v_2)$ . If  $v_1 \pm v_2$  have the same length, the unit cell spanned by  $v_1, v_2$  degenerates to a rectangle,  $\Lambda$  has four non-strict Voronoi vectors  $\pm v_1 \pm v_2$ .

The triple of vector pairs  $\pm v_1, \pm v_2, \mp(v_1 + v_2)$  in Fig. 3 motivates the concept of a superbase with the extra vector  $v_0 = -v_1 - v_2$ , which extends to any dimension  $n$  by setting  $v_0 = -\sum_{i=1}^n v_i$ . For dimensions 2 and 3, Theorem 2.9 will prove that any lattice has an obtuse superbase of vectors whose pairwise scalar products are non-positive and are called *Selling parameters* [31]. For any superbase in  $\mathbb{R}^n$ , the negated parameters  $p_{ij} = -v_i \cdot v_j$  can be interpreted as conorms of lattice characters, functions  $\chi : \Lambda \rightarrow \{\pm 1\}$  satisfying  $\chi(u + v) = \chi(u)\chi(v)$ , see [13, Theorem 6]. So  $p_{ij}$  will be defined as *conorms* only for an obtuse superbase below.

**Definition 2.6 (obtuse superbase, conorms  $p_{ij}$ )** *For any basis  $v_1, \dots, v_n$  in  $\mathbb{R}^n$ , the superbase  $v_0, v_1, \dots, v_n$  includes the vector  $v_0 = -\sum_{i=1}^n v_i$ . The conorms  $p_{ij} = -v_i \cdot v_j$  are the negative scalar products of the vectors above. The superbase is obtuse if all conorms  $p_{ij} \geq 0$ , so all angles between vectors  $v_i, v_j$  are non-acute for distinct indices  $i, j \in \{0, 1, \dots, n\}$ . The superbase is strict if all  $p_{ij} > 0$ . ■*

Formula (1) in [13] has a typo initially defining  $p_{ij}$  as exact Selling parameters, but later Theorems 3, 7, 8 use the non-negative conorms  $p_{ij} = -v_i \cdot v_j \geq 0$ .

The indices of a conorm  $p_{ij}$  are distinct and unordered. We set  $p_{ij} = p_{ji}$  for all  $i, j$ . For  $n = 1$ , the 1-dimensional lattice generated by a vector  $v_1$  has the obtuse superbase consisting of the two vectors  $v_0 = -v_1$  and  $v_1$ , so the only conorm  $p_{01} = -v_0 \cdot v_1 = v_1^2$  is the squared length of  $v_1$ . Any superbase of  $\mathbb{R}^n$  has  $\frac{n(n+1)}{2}$  conorms  $p_{ij}$ , for example, three conorms  $p_{01}, p_{02}, p_{12}$  in dimension 2.

**Definition 2.7 (partial sums  $v_S$ , vonorms  $v_S^2$ )** Let a lattice  $\Lambda \subset \mathbb{R}^n$  have a superbase  $B = \{v_0, v_1, \dots, v_n\}$ . For any proper subset  $S \subset \{0, 1, \dots, n\}$  of indices, consider its complement  $\bar{S} = \{0, 1, \dots, n\} \setminus S$  and the partial sum  $v_S = \sum_{i \in S} v_i$

whose squared lengths  $v_S^2$  are called the vonorms of  $B$  and can be expressed as  $v_S^2 = (\sum_{i \in S} v_i) \cdot (-\sum_{j \in \bar{S}} v_j) = -\sum_{i \in S, j \in \bar{S}} v_j \cdot v_i = \sum_{i \in S, j \in \bar{S}} p_{ij}$ . For  $n = 2$ , we get

$$(2.7a) \quad v_0^2 = p_{01} + p_{02}, \quad v_1^2 = p_{01} + p_{12}, \quad v_2^2 = p_{02} + p_{12}.$$

The above formulae allow us to express the conorms via vonorms as follows

$$(2.7b) \quad p_{12} = \frac{1}{2}(v_1^2 + v_2^2 - v_0^2), \quad p_{01} = \frac{1}{2}(v_0^2 + v_1^2 - v_2^2), \quad p_{02} = \frac{1}{2}(v_0^2 + v_2^2 - v_1^2).$$

So  $p_{ij} = \frac{1}{2}(v_i^2 + v_j^2 - v_k^2)$  for distinct  $i, j \in \{0, 1, 2\}$  and  $k = \{0, 1, 2\} - \{i, j\}$ . ■

Lemma 2.8 will later help to prove that a lattice is uniquely determined up to isometry by an obtuse superbase, hence by its vonorms or, equivalently, conorms.

**Lemma 2.8 (Voronoi vectors  $v_S$  [13, Theorem 3])** For any obtuse superbase  $v_0, v_1, \dots, v_n$  of a lattice, all partial sums  $v_S$  from Definition 2.7 split into  $2^n - 1$  symmetric pairs  $v_S = -v_{\bar{S}}$ , which are Voronoi vectors representing distinct  $2\Lambda$ -classes in  $\Lambda/2\Lambda$ . All Voronoi vectors  $v_S$  are strict if and only if all  $p_{ij} > 0$ . ▲

By Conway and Sloane [13, section 2], any lattice  $\Lambda \subset \mathbb{R}^n$  that has an obtuse superbase is called a *lattice of Voronoi's first kind*. Any lattice in dimensions 2 and 3 is of Voronoi's first kind, which was known to Voronoi [37, p. 277] for  $n = 2$  and certainly proved by Delone [9, Section III.4.3] for  $n = 3$ .

**Theorem 2.9 (reduction to an obtuse superbase)** Any lattice  $\Lambda$  in dimensions 2 and 3 has an obtuse superbase  $\{v_0, v_1, \dots, v_n\}$  so that  $v_0 = -\sum_{i=1}^n v_i$  and all conorms  $p_{ij} = -v_i \cdot v_j \geq 0$  for all distinct indices  $i, j \in \{0, 1, \dots, n\}$ . ▲

Conway and Sloane in [13, section 7] attempted to prove Theorem 2.9 for  $n = 3$  by example, which is corrected in [22]. Appendix A proves Theorem 2.9 for  $n = 2$ . Finding an obtuse superbase is related to solving the shortest vector problem in a lattice. The latter problem is NP-hard [2] in  $\mathbb{R}^n$ , see the great review in [28].

The following result implies that the space of all lattices and general periodic point sets in any  $\mathbb{R}^n$  is continuous, path-connected in the language of topology. Due to Proposition 2.10, if we call any periodic structures equivalent (or similar) when they differ up to any small perturbation of points, then any two point sets become equivalent by the transitivity axiom: if  $A_1 \sim A_2 \sim \dots \sim A_k$  then  $A_1 \sim A_k$ .

**Proposition 2.10** Any periodic point sets  $\Lambda + M = \{v + p \mid v \in \Lambda, p \in M\}$ , where  $\Lambda \subset \mathbb{R}^n$  is a lattice,  $M$  is a finite set (motif) of points in a unit cell of  $\Lambda$ , can be deformed into each other so that coordinates of all points change continuously. ■

*Proof* Starting from any basis  $v_1, \dots, v_n$ , continuously rotate  $v_2, \dots, v_n$  to make all basis vectors pairwise orthogonal. If given periodic sets have different numbers  $m_1 \neq m_2$  of points in their unit cells, we can enlarge their cells in the direction of  $v_1$  by factors  $m_2, m_1$  so that both sets have the same number of  $m = m_1 m_2$  points in their cells. If the coordinates of points  $p \in M$  remain constant in the moving basis  $v_1, \dots, v_n$ , they change continuously in a fixed basis of  $\mathbb{R}^n$ . Then we can continuously elongate  $v_1, \dots, v_n$  to get a sufficiently large unit cubic cell. After two periodic point sets are put in this ‘gas state’ in a common large cube, continuously move all points from one motif into any other configuration without collisions. A composition of the above movements connects any periodic sets. □

Fig. 4 shows how both reduced basis and obtuse superbase discontinuously change up to rigid motion. The invariants of the underlying lattices change continuously in Example 7.6. If we compare bases coordinate-wise, [41, Theorem 15] proved any reduced basis is discontinuous. Theorems 7.5, 7.7 and Corollary 7.9 will settle all (dis)continuity challenges up to isometry and rigid motion in  $\mathbb{R}^2$ .

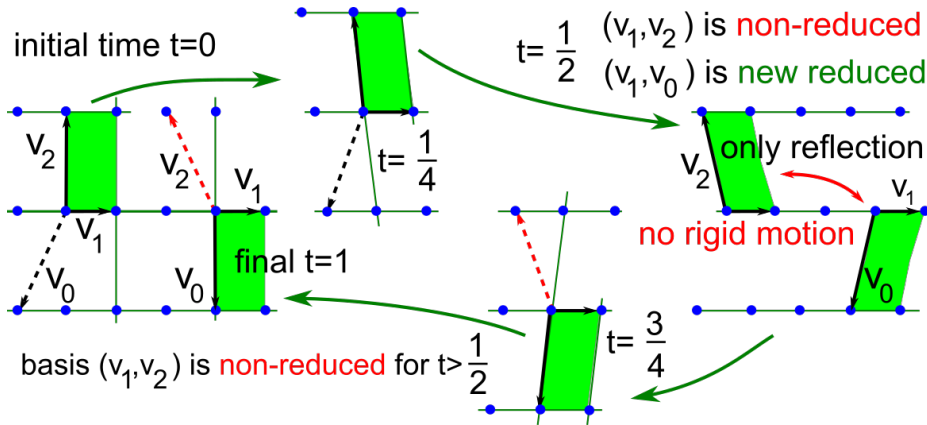


**Fig. 4** Discontinuity of obtuse superbases up to rigid motion. The superbase  $v_1 = (1, 0)$ ,  $v_2(t) = (-t, 2)$ ,  $v_0(t) = (t - 1, -2)$  deforms for  $t \in [0, 1]$ . The initial and final superbases at  $t = 0$  and  $t = 1$  generate the same rectangular lattice but are not related by rigid motion.

Any lattice  $\Lambda \subset \mathbb{R}^2$  with a basis  $v_1, v_2$  defines the *positive quadratic form*

$$Q(x, y) = (xv_1 + yv_2)^2 = q_{11}x^2 + 2q_{12}xy + q_{22}y^2 \geq 0 \text{ for all } x, y \in \mathbb{R},$$

where  $q_{11} = v_1^2$ ,  $q_{22} = v_2^2$ ,  $q_{12} = v_1 \cdot v_2$ . Changing the basis  $v_1, v_2$  (possibly by reflection) is equivalent to replacing  $x, y$  by the linear combinations of the coordinates of  $xv_1 + yv_2$  in a new basis. Conversely, any positive quadratic form  $Q(x, y)$  can be written as a sum  $(a_1x + b_1y)^2 + (a_2x + b_2y)^2$ , see [15, Theorem 2 on p. 116], and defines the lattice with the basis  $v_1 = (a_1, a_2)$ ,  $v_2 = (b_1, b_2)$ .



In 1773 Lagrange [14] proved that any positive quadratic form can be rewritten so that  $0 < q_{11} \leq q_{22}$  and  $-q_{11} \leq 2q_{12} \leq 0$ . The resulting non-acute *reduced* basis  $v_1, v_2$  satisfies  $0 < v_1^2 \leq v_2^2$  and  $-v_1^2 \leq 2v_1 \cdot v_2 \leq 0$  without the new special conditions in Definition 2.3. Alternatively,  $0 \leq 2q_{12} \leq q_{11}$  and  $0 \leq 2v_1 \cdot v_2 \leq v_1^2$  define a non-obtuse reduced basis. The mirror bright2021proof  $\Lambda^\pm$  of  $\Lambda(\frac{1}{4})$  in Fig. 4 (top) generated by the obtuse reduced bases  $v_1 = (1, 0)$ ,  $v_2^\pm = (-\frac{1}{4}, \pm 2)$  have the same reduced form  $Q(x, y) = x^2 - \frac{1}{2}xy + 4y^2$  not distinguishing  $\Lambda^\pm$  up to rigid motion.

If  $v_1, v_2$  form a unique reduced basis, Lemma 4.3 shows that  $\pm\{v_1, v_2, v_1 + v_2\}$  are three shortest Voronoi vectors. Then the *metric tensor*  $(v_1^2, v_1 \cdot v_2, v_2^2)$  is a complete isometry invariant but doesn't distinguish mirror bright2021proof (enantiomorphs). Instead of one scalar product and two squared lengths, Delone used the homogeneous parameters [16, section 29] equal to the conorms  $p_{ij}$  from Definition 2.6:

$$p_{01} = q_{11} + q_{12} = v_1^2 + v_1 \cdot v_2 = v_1 \cdot (v_1 + v_2) = -v_0 \cdot v_1,$$

$$p_{02} = q_{22} + q_{12} = v_2^2 + v_1 \cdot v_2 = v_2 \cdot (v_1 + v_2) = -v_0 \cdot v_2,$$

$$p_{12} = -q_{12} = -v_1 \cdot v_2.$$

The quadratic form becomes a sum of squares:  $Q_\Lambda = p_{01}x^2 + p_{22}y^2 + p_{12}(x - y)^2$ . The inequalities for  $q_{ij}$  are equivalent to the simple ordering  $0 \leq p_{12} \leq p_{01} \leq p_{02}$ , which Definition 3.1 will use to introduce a more convenient root invariant.

The isometry classification in (1.1ab) can be interpreted via group actions, see [18] and [42]. Let  $\mathcal{B}_n$  be the space of all linear bases in  $\mathbb{R}^n$ . Up to a change of basis, all lattices in  $\mathbb{R}^n$  form the  $n^2$ -dimensional orbit space  $\mathcal{L}_n = \mathcal{B}_n/\text{GL}(\mathbb{R}^n)$ , see [18, formula (1.37), p. 34]. Up to orthogonal maps from the group  $O(\mathbb{R}^n)$ , the orbit space of lattices can be identified with the cone  $\mathcal{C}_+(\mathcal{Q}_n) = \mathcal{B}_n/O(\mathbb{R}^n)$  of positive quadratic forms, where  $\mathcal{Q}_n$  denotes the space of real symmetric  $n \times n$  matrices, see [18, formula (1.67), p. 41]. The Lattice Isometry Space  $\text{LIS}(\mathbb{R}^n)$  was called the space of *intrinsic* lattices  $\mathcal{L}_n^o = \mathcal{C}_+(\mathcal{Q}_n)/\text{GL}(\mathbb{Z}^n)$  in [18, formula (1.70), p. 42].

The past approach to uniquely identify an intrinsic lattice (isometry class), say for  $n = 2$ , was to choose a fundamental domain of the action of  $\text{GL}(\mathbb{Z}^2)$  on the cone  $\mathcal{C}_+(\mathcal{Q}_2)$ . This choice is equivalent to a choice of a reduced basis, which can be discontinuous. Mirror reflections of any lattice  $\Lambda$  correspond to quadratic forms  $q_{11}x^2 \pm 2q_{12}xy + q_{22}y^2$  that differ by a sign of  $q_{12}$ . To distinguish mirror bright2021proof of lattices, Definition 3.4 will introduce  $\text{sign}(\Lambda)$ . Then continuous deformations of lattices become continuous paths in a space of invariants, see Remark 4.8.

Proposition 3.10 establishes a 1-1 correspondence between obtuse superbases and reduced bases. The latter bases are common in crystallography and implemented by many fast algorithms [7]. So our lattice input will be any obtuse superbase. Fig. 5 shows logical flows from key concepts to new contributions.

The main results are complete classifications in Theorem 4.2, Corollary 4.6, and metrics on lattice invariants in Definitions 5.1, 5.4. Continuity of invariants in Theorems 7.5, 7.7 convert the Lattice Isometry Space  $\text{LIS}(\mathbb{R}^2)$  into a continuously parameterised map solving Problem 1.1. Definition 6.1 extends the binary chirality to a real-valued deviation of a lattice from a higher-symmetry neighbour.

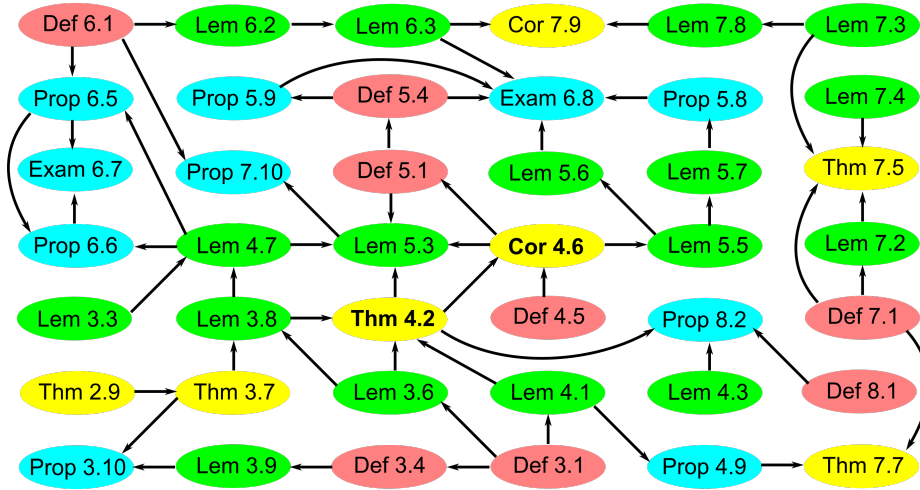


Fig. 5 Major logical connections between new definitions, auxiliary lemmas and main results.

Petitjean [30] comprehensively described past approaches to quantify chirality of bounded objects such as rigid molecules. The most rigorous approach is to use a metric between these rigid objects. However, even for the simplest case of a finite set of points, the Hausdorff-like distances between finite sets require approximate minimisations over infinitely many rotations. Definition 6.1 will introduce chiral distances for 2D lattices, which are easily computable by Propositions 6.5, 6.6.

### 3 Isometry invariants of an obtuse superbase of a 2-dimensional lattice

Definition 3.1 introduces voforms VF and coforms CF, which are triangular cycles whose three nodes are marked by vonorms and conorms, respectively. We start from any obtuse superbase  $B$  of a lattice  $A \subset \mathbb{R}^2$  to define VF, CF, and a root invariant RI. Lemma 3.8(a) will justify that RI depends only on  $A$ , not on  $B$ .

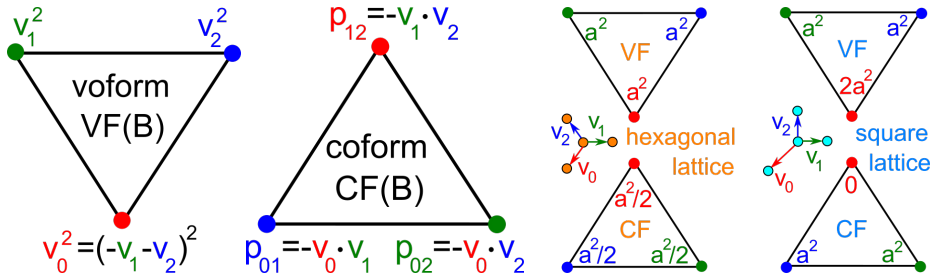


Fig. 6 1st picture: a voform  $VF(B)$  of a 2D lattice with an obtuse superbase  $B = \{v_0, v_1, v_2\}$ . 2nd picture: nodes of a coform  $CF(B)$  are marked by conorms  $p_{ij}$ . 3rd and 4th pictures: VF and CF of the hexagonal and square lattice with a minimum inter-point distance  $a$ .

**Definition 3.1 (voform VF, coform CF, ordered root invariant RI)** For any ordered obtuse superbase  $B$  in  $\mathbb{R}^2$ , the voform  $\text{VF}(B)$  is the cycle on three nodes marked by the vonorms  $v_0^2, v_1^2, v_2^2$ , see Fig. 6. The coform  $\text{CF}(B)$  is the cycle on three nodes marked by the conorms  $p_{12}, p_{02}, p_{01}$ . Since all conorms  $p_{ij} \geq 0$ , we can define the root products  $r_{ij} = \sqrt{p_{ij}}$ . The root invariant  $\text{RI}(B)$  is obtained by writing the three root products  $r_{12}, r_{01}, r_{02}$  in the increasing order. ■

The ordering  $r_{12} \leq r_{01} \leq r_{02}$  is equivalent to  $v_1^2 \leq v_2^2 \leq v_0^2$  by formulae (2.7a). Root products have the same units as original coordinates of basis vectors, for example, Angstroms:  $1\text{\AA} = 10^{-10}\text{m}$ . The ordered root invariant  $\text{RI}(B)$  is more convenient than  $\text{VF}(B)$  and  $\text{CF}(B)$ , which depend on an order of vectors of  $B$ .

**Example 3.2 (a)** A lattice  $\Lambda$  with a rectangular cell of sides  $a \leq b$  has an obtuse superbase  $B$  with  $v_1 = (a, 0)$ ,  $v_2 = (0, b)$ ,  $v_0 = (-a, -b)$ , and  $\text{RI}(B) = (0, a, b)$ .

**(b)** For any lattice  $\Lambda \subset \mathbb{R}^2$  whose Voronoi domain  $V(\Lambda)$  is a mirror-symmetric hexagon, assume that the  $x$ -axis is its line of symmetry. Since  $V(\Lambda)$  is centrally symmetric with respect to the origin  $0$ , the  $y$ -axis is also its line of symmetry, see Fig. 7. Then  $\Lambda$  has the centred rectangular (non-primitive) cell with sides  $2a \leq 2b$ . The obtuse superbase  $B$  with  $v_1 = (2a, 0)$ ,  $v_2 = (-a, b)$ ,  $v_0 = (-a, -b)$  has  $\text{RI}(B) = (a\sqrt{2}, a\sqrt{2}, \sqrt{b^2 - a^2})$  for  $b \geq a\sqrt{3}$ . For  $a \leq b < a\sqrt{3}$ , we should swap  $r_{02} = \sqrt{b^2 - a^2}$  with  $r_{12} = a\sqrt{2}$  to get an ordered root invariant  $\text{RI}(B)$ . ■

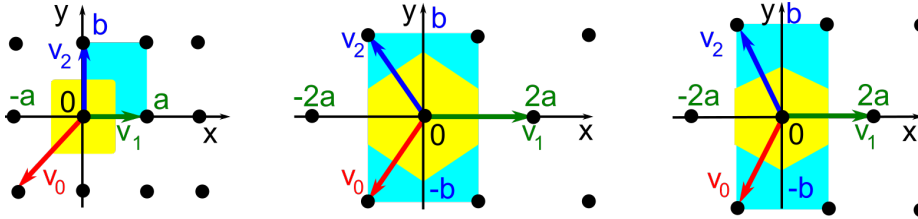


**Fig. 7** Left:  $\Lambda$  has a rectangular cell and obtuse superbase  $B$  with  $v_1 = (a, 0)$ ,  $v_2 = (0, b)$ ,  $v_0 = (-a, -b)$ , see Example 3.2 and Lemma 3.3. Other lattices  $\Lambda$  have a rectangular cell  $2a \times 2b$  and an obtuse superbase  $B$  with  $v_1 = (2a, 0)$ ,  $v_2 = (-a, b)$ ,  $v_0 = (-a, -b)$ . Middle:  $\text{RI}(B) = (\sqrt{b^2 - a^2}, a\sqrt{2}, a\sqrt{2})$ ,  $a \leq b \leq a\sqrt{3}$ . Right:  $\text{RI}(B) = (a\sqrt{2}, a\sqrt{2}, \sqrt{b^2 - a^2})$ ,  $a\sqrt{3} \leq b$ .

A lattice  $\Lambda \subset \mathbb{R}^n$  that can be mapped to itself by a mirror reflection with respect to a  $(n - 1)$ -dimensional hyperspace can be called *mirror-symmetric* or *achiral*. Since a mirror reflection of any lattice  $\Lambda \subset \mathbb{R}^2$  with respect to a line  $L \subset \mathbb{R}^2$  can be realised by a rotation in  $\mathbb{R}^3$  around  $L$  through  $180^\circ$ , the term *achiral* sometimes applies to all 2D lattices and becomes non-trivial only for 3D lattices. This paper for 2D lattices uses the clearer adjective *mirror-symmetric*.

**Lemma 3.3 (root invariants of mirror-symmetric lattices  $\Lambda \subset \mathbb{R}^2$ )** An obtuse superbase  $B$  generates a mirror-symmetric lattice  $\Lambda(B)$  if and only if

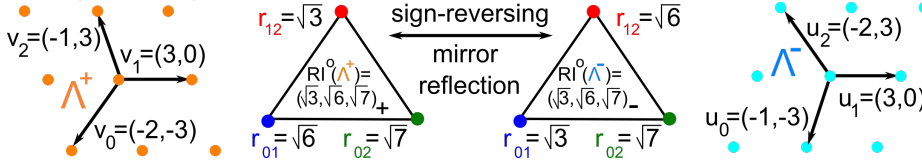
- (3.3a) the root invariant  $\text{RI}(B)$  contains a zero value and  $\Lambda(B)$  is rectangular, or
- (3.3b)  $\text{RI}(B)$  has equal root products and the Voronoi domain of  $\Lambda(B)$  is a square or a hexagon whose symmetry group has two orthogonal axes of symmetry. ▲

*Proof* The part *if*  $\Leftarrow$ . Let  $\text{RI}(B)$  include a zero, which should be the first root product, say  $0 = r_{12} = \sqrt{-v_1 \cdot v_2}$ . The vectors  $v_1, v_2$  of the superbase  $B$  are orthogonal and generate a rectangular lattice, which is mirror-symmetric. If  $\text{RI}(B)$  has two equal root products, say  $r_{01} = r_{02}$ , the conorms are also equal:  $p_{01} = p_{02}$ . Formulae (2.7a) imply that  $v_1^2 = p_{01} + p_{12} = p_{02} + p_{12} = v_2^2$ . The vectors  $v_1, v_2$  have equal lengths and can be swapped ( $v_1 \leftrightarrow v_2$ ) by the reflection in the bisector  $L$  between  $v_1, v_2$ , which preserves  $v_0 = -v_1 - v_2$ , so  $\Lambda(B)$  is mirror-symmetric.

The part *only if*  $\Rightarrow$ . If  $\Lambda(B)$  is mirror-symmetric, then so is its Voronoi domain  $V(\Lambda)$ . If  $V(\Lambda)$  is a rectangle or a mirror-symmetric hexagon as in Fig. 7,  $\text{RI}(B)$  computed in Example 3.2 contains either a zero or two equal root products.  $\square$

**Definition 3.4** ( $\text{sign}(B)$ , the oriented root invariant  $\text{RI}^\circ(B)$ ) *If an obtuse superbase  $B$  generates a mirror-symmetric lattice, set  $\text{sign}(B) = 0$ . Else all vectors of  $B$  have different lengths and angles not equal to  $90^\circ$  by Lemma 3.3. Let  $v_1, v_2$  be the shortest vectors of  $B$  so that  $|v_1| < |v_2|$ . Then  $\text{sign}(B) = \pm 1$  is the sign of the determinant  $\det(v_1, v_2)$  of the matrix with the columns  $v_1, v_2$ . The oriented root invariant  $\text{RI}^\circ(B)$  is obtained by adding  $\text{sign}(B)$  as a superscript to  $\text{RI}(B)$ .  $\blacksquare$*

**Fig. 8** The lattices  $\Lambda, \Lambda'$  are mirror reflections of each other and have oriented root invariants  $\text{RI}^\circ = (\sqrt{3}, \sqrt{6}, \sqrt{7})_\pm$  with opposite signs introduced in Definition 3.4, see Example 3.5.



If  $\text{sign}(B) = 0$ , this zero superscript in  $\text{RI}^\circ(B)$  can be skipped for simplicity, so  $\text{RI}^\circ(B) = \text{RI}(B)$  in this case. Theorem 3.7 will show that  $\text{sign}(B)$  can be considered as an invariant of a lattice  $\Lambda$  up to orientation-preserving similarity.

In Definition 3.4 the determinant  $\det(v_1, v_2)$  is the signed area of the unit cell  $U(v_1, v_2)$  equal to  $|v_1| \cdot |v_2| \sin \angle(v_1, v_2)$ , where the angle is measured from  $v_1$  to  $v_2$  in the anticlockwise direction around the origin  $0 \in \mathbb{R}^2$ . For a strict obtuse superbase  $B$ , all angles between its basis vectors are strictly obtuse. Then  $\text{sign}(B) = +1$  if  $\angle(v_1, v_2)$  is in the positive range  $(90^\circ, 180^\circ)$ , else  $\text{sign}(B) = -1$ .

**Example 3.5 (signs of lattices)** *The lattice  $\Lambda^+$  in the first picture of Fig. 3 has the obtuse superbase  $B$  with  $v_1 = (3, 0)$ ,  $v_2 = (-1, 3)$ ,  $v_0 = (-2, -3)$  of lengths  $3, \sqrt{10}, \sqrt{13}$ , respectively, so  $\Lambda^+$  is not mirror-symmetric. Since  $v_1, v_2$  are the two*

*shortest vectors of  $B^+$  and  $\det(v_1, v_2) = \det \begin{pmatrix} 3 & -1 \\ 0 & 3 \end{pmatrix} > 0$ , we get  $\text{sign}(B^+) = +1$ .*

*The anticlockwise angle is  $\angle(v_1, v_2) = 180^\circ - \arcsin \frac{3}{\sqrt{10}} \approx 108^\circ$ .*

*The lattice  $\Lambda^-$  in the last picture of Fig. 3 is obtained from  $\Lambda^+$  by a mirror reflection and has the obtuse superbase  $B^-$  with  $u_1 = v_1$ ,  $u_2 = (-2, 3)$ ,  $u_0 = (-1, -3)$  of lengths  $3, \sqrt{13}, \sqrt{10}$ , respectively, so  $\Lambda^-$  is not mirror-symmetric. Since*

$u_1, u_0$  are the shortest vectors,  $\det(u_1, u_0) = \det \begin{pmatrix} 3 & -1 \\ 0 & -3 \end{pmatrix} < 0$ , we get  $\text{sign}(B^-) =$

$-1$ . The anticlockwise angle is  $\angle(u_1, u_0) = \arcsin \frac{3}{\sqrt{10}} - 180^\circ \approx -108^\circ$ .  $\blacksquare$

**Lemma 3.6 (RI invariance)** *For an unordered obtuse superbase  $B$  in  $\mathbb{R}^2$ , any isometry preserves  $\text{RI}(B)$ . Any rigid motion preserves  $\text{sign}(B)$  and  $\text{RI}^\circ(B)$ .*  $\blacktriangle$

*Proof* Any isometry of an ordered obtuse superbase  $B$  preserves the lengths and scalar products of the ordered vectors, so  $\text{RI}(B)$  is unchanged. Any re-ordering of vectors of  $B$  permutes conorms.  $\text{RI}(B)$  is unique due to ordered root products.

If a lattice is mirror-symmetric, then so is its image under any rigid motion in  $\mathbb{R}^2$ , hence  $\text{sign}(B) = 0$  is preserved. If  $B$  generates a non-mirror symmetric lattice,  $B$  has unique shortest vectors  $v_1, v_2$ . A rigid motion acts on  $v_1, v_2$  as a special orthogonal matrix with determinant 1, hence preserving  $\det(v_1, v_2)$ ,  $\text{sign}(B)$ .  $\square$

Theorem 3.7 below is crucial for a complete classification of 2D lattices in Theorem 4.2 and Corollary 4.6. Theorem 3.7 highlights that mirror-symmetric lattices have more options for obtuse superbases up to rigid motion. The same rectangular lattice can have two obtuse bases with  $v_1 = (1, 0)$ ,  $v_2 = (0, \pm 2)$ , which are related by reflection in the  $x$ -axis, not by rigid motion. This symmetry-related ambiguity is much harder to resolve for 3D lattices even up to isometry, see [22].

**Theorem 3.7 (isometric obtuse superbases)** *Any lattices  $\Lambda, \Lambda' \subset \mathbb{R}^2$  are isometric if and only if any obtuse superbases of  $\Lambda, \Lambda'$  are isometric. If  $\Lambda, \Lambda'$  are not rectangular, the same conclusion holds for rigid motion instead of isometry. Any rectangular (non-square) lattice has two obtuse superbases related by reflection.*  $\blacktriangle$

*Proof* Part *if* ( $\Leftarrow$ ): any isometry between obtuse superbases of  $\Lambda, \Lambda'$  linearly extends to an isometry  $\Lambda \rightarrow \Lambda'$ . Part *only if* ( $\Rightarrow$ ) means that any obtuse superbase of  $\Lambda$  is unique up to isometry. By Lemma 2.8 for  $n = 2$ , if a lattice  $\Lambda$  has a strict obtuse superbase  $B = \{v_0, v_1, v_2\}$ , the Voronoi vectors of  $\Lambda$  are the pairs of opposite partial sums  $\pm v_0, \pm v_1, \pm v_2$ , see Fig. 3 (left). Hence  $B$  is uniquely determined by the strict Voronoi vectors up to a sign. So  $B$  is one of only two obtuse superbases  $\pm\{v_0, v_1, v_2\}$  related by central symmetry or rotation through  $180^\circ$  around 0. Hence  $\Lambda$  has a unique obtuse superbase up to rigid motion.

If a superbase of  $\Lambda$  is non-strict, one conorm vanishes, say  $p_{12} = 0$ . Then  $v_1, v_2$  span a rectangular unit cell and  $\Lambda$  has four non-strict Voronoi vectors  $\pm v_1 \pm v_2$  with all possible combinations of signs. Hence  $\Lambda$  has four obtuse superbases  $\{v_1, v_2, -v_1 - v_2\}$ ,  $\{-v_1, -v_2, v_1 + v_2\}$ ,  $\{-v_1, v_2, v_1 - v_2\}$ ,  $\{v_1, -v_2, v_2 - v_1\}$ , see Fig. 3. The first two (and the last two) superbases are obtained from each other by rotation through  $180^\circ$  around the origin. Unless the lattice is square, the resulting two classes of superbases are related by reflection, not by rigid motion.  $\square$

**Lemma 3.8 (lattice invariants) (a)** *For any obtuse superbase  $B$  of a lattice  $\Lambda \subset \mathbb{R}^2$ , the root invariant  $\text{RI}(B)$  is an isometry invariant of  $\Lambda$  and can be denoted by  $\text{RI}(\Lambda)$ . Similarly,  $\text{RI}^\circ(\Lambda)$  and  $\text{sign}(\Lambda)$  are invariants of a lattice  $\Lambda$  up to rigid motion and orientation-preserving similarity, respectively.*

**(b)** *A lattice  $\Lambda \subset \mathbb{R}^2$  is mirror-symmetric if and only if  $\text{sign}(\Lambda) = 0$ .*  $\blacktriangle$

*Proof (a)* An obtuse superbase  $B$  of any lattice  $\Lambda$  is unique up to isometry by Theorem 3.7. Lemma 3.6 implies that the root invariant  $\text{RI}$  is an isometry invariant of  $\Lambda$ , independent of any obtuse superbase  $B$ , hence can be denoted by  $\text{RI}(\Lambda)$ .

Since an obtuse superbase  $B$  of any non-mirror-symmetric lattice  $\Lambda$  is unique up to rigid motion by part (a), Lemma 3.6 implies that  $\text{sign}(B)$  and  $\text{RI}^\circ(B)$  are invariant up to rigid motion, hence can be denoted by  $\text{sign}(\Lambda)$  and  $\text{RI}^\circ(\Lambda)$ , respectively. If  $\Lambda$  is mirror-symmetric, then any rigid motion preserves  $\text{sign}(\Lambda) = 0$  as well as  $\text{RI}(\Lambda)$ . So  $\text{RI}^\circ(\Lambda)$  is invariant up to rigid motion for all  $\Lambda \subset \mathbb{R}^2$ .

Any orientation-preserving similarity is a composition of a rigid motion and a uniform scaling (or a dilation) of all vectors by a factor  $s > 0$ . This similarity preserves any symmetries of the lattice  $\Lambda$  and multiplies the determinant  $\det(v_1, v_2)$  from Definition 3.4 by  $s^2 > 0$ , hence preserving  $\text{sign}(\Lambda)$ .

(b) By Definition 3.4 any mirror-symmetric lattice has  $\text{sign}(\Lambda) = 0$ . Any basis  $v_1, v_2$  of a non-mirror symmetric lattice  $\Lambda$  has  $\det(v_1, v_2) \neq 0$ , so  $\text{sign}(\Lambda) \neq 0$ .  $\square$

For any lattices  $\Lambda^\pm$  related by reflection, their unoriented root invariants  $\text{RI}(\Lambda^\pm)$  are identical, while  $\text{RI}^\circ(\Lambda^\pm)$  differ by sign. Lemma 3.9 computes  $\text{sign}(\Lambda)$  from any obtuse superbase whose first vector can be assumed to be  $v_1 = (1, 0)$ .

**Lemma 3.9 (geometry of signs)** (a) *Up to orientation-preserving similarity, any lattice  $\Lambda \subset \mathbb{R}^2$  has an obtuse superbase with  $v_1 = (1, 0)$  and  $v_2 = (x, y)$ , where  $(x, y)$  belongs to the region  $\text{Obt} = \{-1 \leq x \leq 0 < y, x^2 + x + y^2 \geq 0\}$ . Then  $\text{sign}(\Lambda)$  from Definition 3.4 is determined by  $(x, y)$  in Fig. 9, see also Table 1.*

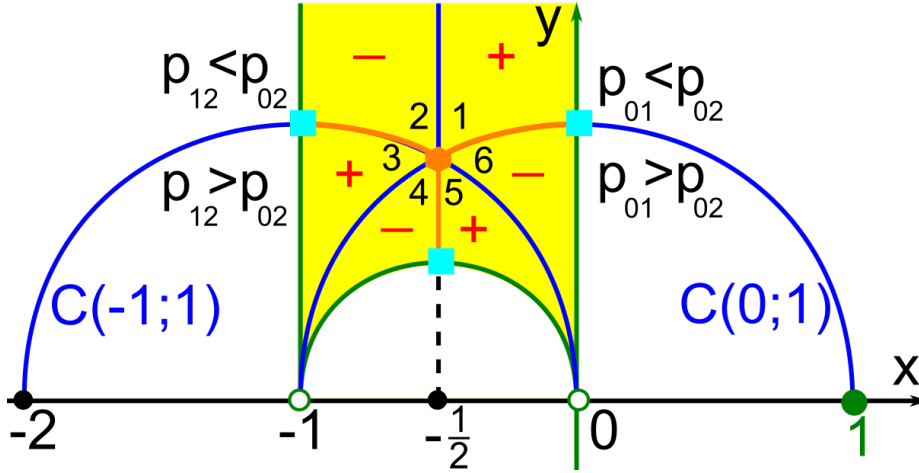


**Fig. 9** The yellow region  $\text{Obt}$  is the fundamental domain of  $\text{SL}(\mathbb{R}^2)$  and is split into six subregions by the vertical line  $x = -\frac{1}{2}$  and the circles  $C(0; 1) = \{(x, y) \in \mathbb{R}^2 \mid x^2 + y^2 = 1\}$  and  $C(-1; 1) = \{(x, y) \in \mathbb{R}^2 \mid x^2 + 2x + y^2 = 0\}$ , see Lemma 3.9(a) and Table 1.

(b) *Up to similarity, any lattice  $\Lambda \subset \mathbb{R}^2$  with an obtuse superbase  $v_0, v_1, v_2$  can be represented by up to six points  $(x, y)$  in the subregions of  $\text{Obt}$ . Swapping  $v_0 \leftrightarrow v_2$  is realised by the reflection in the line  $x = -\frac{1}{2}$ , so  $v_2 = (x, y) \mapsto (-1-x, y)$ . Swapping and re-scaling the vectors  $v_1 \leftrightarrow v_2$  is realised by the inversion with respect to the circle  $x^2 + y^2 = 1$  so that  $v_2 \mapsto v_1 \mapsto \frac{v_2}{x^2 + y^2}$ , see Fig. 10 (right).  $\blacktriangle$*

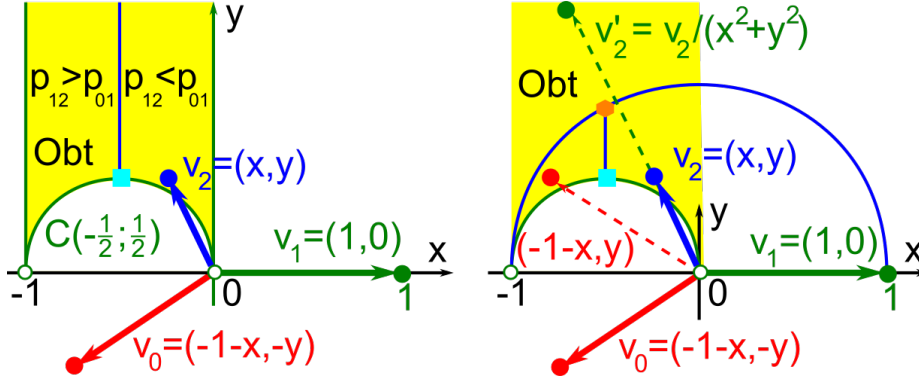


**Fig. 10 Left:** if  $\Lambda$  has an obtuse superbase with  $v_1 = (1, 0)$ ,  $v_2 = (x, y)$ , then  $\text{sign}(\Lambda)$  is determined by  $(x, y) \in \text{Obt}$  above the circle  $C(-\frac{1}{2}; \frac{1}{2}) = \{(x, y) \in \mathbb{R}^2 \mid x^2 + x + y^2 = 0\}$ . **Right:** re-ordering and re-scaling vectors of an obtuse superbase  $\{v_0, v_1, v_2\}$  is realised by the symmetries acting on  $v_2 = (x, y)$  within the yellow region  $\text{Obt}$ , see Lemma 3.9(b).

**Table 1** The sign of a lattice  $\Lambda \subset \mathbb{R}^2$  can be found from an obtuse superbase with  $v_1 = (1, 0)$ ,  $v_2 = (x, y)$ , see Lemma 3.9(a), Fig. 9. If any inequality becomes equality, then  $\text{sign}(\Lambda) = 0$ .

$k$	$\text{sign}(\Lambda)$	conditions on $v_2 = (x, y)$ in the $k$ -th subregion in Fig. 9	$p_{ij}$ inequalities
1	+	$-\frac{1}{2} < x < 0, \quad x^2 + y^2 > 1$	$p_{12} < p_{01} < p_{02}$
2	-	$-1 < x < -\frac{1}{2}, \quad x^2 + 2x + y^2 > 0$	$p_{01} < p_{12} < p_{02}$
3	+	$-1 < x < -\frac{1}{2}, \quad x^2 + y^2 > 1, \quad x^2 + 2x + y^2 < 0$	$p_{01} < p_{02} < p_{12}$
4	-	$-1 < x < -\frac{1}{2}, \quad x^2 + y^2 < 1, \quad x^2 + x + y^2 > 0$	$p_{02} < p_{01} < p_{12}$
5	+	$-\frac{1}{2} < x < 0, \quad x^2 + x + y^2 > 0, \quad x^2 + 2x + y^2 < 0$	$p_{02} < p_{12} < p_{01}$
6	-	$-\frac{1}{2} < x < 0, \quad x^2 + y^2 < 1, \quad x^2 + 2x + y^2 > 0$	$p_{12} < p_{02} < p_{01}$

*Proof (a)* Let  $B = \{v_0, v_1, v_2\}$  be an obtuse superbase of  $\Lambda$ . Any point  $p \in \Lambda$  can be translated to the origin. Then a suitable rotation puts the basis vector  $v_1$  along the positive  $x$ -axis so that  $v_1 = (s, 0)$  for  $s > 0$ . The uniform scaling by the factor  $s$ , maps  $v_1$  to  $(1, 0)$ . Since both vectors  $v_0, v_2$  have non-acute angles with  $v_1$ , they should have non-positive  $x$ -coordinates. Since the vectors  $v_0, v_2$  have a non-acute angle, one of them should be in the second quadrant  $\{x \leq 0 < y\}$ . Since we can swap  $v_0, v_2$  without affecting  $\Lambda$ , we can assume that  $v_2 = (x, y)$  for  $x \leq 0 < y$ . Then  $v_0 = (-1 - x, -y)$ . The ordered superbase  $B = \{v_0, v_1, v_2\}$  has the conorms

$$p_{12} = -v_1 \cdot v_2 = -x \geq 0, \quad p_{01} = -v_0 \cdot v_1 = 1 + x, \quad p_{02} = -v_0 \cdot v_2 = x^2 + x + y^2.$$

Since all conorms should be non-negative, we need that  $0 \leq p_{01} = 1 + x$ ,  $x \geq -1$ . Also  $0 \leq p_{02} = x^2 + x + y^2 = (x + \frac{1}{2})^2 - \frac{1}{4} + y^2$ , so  $(x + \frac{1}{2})^2 + y^2 \geq \frac{1}{4}$ . The endpoint  $(x, y)$  of  $v_2$  should be in the vertical strip  $\{-1 \leq x \leq 0\}$  non-strictly above the green circle  $C(-\frac{1}{2}; \frac{1}{2})$  with the centre  $(-\frac{1}{2}, 0)$  and radius  $\frac{1}{2}$  in Fig. 9. The yellow

**Table 2** Inequalities between conorms are interpreted in terms of endpoints  $(x, y)$  of a vector  $v_2$  complementing  $v_1 = (1, 0)$  in an obtuse superbase  $\{v_0, v_1, v_2\}$ , see Lemma 3.9.

$p_{ij}$ inequality	condition on $(x, y)$	subregion within the yellow region Obt in Fig. 9
$p_{02} \geq 0$	$x^2 + x + y^2 \geq 0$	the region Obt is non-strictly above $C(-\frac{1}{2}; \frac{1}{2})$
$p_{12} < p_{01}$	$-\frac{1}{2} < x < 0$	the right hand side vertical strip of the region Obt
$p_{01} < p_{02}$	$x^2 + y^2 > 1$	the subregion in Obt above the circle $C(0; 1)$
$p_{12} < p_{02}$	$x + 2x + y^2 > 0$	the subregion in Obt above the circle $C(-1; 1)$

region Obt of allowed endpoints  $(x, y)$  of  $v_2$  in Fig. 9 is bounded by the vertical lines  $x = 0$ ,  $x = -1$  and the green circle  $C(-\frac{1}{2}; \frac{1}{2})$ . All boundary points represent all rectangular lattices. For example, the points  $(x, y) = (0, 1)$  and  $(x, y) = (-1, 1)$  in the vertical boundaries represent the same square lattice. For  $(x, y) = (-\frac{1}{2}, \frac{1}{2})$  in the green circle  $C(-\frac{1}{2}; \frac{1}{2})$ , the vectors  $v_0 = (-\frac{1}{2}, -\frac{1}{2})$  and  $v_2 = (-\frac{1}{2}, \frac{1}{2})$  span a square unit cell with edge-length  $\frac{1}{\sqrt{2}}$ . Now we split the yellow region into three pairs of symmetric subregions according to inequalities between three conorms.

The inequality  $p_{12} < p_{01}$  is equivalent to  $-x < 1 + x$ ,  $x > -\frac{1}{2}$ , see Table 2. The inequality  $p_{01} < p_{02}$  is equivalent to  $1 + x < x^2 + x + y^2$ ,  $x^2 + y^2 > 1$ , so the point  $(x, y)$  is above the circle  $C(0; 1)$  with the centre  $(0, 0)$  and radius 1 in Fig. 9. The inequality  $p_{12} < p_{02}$  is equivalent to  $-x < x^2 + x + y^2$ ,  $(x + 1)^2 + y^2 > 1$ , so the point  $(x, y)$  is above the circle  $C(-1; 1)$  with the centre  $(-1, 0)$  and radius 1.

The inequalities on  $p_{ij}$  from Table 2 justify that the region Obt splits into six subregions split by the vertical line  $x = -\frac{1}{2}$  and two circles  $C(-1; 0)$  and  $C(0; 1)$ . Each subregion is defined by one of six possible orderings of the conorms  $p_{12}, p_{01}, p_{02}$ , see the last column of Table 1. To check the signs in the second column of Table 1, notice that if  $p_{ij}$  is a minimal conorm, the formula  $p_{ij} = \frac{1}{2}(v_i^2 + v_j^2 - v_k^2)$  from (2.7b) implies that  $v_i, v_j$  are the shortest of three vectors  $v_0, v_1, v_2$ .

For example, Table 1 says that  $v_1 = (1, 0)$  and  $v_2$  are the two shortest vectors in the cases of the first and last rows. In the first row,  $v_2 = (x, y)$  has the length  $|v_2| = \sqrt{x^2 + y^2} > 1 = |v_1|$ , hence by Definition 3.4  $\text{sign}(A)$  equals the sign of  $\det(v_1, v_2) = y > 0$ . In the last row,  $v_2 = (x, y)$  has the length  $|v_2| = \sqrt{x^2 + y^2} < 1 = |v_1|$ , hence by Definition 3.4  $\text{sign}(A)$  equals the sign of  $\det(v_2, v_1) = -y < 0$ . The signs in the remaining four rows of Table 1 are similarly checked.

If any of the strict inequalities above becomes equality, we get a point either on the boundary of Obt (representing all rectangular lattices in  $\mathbb{R}^2$ ) or in one of the lines  $x = -\frac{1}{2}$  or the circles  $C(0; 1)$  and  $C(-1; 1)$ . These internal curves contain points  $(x, y)$  representing centred rectangular lattices. For instance, the triple intersection of the internal curves at  $(x, y) = (-\frac{1}{2}, \frac{\sqrt{3}}{2})$  represents all hexagonal lattices. All these lattices are mirror-symmetric and have  $\text{sign}(A) = 0$ .

**(b)** Any two vectors of an obtuse superbase  $B = \{v_0, v_1, v_2\}$  can be mapped by similarity to  $(1, 0)$  and  $(x, y)$ . Each of the resulting six pairs  $(x, y)$  belongs to one of the six subregions marked by  $k = 1, 2, 3, 4, 5, 6$  in the middle picture of Fig. 9. It suffices to understand the action of two transpositions  $v_0 \leftrightarrow v_2$  and  $v_1 \leftrightarrow v_2$ .



When we swap  $v_2 = (x, y)$  and  $v_0 = (-1 - x, -y)$ , while keeping  $v_1 = (x, y)$  fixed, we reflect the lattice  $\Lambda(B)$  generated by  $B$  in the  $x$ -axis so that  $v_1 = (x, y)$  has an obtuse angle to the image  $(-1 - x, y)$  of  $v_0$ . This new vector  $(-1 - x, y)$  plays the role of  $v_2$  in the reflected lattice and is symmetric to  $v_2 = (x, y)$  in the vertical line  $x = -\frac{1}{2}$  within the yellow region  $\text{Obt}$  in Fig. 10 (right).

When we swap  $v_1 = (1, 0)$  and  $v_2 = (x, y)$ , the second vector is divided by its length  $|v_2| = \sqrt{x^2 + y^2}$ . Hence the first vector  $v_1$  maps to the vector that is parallel to  $v_2 = (x, y)$  and has the length  $1/\sqrt{x^2 + y^2}$ . This new vector  $v'_2 = v_2/(x^2 + y^2)$  plays the role of  $v_2$  and is obtained from  $v_2 = (x, y)$  by the inversion with respect to the circle  $x^2 + y^2 = 1$ . The inversion keeps all points on  $x^2 + y^2 = 1$  fixed, maps the  $y$ -axis  $x = 0$  to itself, swaps the half-line  $\{x = 0, y > 0\}$  with the upper half-circle  $\{x^2 + x + y^2 = 0, y > 0\}$ . Compositions of the symmetry in  $x = -\frac{1}{2}$  and this inversion generate up to six bright2021proof of  $(x, y)$  in the six subregions of  $\text{Obt}$ , though the point  $(x, y) = (-\frac{1}{2}, \frac{\sqrt{3}}{2})$  representing all hexagonal lattices is fixed.  $\square$

**Proposition 3.10 (reduced bases)** (a) *Up to isometry in  $\mathbb{R}^2$ , all reduced bases  $v_1, v_2$  from Definition 2.3 are in a 1-1 correspondence with all obtuse superbases  $B = \{v_0, v_1, v_2\}$  such that  $|v_1| \leq |v_2| \leq |v_0|$ . Up to isometry, any lattice  $\Lambda \subset \mathbb{R}^2$  has a unique reduced basis specified by the conditions of Definition 2.3.*

(b) *Up to rigid motion, any lattice has a unique reduced basis in Definition 2.3.  $\blacktriangle$*

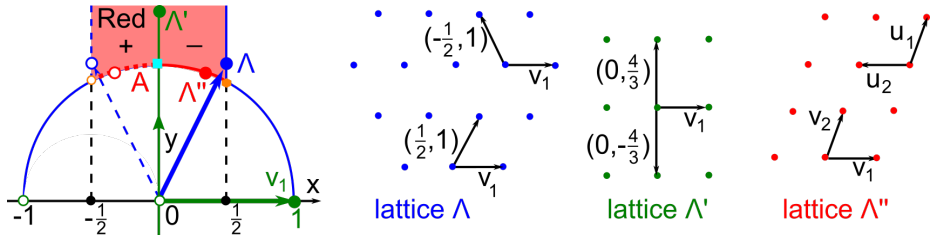


**Fig. 11** **Left:** any reduced basis in Definition 2.3 up to orientation-preserving similarity maps to  $v_1 = (1, 0)$  and  $v_2 = (x, y) \in \text{Red}$  from Proposition 3.10. **Right:** for each of the lattices  $\Lambda, \Lambda', \Lambda''$  represented by small blue, green, red circles/disks on the right, the conditions of Definition 2.3 choose one reduced basis among two bases that differ up to rigid motion.

*Proof (a)* Up to similarity by Lemma 3.9(b), any lattice  $\Lambda$  has an obtuse superbase  $B = \{v_0, v_1, v_2\}$  with  $v_1 = (1, 0)$  and  $v_2 = (x, y)$ , where the point  $(x, y)$  belongs to the yellow region  $\text{Obt}$  in Fig. 9. By Lemma 3.9(b) the six permutations of  $v_0, v_1, v_2$  are realised by internal symmetries of  $\text{Obt}$ , so we may assume that  $|v_1| \leq |v_2| \leq |v_0|$ . The equivalent inequalities in conorms  $p_{12} \leq p_{01} \leq p_{02}$  define the 1st subregion of  $\text{Obt}$  in Fig. 9, which coincides with the closure of the region  $\overline{\text{Red}}_+ = \{(x, y) \in \mathbb{R}^2 \mid x^2 + y^2 \geq 1, -\frac{1}{2} \leq x \leq 0 < y\}$  in Fig. 11.

Due to uniqueness of  $B$  up to isometry by Theorem 3.7, the position of  $v_2 = (x, y) \in \overline{\text{Red}}_+$  is unique for  $\Lambda$ . Up to uniform scaling and reflection  $y \leftrightarrow -y$ , the

closure  $\overline{\text{Red}}_+$  is defined by the same conditions  $v_1^2 \leq v_2^2 = x^2 + y^2$  and  $-\frac{1}{2} \leq \frac{v_1 \cdot v_2}{v_1^2} = x \leq 0$  as a reduced basis whose uniqueness up to isometry follows now.

(b) If orientation should be preserved, Theorem 3.7 proves the uniqueness of the obtuse superbase  $B = \{v_0, v_1, v_2\}$  from part (a) up to rigid motion for any non-rectangular lattice  $\Lambda$ . Cyclic permutations of  $v_0, v_1, v_2$  allow us to assume that  $v_1$  is the shortest vector. The equivalent condition on conorms says that  $p_{02}$  is the largest, hence  $v_2 = (x, y)$  belongs to the first two subregions of Obt in Fig. 9.

For the first open subregion with  $\text{sign}(B) = +1$ , the conditions  $v_1^2 < v_2^2 = x^2 + y^2$ ,  $-\frac{1}{2} < x = \frac{v_1 \cdot v_2}{v_1^2} < 0 < y = \det(v_1, v_2)$  of Definition 2.3 specify the interior  $\overline{\text{Red}}_+$ , so the basis  $\{v_1, v_2\}$  is reduced. For the second open subregion with  $\text{sign}(B) = -1$ , another basis  $\{v_1, v_1 + v_2\}$  is reduced by Definition 2.3 because the shifted point  $v_1 + v_2 = (x + 1, y)$  belongs to the interior of the right-half region in Fig. 11 (left):  $\overline{\text{Red}}_- = \{(x, y) \in \mathbb{R}^2 \mid x^2 + y^2 \geq 1, 0 < x < \frac{1}{2}, 0 < y\}$ .

It remains to consider singular cases. We include the common boundary line  $x = \frac{v_1 \cdot v_2}{v_1^2} = -\frac{1}{2}$  and the boundary round arcs of both subregions represent mirror-symmetric lattices with a unique (up to rigid motion) obtuse superbase. We exclude these boundaries from the first region, include them into the second region and shift by  $x \mapsto x + 1$  so that the unique reduced basis  $v_1, v_1 + v_2$  satisfies the conditions  $\frac{v_1 \cdot v_2}{v_1^2} = \frac{1}{2}$  and  $v_1 \cdot v_2 \geq 0$  for  $|v_1| = |v_2|$  in Definition 2.3.

The above boundaries in Fig. 11 (left) include the blue and red points representing the basis vectors  $v_2 = (x, y)$  of the lattices  $\Lambda, \Lambda''$ , respectively.

The final boundary lines  $x = -1$  and  $x = 0$  represent rectangular lattices with a unit cell  $a \times b$  for  $0 < a < b$  and two obtuse superbases related by reflection, not by rigid motion, for example  $v_1 = (a, 0)$ ,  $v_2 = (0, \pm b)$ . In this case there is no 1-1 correspondence between obtuse superbases and reduced bases. Definition 2.3 selects a unique reduced basis  $v_1 = (a, 0)$ ,  $v_2 = (0, b)$  due to  $\det(v_1, v_2) > 0$ .  $\square$

The dotted arc  $A$  in Fig. 11 (left) should be indeed excluded from [18, Fig. 1.3 on p. 85], otherwise the lattice  $\Lambda''$  in the last picture of Fig. 11 has two potential reduced bases  $v_1 = (1, 0)$ ,  $v_2 = (\frac{1}{3}, \frac{2\sqrt{2}}{3})$  and  $u_1 = (\frac{1}{3}, \frac{2\sqrt{2}}{3})$  and  $u_2 = (-1, 0)$ . Indeed, all basis vectors have length 1 and the second basis can be rotated to  $u'_1 = (1, 0)$ ,  $u'_2 = (-\frac{1}{3}, \frac{2\sqrt{2}}{3}) \in A$ . The second basis  $(u_1, u_2)$  of the same lattice  $\Lambda''$  is related to  $(v_1, v_2)$  by a reflection, but not by rigid motion. So the region Red with the excluded left boundary for  $x < 0$  contains a unique vector  $v_2 = (x, y)$  of a reduced basis up to orientation-preserving similarity. Forgetting about the uniform scaling, we get uniqueness of a reduced basis up to rigid motion.

The region Red in Fig. 11 (left) is a fundamental domain of all bases by the action of  $\text{SO}(\mathbb{R}^2) \times \mathbb{R}_+$  and  $\text{GL}(\mathbb{Z}^2)$  in the sense that any lattice up to orientation-preserving similarity can be represented by a unique point  $(x, y) \in \text{Red}$ . Red or any other half-open fundamental domain of a group action suffers from *discontinuity on boundary* when close lattices are represented by distant bases. For each of the lattices  $\Lambda, \Lambda''$  in Fig. 11, a slight perturbation of the non-reduced basis makes

it reduced but distant from the initial reduced basis up to rigid motion. The discontinuity above can be resolved by identifying boundary points of of Red by the reflection  $x \leftrightarrow -x$ . Section 4 will describe a simpler way to continuously parameterise lattices up to orientation-preserving similarity in Corollary 4.6.

#### 4 Complete classifications of 2D lattices up to isometry and similarity

Lemma 3.8 showed that  $\text{RI}(\Lambda)$ ,  $\text{RI}^\circ(\Lambda)$  are invariants of lattices up to isometry and rigid motion, respectively. To prove completeness of the invariants in Theorem 4.2, Lemma 4.1 reconstructs an obtuse superbase of  $\Lambda$ . Corollary 4.6 will classify lattices up to similarity by projected invariants introduced in Definition 4.5.

**Lemma 4.1 (superbase reconstruction)** *An obtuse superbase  $B = \{v_0, v_1, v_2\}$  of a lattice  $\Lambda \subset \mathbb{R}^2$  can be uniquely reconstructed up to isometry and up to rigid motion from its root invariant  $\text{RI}(\Lambda)$  and its oriented root invariant  $\text{RI}^\circ(\Lambda)$ , respectively. If  $\text{RI}(\Lambda) = (r_{12}, r_{01}, r_{02})$ , the basis vectors  $v_1, v_2$  are determined by*

$$|v_1| = \sqrt{r_{12}^2 + r_{01}^2}, \quad |v_2| = \sqrt{r_{12}^2 + r_{02}^2}, \quad \cos \angle(v_1, v_2) = \frac{-r_{12}^2}{\sqrt{r_{12}^2 + r_{01}^2} \sqrt{r_{12}^2 + r_{02}^2}},$$

and span a primitive unit cell of the area  $A(\Lambda) = \sqrt{r_{12}^2 r_{01}^2 + r_{12}^2 r_{02}^2 + r_{01}^2 r_{02}^2}$ .  $\blacktriangle$

*Proof* Assuming that a root invariant  $\text{RI}(\Lambda)$  is ordered as  $r_{12} \leq r_{01} \leq r_{02}$ , we will build an obtuse superbase  $\{v_0, v_1, v_2\}$  such that  $r_{ij} = \sqrt{-v_i \cdot v_j}$  for any distinct  $i, j \in \{0, 1, 2\}$ . Find the lengths from (2.7a):  $|v_i| = \sqrt{p_{12}^2 + p_{0i}^2} = \sqrt{r_{12}^2 + r_{0i}^2}$  for  $i = 1, 2$ . Using  $v_1 \cdot v_2 = -r_{12}^2$ , the anticlockwise angle has  $\cos \angle(v_1, v_2) = \frac{v_1 \cdot v_2}{|v_1| \cdot |v_2|} = \frac{-r_{12}^2}{\sqrt{r_{12}^2 + r_{01}^2} \sqrt{r_{12}^2 + r_{02}^2}}$ . The unit cell  $U(v_1, v_2)$  has the area

$$\begin{aligned} A(\Lambda) &= |v_1| \cdot |v_2| \sin \alpha = |v_1| \cdot |v_2| \sqrt{1 - \cos^2 \alpha} = \sqrt{|v_1|^2 |v_2|^2 - (v_1 \cdot v_2)^2} = \\ &= \sqrt{(r_{12}^2 + r_{01}^2)(r_{12}^2 + r_{02}^2) - r_{12}^4} = \sqrt{r_{12}^2 r_{01}^2 + r_{12}^2 r_{02}^2 + r_{01}^2 r_{02}^2}. \end{aligned}$$

Up to rigid motion, the length  $|v_1|$  is enough to fix the vector  $v_1$  along the positive  $x$ -axis. The length  $|v_2|$  and  $\cos \angle(v_1, v_2)$  determine the position of  $v_2$  relative to the fixed vector  $v_1$  up to reflection in the  $x$ -axis. Up to isometry or if  $\text{sign}(\Lambda) = 0$  (when  $\Lambda$  is mirror-symmetric), the above options for  $v_2$  are not important. If  $\text{sign}(\Lambda) = +1$ , then we choose  $v_2$  in the upper half-plane above the  $x$ -axis so that  $\angle(v_1, v_2) \in (90^\circ, 180^\circ)$ , otherwise we put  $v_2$  into the lower half-plane.

Finally,  $v_0 = -v_1 - v_2$  and the reconstructed ordered obtuse superbase  $B = \{v_0, v_1, v_2\}$  is unique up to isometry and up to rigid motion by Theorem 3.7.  $\square$

**Theorem 4.2 (isometric 2D lattices  $\leftrightarrow$  root invariants)** *Any lattices  $\Lambda, \Lambda' \subset \mathbb{R}^2$  are isometric if and only if their root invariants coincide:  $\text{RI}(\Lambda) = \text{RI}(\Lambda')$ . Any lattices  $\Lambda, \Lambda'$  are related by rigid motion if and only if  $\text{RI}^\circ(\Lambda) = \text{RI}^\circ(\Lambda')$ .  $\blacktriangle$*

*Proof* The part *only if* ( $\Rightarrow$ ) follows from Lemma 3.8(a) saying that  $\text{RI}(\Lambda)$ ,  $\text{RI}^\circ(\Lambda)$  are invariant under isometry and rigid motion, respectively. The part *if* ( $\Leftarrow$ ) follows from Lemma 4.1 reconstructing a superbase from  $\text{RI}(\Lambda)$  or  $\text{RI}^\circ(\Lambda)$ .  $\square$

The above classification helps prove that some other isometry invariants of lattices are also complete and continuous. By (2.7ab) the voform  $\text{VF} = (v_0^2, v_1^2, v_2^2)$  and coform  $\text{CF} = (p_{12}, p_{01}, p_{02})$  are both complete if considered up to  $3!$  permutations. The root invariant  $\text{RI}$  is a uniquely ordered version of  $\text{CF}$  and deserves its own name. The square roots  $r_{ij} = \sqrt{p_{ij}}$  have original units of vector coordinates.

The oriented part of Theorem 4.2 didn't appear in the past to the best of our knowledge. Conway and Sloane studied 2D lattices in [13, section 6] only up to general isometry including reflections. Here is the closest formal claim from [13].

**Lemma 4.3 ([13, Theorem 7])** *For any obtuse superbase  $(v_0, v_1, v_2)$  of a lattice  $A \subset \mathbb{R}^2$ , the vonorms  $v_0^2, v_1^2, v_2^2$  are squared lengths of shortest Voronoi vectors.  $\blacktriangle$*

Theorem 4.2 and Lemma 4.3 imply that, after taking square roots of vonorms, the ordered lengths, say  $|v_1| \leq |v_2| \leq |v_0|$ , form a complete invariant that should satisfy the triangle inequality  $|v_1| + |v_2| \geq |v_0|$ . This inequality is the only disadvantage of the complete invariant  $|v_1| \leq |v_2| \leq |v_0|$  in comparison with ordered root products  $r_{12} \leq r_{01} \leq r_{02}$ , which are easier to visualise in Fig. 12, 13.

Classification Theorem 4.2 says that all isometry classes of lattices  $A \subset \mathbb{R}^2$  are in a 1-1 correspondence with all ordered triples  $0 \leq r_{12} \leq r_{01} \leq r_{02}$  of root products in  $\text{RI}(A)$ . Only the smallest root product  $r_{12}$  can be zero, two others  $r_{01} \leq r_{02}$  should be positive, otherwise  $v_1^2 = r_{12}^2 + r_{01}^2 = 0$  by formulae (2.7a).

We explicitly describe the set of all possible root invariants, which will be later converted into metric spaces with continuous metrics in Definitions 5.1 and 5.4.

**Definition 4.4 (triangular cone TC)** *All root invariants  $\text{RI}(A) = (r_{12}, r_{01}, r_{02})$  of lattices  $A \subset \mathbb{R}^2$  live in the triangular cone  $\text{TC} = \{0 \leq r_{12} \leq r_{01} \leq r_{02}\}$  within the octant  $\text{Oct} = [0, +\infty)^3$  excluding the axes in the coordinates  $r_{12}, r_{01}, r_{02}$ , see Fig. 12 (left). The boundary  $\partial(\text{TC})$  of the cone  $\text{TC}$  consists of root invariants of all mirror-symmetric lattices from Lemma 3.3: the bisector planes  $\{r_{01} = r_{02}\}$  and  $\{r_{12} = r_{01}\}$  within  $\text{TC}$ . The orange line  $\{0 < r_{12} = r_{01} = r_{02}\} \subset \partial(\text{TC})$  in Fig. 12 (left) consists of root invariants of hexagonal lattices with a minimum inter-point distance  $r_{12}\sqrt{2}$ . The blue line  $\{r_{12} = 0 < r_{01} = r_{02}\} \subset \partial(\text{TC})$  consists of root invariants of square lattices with a minimum inter-point distance  $r_{01}$ .  $\blacksquare$*

To classify lattices up to similarity, it is convenient to scale them by the size  $\sigma(A) = r_{12} + r_{01} + r_{02}$ . This sum is a simpler uniform measure of size than (say) the unit cell area  $A(A)$  from Lemma 4.1, which can be small even for long cells.

**Definition 4.5 (projected invariants  $\text{PI}(A)$  and  $\text{PI}^\circ(A)$ )** *The triangular projection  $\text{TP} : \text{TC} \rightarrow \{r_{12} + r_{01} + r_{02} = 1\}$  divides each coordinate by the size  $\sigma(A) = r_{12} + r_{01} + r_{02}$  and gives  $\overline{\text{RI}}(A) = (\bar{r}_{12}, \bar{r}_{01}, \bar{r}_{02}) = \frac{(r_{12}, r_{01}, r_{02})}{r_{12} + r_{01} + r_{02}}$  in  $\text{TC} \cap \{r_{12} + r_{01} + r_{02} = 1\}$ . Then we map  $(\bar{r}_{12}, \bar{r}_{01}, \bar{r}_{02})$  to the projected invariant  $\text{PI}(A) = (x, y)$  with  $x = \bar{r}_{02} - \bar{r}_{01} \in [0, 1)$  and  $y = 3\bar{r}_{12} \in [0, 1]$  in the quotient triangle  $\text{QT} = \{(x, y) \in \mathbb{R}^2 \mid 0 \leq x < 1, 0 \leq y \leq 1, x + y \leq 1\}$ , see Fig. 13.*

*All oriented root invariants  $\text{RI}^\circ(A)$  live in the doubled cone  $\text{DC}$  that is the union of two triangular cones  $\text{TC}^\pm$ , where we identify any two boundary points representing the same root invariant  $\text{RI}(A)$  with  $\text{sign}(A) = 0$ . The oriented projected invariant  $\text{PI}^\circ(A) = (x, y)^\pm$  is  $\text{PI}(A)$  with the superscript from  $\text{sign}(A)$ .  $\blacksquare$*

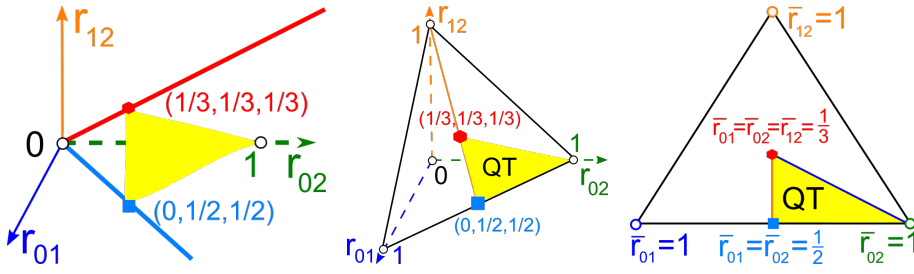


**Fig. 12** **Left:** the triangular cone  $TC = \{(r_{12}, r_{01}, r_{02}) \in \mathbb{R}^3 \mid 0 \leq r_{12} \leq r_{01} \leq r_{02} \neq 0\}$  represents the space RIS of all root invariants of 2D lattices, see Definition 4.4. **Middle:** TC projects to the quotient triangle  $QT = TC \cap \{r_{12} + r_{01} + r_{02} = 1\}$  representing the space LSS of 2D lattices up to similarity, see Corollary 4.6. **Right:** the quotient triangle QT can be parameterised by  $x = \bar{r}_{02} - \bar{r}_{01} \in [0, 1]$  and  $y = 3\bar{r}_{12} \in [0, 1]$ , see QT also in Fig. 13.

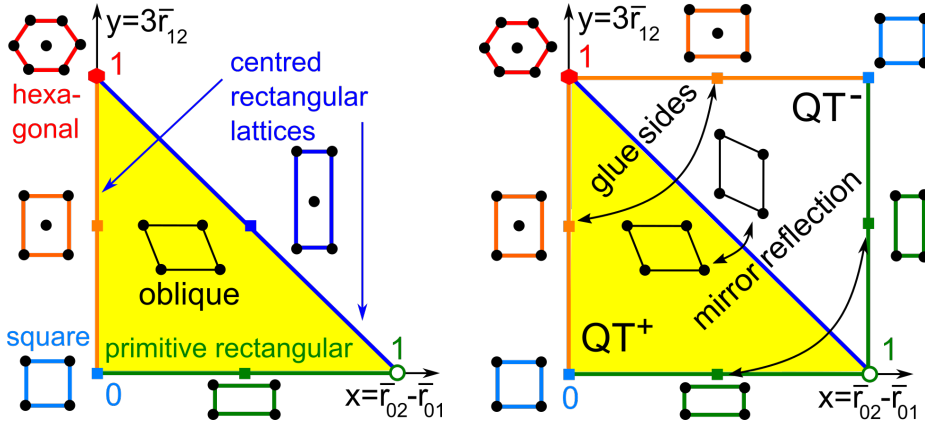


**Fig. 13** **Left:** all projected invariants  $PI(A)$  of lattices  $A \subset \mathbb{R}^2$  live in the quotient triangle QT from Fig. 12, which is parameterised by  $x = \bar{r}_{02} - \bar{r}_{01} \in [0, 1]$  and  $y = 3\bar{r}_{12} \in [0, 1]$ . **Right:** mirror reflections  $A^\pm$  of any non-mirror-symmetric lattice can be represented by a pair of points in the quotient square  $QS = QT^+ \cup QT^-$  symmetric in the diagonal  $x + y = 1$ .

The inequality  $1 \geq x + y = (\bar{r}_{02} - \bar{r}_{01}) + 3\bar{r}_{12}$  follows after multiplying both sides by the size  $\sigma(A)$ , because  $r_{12} + r_{01} + r_{02} \geq (r_{02} - r_{01}) + 3r_{12}$  becomes  $r_{01} \geq r_{12}$ .

The set of oriented projected invariants  $PI^\circ$  is visualised in Fig. 13 (right) as the *quotient square* QS obtained by gluing the quotient triangle  $QT^+$  with its mirror image  $QT^-$ . The boundaries of both triangles excluding the vertex  $(x, y) = (1, 0)$  are glued by the diagonal reflection  $(x, y) \leftrightarrow (1 - y, 1 - x)$ . Any pair of points  $(x, y) \in QT^+$  and  $(1 - y, 1 - x) \in QT^-$  in Fig. 13 (right) represent mirror bright2021proof of a lattice up to similarity, see Corollary 4.6. So QS is a topological sphere without a single point and will be parameterised by geographic-style coordinates in [11].

Following Fig. 6, any square lattice has a root invariant  $RI = (0, a, a)$ , so its projected invariant  $PI = (0, 0)$  is at the bottom left vertex of QT in Fig. 13 (left), identified with top right vertex of QS in Fig. 13 (right). Any hexagonal lattice has a root invariant  $RI = (a, a, a)$ , so its projected invariant  $PI = (0, 1)$  is at the top left vertex of QT in Fig. 13 (left), identified with bottom right vertex of QS.

By Example 3.2(a) any rectangular lattice has  $\text{RI} = (0, a, b)$  for  $a < b$ , hence its projected invariant  $\text{PI} = (\frac{b-a}{a+b}, 0)$  belongs to the bottom edge of QT identified with the top edge of QS. By Example 3.2(b) any lattice with a mirror-symmetric Voronoi domain has RI with 0 or two equal root products. Such lattices have a rhombic unit cell and form the centred rectangular Bravais class. Their projected invariants belong to the vertical edges and diagonal of QS in Fig. 13 (right). The companion paper [11] discusses Bravais classes of 2-dimensional lattices in detail.

In the theory of complex functions, any lattice  $\Lambda \subset \mathbb{R}^2$  can be considered as a subgroup of the complex plane  $\mathbb{C}$  whose quotient  $\mathbb{C}/\Lambda$  is a torus. By the Riemann mapping theorem any compact Riemann surface of genus 1 is conformally equivalent (holomorphically homeomorphic) to the quotient  $\mathbb{C}/\Lambda$  for some lattice  $\Lambda$ , see [21, Section 5.3]. Such tori  $\mathbb{C}/\Lambda$  and  $\mathbb{C}/\Lambda'$  are *conformally equivalent* if and only if  $\Lambda, \Lambda'$  are similar, see [20, Theorem 6.1.4]. The spaces  $\text{LSS}(\mathbb{R}^2)$  and  $\text{LSS}^\circ(\mathbb{R}^2)$  of all lattices  $\Lambda \subset \mathbb{C} = \mathbb{R}^2$  up to similarity and orientation-preserving similarity are the quotient triangle QT and square QS, respectively, see Fig. 13.

**Corollary 4.6 (similar lattices  $\leftrightarrow$  projected invariants PI)** *Lattices  $\Lambda, \Lambda' \subset \mathbb{R}^2$  are similar (related by an isometry composed with a uniform scaling) if and only if their projected invariants are equal:  $\text{PI}(\Lambda) = \text{PI}(\Lambda')$ . The lattices  $\Lambda, \Lambda'$  are related by an orientation-preserving similarity if and only if  $\text{PI}^\circ(\Lambda) = \text{PI}^\circ(\Lambda')$ .  $\blacktriangle$*

*Proof* follows from Theorem 4.2 because a uniform scaling of all basis vectors  $v_i \mapsto sv_i$  by a factor  $s > 0$  multiplies all root products  $r_{ij} = \sqrt{-v_i \cdot v_j}$  by  $s$ , which is neutralised by the triangular projection TP from Definition 4.4.  $\square$

**Lemma 4.7 (criteria of mirror-symmetric lattices in  $\mathbb{R}^2$ )** *A lattice  $\Lambda$  in  $\mathbb{R}^2$  is mirror-symmetric if and only if one of the following equivalent conditions holds:  $\text{sign}(\Lambda) = 0$  or  $\text{RI}(\Lambda) \in \partial\text{TC}$  or  $\text{PI}(\Lambda) \in \partial\text{QT}$ . So the boundaries of the triangular cone TC and the quotient triangle QT consist of root invariants and projected invariants, respectively, of all mirror-symmetric lattices  $\Lambda \subset \mathbb{R}^2$ .  $\blacktriangle$*

*Proof* By Lemma 3.8 a lattice  $\Lambda$  is mirror-symmetric if and only if  $\text{sign}(\Lambda) = 0$ . By Lemma 3.3 any mirror-symmetric lattice  $\Lambda$  has  $\text{RI}(\Lambda)$  with 0 (rectangular lattice) or with two equal root products (centred rectangular lattices). The last conditions on RI define the boundary  $\partial\text{TC}$  of the triangular cone in Fig. 12 or, equivalently, the projected invariant  $\text{PI}(\Lambda)$  belongs to the boundary of QT in Fig. 13 (left).  $\square$

**Remark 4.8 (lattices via group actions)** *Another parameterisation of the Lattice Similarity Space  $\text{LSS}(\mathbb{R}^2)$  can be obtained from a fundamental domain of the action of  $\text{GL}(\mathbb{Z}^2) \times \mathbb{R}_+^\times$  on the cone  $\mathcal{C}_+(\mathcal{Q}_2)$  of positive quadratic forms. Recall that any lattice  $\Lambda \subset \mathbb{R}^2$  with a basis  $v_1, v_2$  defines the positive quadratic form*

$$Q_\Lambda(x, y) = (xv_1 + yv_2)^2 = v_1^2x^2 + 2v_1v_2xy + v_2^2y^2 = q_{11}x^2 + 2q_{12}xy + q_{22}y^2 \geq 0$$

*whose positivity for all  $(x, y) \in \mathbb{R}^2 - 0$  means that  $q_{12}^2 < q_{11}q_{22}$ . The cone  $\mathcal{C}_+(\mathcal{Q}_2)$  of all positive quadratic forms projects to the unit disk  $\xi^2 + \eta^2 < 1$  parameterised by  $\xi = \frac{q_{22} - q_{11}}{q_{11} + q_{22}}$  and  $\eta = \frac{-2q_{12}}{q_{11} + q_{22}}$ . Indeed, the positivity condition  $q_{12}^2 < q_{11}q_{22}$  for the form  $Q_\Lambda(x, y)$  is equivalent to  $\xi^2 + \eta^2 < 1$  in the coordinates above.*

*$Q_\Lambda$  has a reduced (non-acute) form if  $0 \leq -2q_{12} \leq q_{11} \leq q_{22}$  and  $q_{11} > 0$ , see [18, formula (1.130) on p. 75]. The above conditions define the fundamental*

domain  $T = \{0 \leq \xi < 1, 0 \leq \eta \leq \frac{1}{2}, \xi + 2\eta \leq 1\}$ , see [42, Fig. 8.1]. This non-isosceles triangle is one of the infinitely many triangular domains within the disk  $\xi^2 + \eta^2 < 1$  in [18, Fig. 1.2 on p. 82] or [42, Fig. 6.2]. Choosing one triangular domain is equivalent to choosing a reduced basis up to isometry, not up to rigid motion. For instance, the mirror-symmetric bases  $v_1 = (1, 0)$ ,  $v_2^\pm = (-\frac{1}{2}, \pm 1)$  have the same reduced non-acute form  $x^2 - xy + \frac{5}{4}y^2$  represented only by  $(\xi, \eta) = (\frac{1}{9}, \frac{4}{9})$ . The above ambiguity up to rigid motion is resolved by  $\text{sign}(\Lambda)$  in the twice larger space  $\text{LSS}^\circ(\mathbb{R}^2)$  visualised as the quotient square QS, see Example 7.6.

More importantly, the inverse map from  $\text{RI}^\circ(\Lambda)$  to a reduced basis is discontinuous at any rectangular lattice  $\Lambda$  with a unit cell  $a \times b$ . Indeed, slight perturbations of  $\Lambda$  have unique reduced bases that are not close to each other, being close to the distant bases  $(a, 0)$ ,  $(0, \pm b)$ , which are not equivalent up to rigid motion for  $a < b$ . This discontinuity of lattice bases will emerge in  $\mathbb{R}^3$  even up to isometry [22]. In  $\mathbb{R}^2$ , Corollary 7.9 will completely settle the basis discontinuity up to rigid motion.

Another complete invariant is the ordered voform  $v_1^2 \leq v_2^2 \leq v_0^2$  or the lengths  $|v_1| \leq |v_2| \leq |v_0|$  of the three shortest Voronoi vectors from Lemma 4.3. However, this invariant doesn't extend even to dimension  $n = 3$  due to a 6-parameter family of pairs of non-isometric lattices  $\Lambda_1 \not\cong \Lambda_2$  that have the same lengths of seven shortest Voronoi vectors in  $\mathbb{R}^3$ , see [22]. The above reasons justify the choice of homogeneous coordinates  $r_{ij}$ , which easily extend to higher dimensions. ■

The projected invariant  $\text{PI} = (x, y)$  obtained from  $\text{RI}$  is preferable to the coordinates  $(\xi, \eta)$ , which define a non-isosceles triangle, while the isosceles quotient triangle QT will lead to easier formulae for metrics in the next section. Since the metric tensor  $(v_1^2, v_1 \cdot v_2, v_2^2) = (q_{11}, q_{12}, q_{22})$  and its 3-dimensional analogue are more familiar to crystallographers, we will rephrase key results from sections 5-6 by using these non-homogeneous coordinates in the companion paper [11].

**Proposition 4.9 (inverse design of 2D lattices)** *For  $\sigma > 0$  and any point  $(x, y)$  in the quotient triangle QT, there is a unique (up to isometry) lattice  $\Lambda$  with the projected invariant  $\text{PI}(\Lambda) = (x, y)$  and size  $\sigma = r_{12} + r_{01} + r_{02}$ . Then*

$$(4.9a) \quad \text{RI}(\Lambda) = (r_{12}, r_{01}, r_{02}) = \left( \frac{\sigma}{3}y, \frac{\sigma}{6}(3 - 3x - y), \frac{\sigma}{6}(3 + 3x - y) \right).$$

If  $(x, y)$  is in the interior of QT, the invariant  $\text{RI}$  defines a pair of lattices  $\Lambda^\pm$  that have opposite signs and unique (up to isometry) reduced basis vectors  $v_1, v_2$  with the lengths  $|v_1| = \sqrt{r_{12}^2 + r_{01}^2}$ ,  $|v_2| = \sqrt{r_{12}^2 + r_{02}^2}$  and the anticlockwise angle

$$(4.9b) \quad \angle(v_1, v_2) = \arccos \frac{-4y^2}{\sqrt{(9x^2 + 5y^2 - 6y + 9)^2 - 36x^2(3 - y)^2}}. \quad \blacktriangle$$

*Proof* In Definition 4.5 the projected invariant  $\text{PI}(\Lambda) = (x, y)$  is obtained from the

$$\text{coordinates } (\bar{r}_{12}, \bar{r}_{01}, \bar{r}_{02}) \text{ of } \overline{\text{RI}}(\Lambda) \text{ satisfying the equations } \begin{cases} x = \bar{r}_{02} - \bar{r}_{01}, \\ y = 3\bar{r}_{12}, \\ \bar{r}_{12} + \bar{r}_{01} + \bar{r}_{02} = 1. \end{cases}$$

The solution is  $\overline{\text{RI}}(\Lambda) = (\bar{r}_{12}, \bar{r}_{01}, \bar{r}_{02}) = (\frac{y}{3}, \frac{1}{2} - \frac{x}{2} - \frac{y}{6}, \frac{1}{2} + \frac{x}{2} - \frac{y}{6})$ . Multiplying all coordinates by the size  $\sigma = r_{12} + r_{01} + r_{02}$  gives the root invariant in (4.9a).

By Proposition 3.10 a (unique up to isometry) reduced basis  $v_1, v_2$  consist of two shortest vectors of an obtuse superbase. Lemma 4.1 implies the formulae for  $|v_1|, |v_2|$ . The angle formula from Lemma 4.1 can be expressed in  $x, y$  as follows:

$$\begin{aligned} \cos \angle(v_1, v_2) &= \frac{-r_{12}^2}{|v_1| \cdot |v_2|} = \frac{-y^2/9}{\frac{1}{6}\sqrt{(2y)^2 + (3-3x-y)^2} \frac{1}{6}\sqrt{(2y)^2 + (3+3x-y)^2}} = \\ &= \frac{-4y^2}{\sqrt{4y^2 + (3-y)^2 + 9x^2 + 6x(3-y)} \sqrt{4y^2 + (3-y)^2 + 9x^2 - 6x(3-y)}} = \\ &= \frac{-4y^2}{\sqrt{(9x^2 + 5y^2 - 6y + 9) + 6x(3-y)} \sqrt{(9x^2 + 5y^2 - 6y + 9) - 6x(3-y)}}. \quad \square \end{aligned}$$

Example 4.10 shows the power of Proposition 4.9 based on Theorem 4.2 and Corollary 4.6 for inverse design by sampling the square QS at interesting places.

Fig. 14 (right) visualises the doubled cone DC of oriented root invariants  $\text{RI}^\circ$  from Definition 3.4 by uniting the triangular cone  $\text{TC} = \{0 \leq r_{12} \leq r_{01} \leq r_{02}\}$  with its mirror reflection in the vertical plane  $\{r_{01} = r_{02}\}$  including the  $r_{12}$ -axis.

The lattice  $\Lambda_0$  with  $\text{RI} = (1, 1, 4)$  is represented by two boundary points of DC identified by  $(r_{01}, r_{02}) \leftrightarrow (r_{02}, r_{01})$ . The lattices  $\Lambda_\infty^\pm$  with the root invariant  $\text{RI} = (r_{12}, r_{01}, r_{02}) = (1, 4, 7)$  are represented by  $(1, 4, 7)$  and its mirror image  $(1, 7, 4)$  in DC related by the reflection in the vertical bisector plane  $r_{01} = r_{02}$  containing the root invariants of  $\Lambda_4, \Lambda_6$ . The superscript shows  $\text{sign}(\Lambda_\infty^\pm) = \pm 1$ .

**Example 4.10 (inverse design of 2D lattices)** *We will inversely design the lattices  $\Lambda_4, \Lambda_6, \Lambda_0, \Lambda_2^\pm, \Lambda_\infty^\pm$ , see their visualised invariants in Fig. 14 (right).*

**( $\Lambda_4$ )** *We design the square lattice  $\Lambda_4$  starting from its projected invariant at the origin  $\text{PI}(\Lambda_4) = (0, 0) \in \text{QT}$ , which is identified with the top right vertex  $(1, 1) \in \text{QS}$  in Fig. 14 (left). Formula (4.9a) for the size  $\sigma(\Lambda_4) = 2$  (only to get simplest integers) gives  $\text{RI}(\Lambda_4) = (0, 1, 1)$ . An obtuse superbase  $\{v_0, v_1, v_2\}$  can be reconstructed by Lemma 4.1. The vonorms are  $v_1^2 = v_2^2 = 0^2 + 1^2 = 1$ ,  $v_0^2 = 1^2 + 1^2 = 2$ . We can choose the standard obtuse superbase  $v_1 = (1, 0)$ ,  $v_2 = (0, 1)$ ,  $v_0 = (-1, -1)$ .*

**( $\Lambda_6$ )** *We design the hexagonal lattice  $\Lambda_6$  starting from the projected invariant at the top left vertex  $\text{PI}(\Lambda_6) = (0, 1) \in \text{QT}$ , which is identified with the bottom right vertex  $(1, 0) \in \text{QS}$  in Fig. 14 (left). Formula (4.9a) for the size  $\sigma(\Lambda_6) = 3$  (only to get simplest integers) gives  $\text{RI}(\Lambda_6) = (1, 1, 1)$ . To reconstruct an obtuse superbase  $\{v_0, v_1, v_2\}$  by Lemma 4.1, find the vonorms  $v_1^2 = v_2^2 = v_0^2 = 1^2 + 1^2 = 2$ . Formula (4.9b) gives the angle  $\angle(v_1, v_2) = \arccos \frac{-4}{\sqrt{(5-6+9)^2}} = \arccos(-\frac{1}{2}) = 120^\circ$ .*

*We can choose the superbase  $v_1 = (\sqrt{2}, 0)$ ,  $v_2 = (-\frac{1}{\sqrt{2}}, \frac{\sqrt{3}}{\sqrt{2}})$ ,  $v_0 = (-\frac{1}{\sqrt{2}}, -\frac{\sqrt{3}}{\sqrt{2}})$ .*

**( $\Lambda_0$ )** *We inversely design the lattice  $\Lambda_0$  in Fig. 14 starting from  $\text{PI}(\Lambda_0) = (x, y)$  at the centre  $(\frac{1}{2}, \frac{1}{2}) \in \text{QS}$ . Formula (4.9a) for the size  $\sigma(\Lambda_0) = 6$  (only to get simplest integers) gives  $\text{RI}(\Lambda_0) = (1, 1, 4)$ . To reconstruct an obtuse superbase  $\{v_0, v_1, v_2\}$  by Lemma 4.1, find the vonorms  $v_1^2 = 1^2 + 1^2 = 2$ ,  $v_2^2 = v_0^2 = 1^2 + 4^2 = 17$ .*

*Formula (4.9b) gives the angle  $\angle(v_1, v_2) = \arccos \frac{-4}{\sqrt{(\frac{9}{4} + \frac{5}{4} - 3 + 9)^2 - 9(\frac{5}{4})^2}} =$*



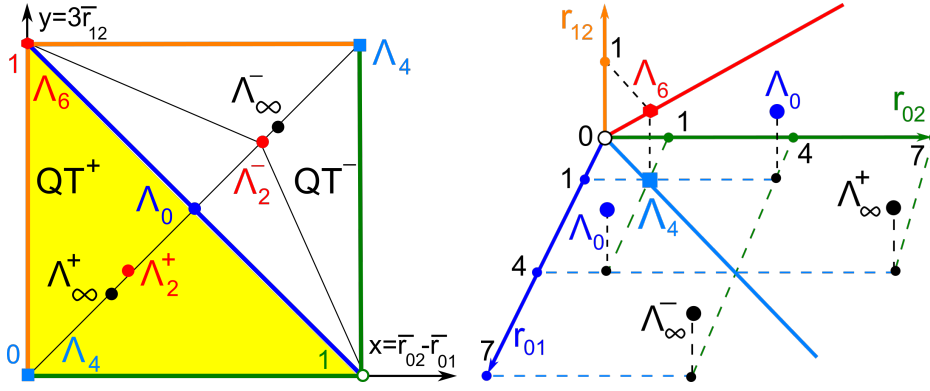


**Fig. 14** **Left:**  $QS = QT^+ \cup QT^-$  includes mirror-symmetric lattices  $\Lambda_4, \Lambda_6, \Lambda_0$  and non-mirror-symmetric lattices  $\Lambda_\infty^\pm$ , see Example 5.2 and Table 3 later. **Right:** the doubled cone DC is visualised as  $\{0 \leq r_{12} \leq \min\{r_{01}, r_{02}\} > 0\}$  bounded by the planes  $\{r_{12} = 0\}$ ,  $\{r_{12} = r_{01}\}$ ,  $\{r_{12} = r_{02}\}$  with the identifications  $(r_{12}, r_{01}, r_{02}) \leftrightarrow (r_{12}, r_{02}, r_{01})$  on the boundary  $\partial DC$ .

$\arccos(-\frac{1}{\sqrt{34}}) \approx 99.9^\circ$ . We can choose the following superbase, see Fig. 15:  $v_1 = (\sqrt{2}, 0)$ ,  $v_2 = |v_2|(\cos \angle(v_1, v_2), \sin \angle(v_1, v_2)) = (-\frac{1}{\sqrt{2}}, \frac{\sqrt{33}}{\sqrt{2}})$ ,  $v_0 = (-\frac{1}{\sqrt{2}}, -\frac{\sqrt{33}}{\sqrt{2}})$ .

( $\Lambda_2$ ) We inversely design the lattice  $\Lambda_2$  in Fig. 14 starting from their projected invariants  $PI(\Lambda_2) = (\frac{1}{2+\sqrt{2}}, \frac{1}{2+\sqrt{2}})$ , which will maximise the chiral distance  $PC[D_2]$  in Theorem 6.6(a). Formula (4.9a) for the size  $\sigma(\Lambda_2) = 6$  (only to simplify the root invariant) gives  $RI(\Lambda_2) = (2 - \sqrt{2}, 2\sqrt{2} - 1, 5 - \sqrt{2})$ . Since all root products are non-zero and distinct, by Lemma 3.3 there is a pair of lattices  $\Lambda_2^\pm$  with  $\text{sign}(\Lambda_2^\pm) = \pm 1$ . The lattices  $\Lambda_2^\pm$  are related by reflection, not by rigid motion.

To reconstruct an obtuse superbase  $\{v_0, v_1, v_2\}$  of  $\Lambda_2^\pm$  by Lemma 4.1, find  $v_0^2 = (2\sqrt{2} - 1)^2 + (5 - \sqrt{2})^2 = (9 - 4\sqrt{2}) + (27 - 10\sqrt{2}) = 36 - 14\sqrt{2} \approx 16.2$ ,  $v_1^2 = (2 - \sqrt{2})^2 + (2\sqrt{2} - 1)^2 = (6 - 4\sqrt{2}) + (9 - 4\sqrt{2}) = 15 - 8\sqrt{2} \approx 3.7$ ,  $v_2^2 = (2 - \sqrt{2})^2 + (5 - \sqrt{2})^2 = (6 - 4\sqrt{2}) + (27 - 10\sqrt{2}) = 33 - 14\sqrt{2} \approx 13.2$ , and the anticlockwise angle  $\angle(v_1, v_2) = \arccos \frac{-r_{12}^2}{|v_1| \cdot |v_2|} \approx 92.8^\circ$ . Then  $\Lambda_2^\pm$  have

the following obtuse superbases in Fig. 15:  $v_1 = (\sqrt{15 - 8\sqrt{2}}, 0) \approx (1.9, 0)$ ,  $v_2 = |v_2|(\cos \angle(v_1, v_2), \sin \angle(v_1, v_2)) \approx (-0.18, 3.63)$ ,  $v_0 \approx (-1.72, -3.63)$ .

( $\Lambda_\infty$ ) We inversely design the lattice  $\Lambda_\infty$  in Fig. 15 starting from  $PI(\Lambda_\infty) = (x, y)$  at the mid-point  $(\frac{1}{4}, \frac{1}{4})$  of the segment between  $PI(\Lambda_4), PI(\Lambda_0) \in QT$ . Formula (4.9a) for the size  $\sigma(\Lambda_\infty) = 12$  (only to simplify the root invariant) gives  $RI(\Lambda_\infty) = (1, 4, 7)$ . Since all root products are non-zero and distinct, by Lemma 3.3 there is a pair of lattices  $\Lambda_\infty^\pm$  of opposite signs  $\text{sign}(\Lambda_\infty^\pm) = \pm 1$ .

To reconstruct an obtuse superbase  $\{v_0, v_1, v_2\}$  of  $\Lambda_\infty^\pm$  by Lemma 4.1, find the vonorms  $v_0^2 = 4^2 + 7^2 = 65$ ,  $v_1^2 = 1^2 + 4^2 = 17$ ,  $v_2^2 = 1^2 + 7^2 = 50$ , and the anticlockwise angle  $\angle(v_1, v_2) = \arccos \frac{-r_{12}^2}{|v_1| \cdot |v_2|} = \arccos(-\frac{1}{\sqrt{850}}) \approx 92^\circ$ . Then  $\Lambda_\infty^\pm$  have the following obtuse superbases in Fig. 15:  $v_1 = (\sqrt{17}, 0) \approx (4.12, 0)$ ,

$$v_2^\pm = |v_2|(\cos \angle(v_1, v_2), \sin \angle(v_1, v_2)) = \left(-\frac{1}{\sqrt{17}}, \pm \frac{\sqrt{849}}{\sqrt{17}}\right) \approx (-0.24, \pm 7.1),$$

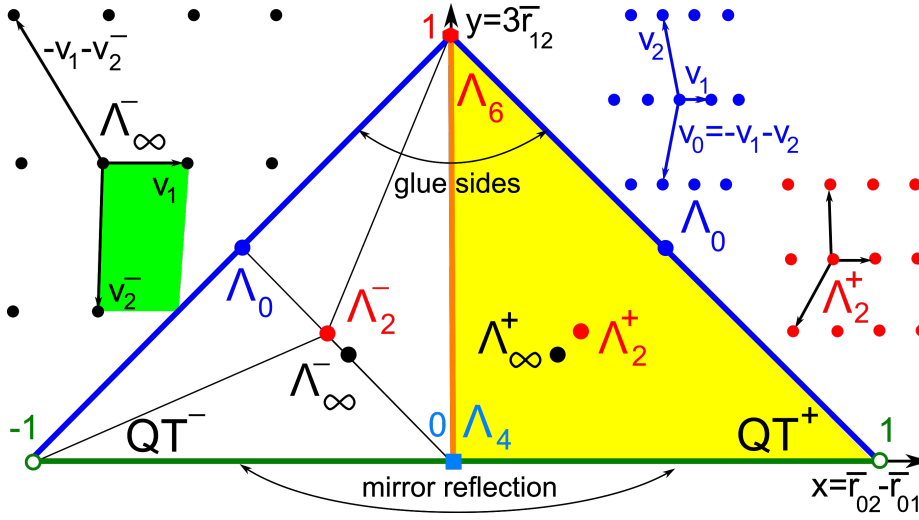


**Fig. 15** The doubled cone DC in Fig. 14 (right) projects to the doubled triangle DT parameterised by  $x \in (-1, 1)$ ,  $y \in [0, 1]$  and obtained by gluing two copies  $QT^\pm$  of the quotient triangle along vertical sides instead of hypotenuses as in QS, see Example 4.10 and Table 3.

$$v_0^\pm = -v_1 - v_2^\pm = \left(-\frac{16}{\sqrt{17}}, \mp \frac{\sqrt{849}}{\sqrt{17}}\right) \approx (-3.88, \mp 7.1), \text{ see all forms in Table 3. } \blacksquare$$

**Table 3** Various invariants of the lattices computed in Example 4.10, see Fig. 14 and 15.

$A$	$A_4$	$A_6$	$A_0$	$A_2^\pm$	$A_\infty^\pm$
$\sigma(A)$	2	3	6	6	12
$PI(A)$	(0, 0)	(0, 1)	$\left(\frac{1}{2}, \frac{1}{2}\right)$	$\left(\frac{1}{2+\sqrt{2}}, \frac{1}{2+\sqrt{2}}\right)$	$\left(\frac{1}{4}, \frac{1}{4}\right)$
$RI^o(A)$	(0, 1, 1)	(1, 1, 1)	(1, 1, 4)	$(2 - \sqrt{2}, 2\sqrt{2} - 1, 5 - \sqrt{2})^\pm$	$(1, 4, 7)^\pm$
$VF(A)$	(2, 1, 1)	(2, 2, 2)	(17, 2, 17)	$(15 - 8\sqrt{2}, 33 - 14\sqrt{2}, 36 - 14\sqrt{2})$	(65, 17, 50)

## 5 Metrics on spaces of lattices up to isometry, rigid motion, similarity

All lattices  $A \subset \mathbb{R}^2$  are uniquely represented up to isometry and similarity by their invariants  $RI \in TC$  and  $PI \in QT$ , respectively. Then any metric  $d$  on the triangular cone  $TC \subset \mathbb{R}^3$  or the quotient triangle  $QT \subset \mathbb{R}^2$  gives rise to a metric in Definition 5.1 on the spaces LIS and LSS, respectively. The oriented case in Definition 5.4 will be harder because of identifications on the boundary  $\partial TC$ .

**Definition 5.1 (root metrics RM, projected metrics PM)** Any metric  $d$  on  $\mathbb{R}^3$  defines the root metric  $RM(A_1, A_2) = d(RI(A_1), RI(A_2))$  on lattices  $A_1, A_2 \subset \mathbb{R}^2$  up to isometry. The Root Invariant Space  $RIS = (TC, d)$  is the triangular cone

with a fixed metric  $d$ . If we use the Minkowski norm  $M_q(v) = \|v\|_q = (\sum_{i=1}^n |x_i|^q)^{1/q}$  of a vector  $v = (x_1, \dots, x_n) \in \mathbb{R}^n$  for any real  $q \in [1, +\infty]$ , the root metric is denoted by  $\text{RM}_q(\Lambda_1, \Lambda_2) = \|\text{RI}(\Lambda_1) - \text{RI}(\Lambda_2)\|_q$ . The limit case  $q = +\infty$  uses  $\|v\|_\infty = \max_{i=1, \dots, n} |x_i|$ . The projected metric  $\text{PM}(\Lambda_1, \Lambda_2) = d(\text{PI}(\Lambda_1), \text{PI}(\Lambda_2))$  is on lattices up to similarity for any metric  $d$  on  $\mathbb{R}^2$ . The space of projected invariants  $\text{PIN} = (\text{QT}, d)$  is the quotient triangle with a metric  $d$ . The notation  $\text{PM}_q(\Lambda_1, \Lambda_2) = \|\text{PI}(\Lambda_1) - \text{PI}(\Lambda_2)\|_q$  includes a parameter  $q \in [1, +\infty]$  of  $M_q$ . ■

The Minkowski distance  $M_q$  for  $q = 2$  is Euclidean. The root metric  $\text{RM}_q$  can take any large values in original units of vector coordinates such as Angstroms. The projected metric  $\text{PM}_q$  is unitless and the space  $\text{PIN} = (\text{QT}, d)$  is bounded.

**Table 4** Metrics  $\text{RM}_q$  and  $\text{PM}_q$  for the lattices from Example 5.2 and shown Fig. 14 and 15.

$\text{RM}_\infty$	$\Lambda_4$	$\Lambda_6$	$\Lambda_0$	$\Lambda_\infty^\pm$	$\text{PM}_\infty$	$\Lambda_4$	$\Lambda_6$	$\Lambda_0$	$\Lambda_\infty^\pm$
$\text{RI}(\Lambda_4) = (0, 1, 1)$	0	1	3	6	$\text{PI}(\Lambda_4) = (0, 0)$	0	1	$\frac{1}{2}$	$\frac{1}{4}$
$\text{RI}(\Lambda_6) = (1, 1, 1)$	1	0	3	6	$\text{PI}(\Lambda_6) = (0, 1)$	1	0	$\frac{1}{2}$	$\frac{3}{4}$
$\text{RI}(\Lambda_0) = (1, 1, 4)$	3	3	0	3	$\text{PI}(\Lambda_0) = (\frac{1}{2}, \frac{1}{2})$	$\frac{1}{2}$	$\frac{1}{2}$	0	$\frac{1}{4}$
$\text{RI}(\Lambda_\infty^\pm) = (1, 4, 7)$	6	6	3	0	$\text{PI}(\Lambda_\infty^\pm) = (\frac{1}{4}, \frac{1}{4})$	$\frac{1}{4}$	$\frac{3}{4}$	$\frac{1}{4}$	0

$\text{RM}_q$ for $q \in [1, +\infty)$	$\Lambda_4$	$\Lambda_6$	$\Lambda_0$	$\Lambda_\infty^\pm$
$\text{RI}(\Lambda_4) = (0, 1, 1)$	0	1	$(1 + 3^q)^{1/q}$	$(1 + 3^q + 6^q)^{1/q}$
$\text{RI}(\Lambda_6) = (1, 1, 1)$	1	0	3	$(3^q + 6^q)^{1/q}$
$\text{RI}(\Lambda_0) = (1, 1, 4)$	$(1 + 3^q)^{1/q}$	3	0	$3 \cdot 2^{1/q}$
$\text{RI}(\Lambda_\infty^\pm) = (1, 4, 7)$	$(1 + 3^q + 6^q)^{1/q}$	$(3^q + 6^q)^{1/q}$	$3 \cdot 2^{1/q}$	0

$\text{PM}_q$ for $q \in [1, +\infty)$	$\Lambda_4$	$\Lambda_6$	$\Lambda_0$	$\Lambda_\infty^\pm$
$\text{PI}(\Lambda_4) = (0, 0)$	0	1	$2^{(1/q)-1}$	$2^{(1/q)-2}$
$\text{PI}(\Lambda_6) = (0, 1)$	1	0	$2^{(1/q)-1}$	$\frac{1}{4}(1 + 3^q)^{1/q}$
$\text{PI}(\Lambda_0) = (\frac{1}{2}, \frac{1}{2})$	$2^{(1/q)-1}$	$2^{(1/q)-1}$	0	$2^{(1/q)-2}$
$\text{PI}(\Lambda_\infty^\pm) = (\frac{1}{4}, \frac{1}{4})$	$2^{(1/q)-2}$	$\frac{1}{4}(1 + 3^q)^{1/q}$	$2^{(1/q)-2}$	0

**Example 5.2 (metrics  $\text{RM}_q, \text{PM}_q$ )** Table 4 summarises metric computations for the lattices  $\Lambda_4, \Lambda_6, \Lambda_0, \Lambda_\infty^\pm$ , which were inversely designed in Example 4.10. ■

**Lemma 5.3 (metric axioms for  $\text{RM}, \text{PM}$ )** (a) Any metrics  $\text{RM}$  and  $\text{PM}$  from Definition 5.1 satisfy all metric axioms in (1.1c) on the Lattice Isometry Space  $\text{LIS}(\mathbb{R}^2)$  and the Lattice Similarity Space  $\text{LSS}(\mathbb{R}^2)$ , respectively. ▲

*Proof* The metric axioms for  $\text{RM}, \text{PM}$  from Definition 5.1 follow from the same axioms for an underlying metric  $d$ . Only the first axiom is non-trivial: by the first

axiom for  $d$  we know that  $\text{RM}(\Lambda_1, \Lambda_2) = d(\text{RI}(\Lambda_1), \text{RI}(\Lambda_2)) = 0$  if and only if  $\text{RI}(\Lambda_1) = \text{RI}(\Lambda_2)$ . Now Theorem 4.2 says that  $\text{RI}(\Lambda_1) = \text{RI}(\Lambda_2)$  is equivalent to  $\Lambda_1, \Lambda_2$  being isometric. Corollary 4.6 classifying lattices up to similarity by projected invariants similarly justifies the first axiom for  $\text{PM}(\Lambda_1, \Lambda_2)$ .  $\square$

Since the mirror bright2021proof  $\Lambda_\infty^\pm$  have the same root invariant  $\text{RI}(\Lambda_\infty^\pm) = (1, 4, 7)$ , for any lattice  $\Lambda$ , the distances  $\text{RM}(\Lambda, \Lambda_\infty^\pm)$  and  $\text{PM}(\Lambda, \Lambda_\infty^\pm)$  are independent of  $\text{sign}(\Lambda_\infty^\pm) = \pm 1$ . Any mirror bright2021proof  $\Lambda^\pm$  have  $\text{RM}(\Lambda^+, \Lambda^-) = 0 = \text{PM}(\Lambda^+, \Lambda^-)$  because  $\Lambda^\pm$  are isometric to each other. The metric  $\text{RM}$  from Definition 5.1 is well-defined only for lattices up to any isometry including reflections.

Definition 5.4 introduces the metric  $\text{RM}^\circ$  on lattices up to rigid motion so that  $\text{RM}^\circ(\Lambda^+, \Lambda^-) > 0$  on mirror bright2021proof of a non-mirror-symmetric lattice, see Fig. 16.

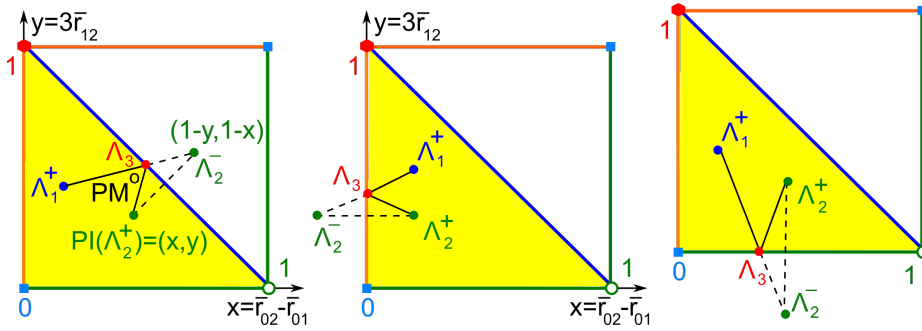


**Fig. 16** By Definition 5.4, the projected metric  $\text{PM}_2(\Lambda_1^+, \Lambda_2^-)$  is the minimum sum  $\text{PM}_2(\Lambda_1^+, \Lambda_3) + \text{PM}_2(\Lambda_3, \Lambda_2^-)$  achieved in the left image, see computations in Proposition 5.8.

**Definition 5.4 (orientation-aware metrics  $\text{RM}^\circ, \text{PM}^\circ$ )** For lattices  $\Lambda_1, \Lambda_2 \subset \mathbb{R}^2$  with  $\text{sign}(\Lambda_1)\text{sign}(\Lambda_2) \geq 0$ , the orientation-aware root metric is  $\text{RM}^\circ(\Lambda_1, \Lambda_2) = \text{RM}(\Lambda_1, \Lambda_2)$  as in Definition 5.1. If any lattices  $\Lambda_1, \Lambda_2$  have opposite signs, set  $\text{RM}^\circ(\Lambda_1, \Lambda_2) = \inf_{\text{sign}(\Lambda_3)=0} (\text{RM}(\Lambda_1, \Lambda_3) + \text{RM}(\Lambda_2, \Lambda_3))$ . The orientation-based metric  $\text{PM}^\circ(\Lambda_1, \Lambda_2)$  is defined by the same formula, where we replace  $\text{RM}$  by  $\text{PM}$ .  $\blacksquare$

The infimum in  $\text{RM}^\circ(\Lambda_1, \Lambda_2)$  is the greatest lower bound defining a metric on a union of metric spaces glued by isometries. Theoretically, this bound may not be achieved over a non-compact domain. When using a Minkowski base metric  $M_q$ , Propositions 5.8-5.9 explicitly compute  $\text{RM}_q^\circ, \text{PM}_q^\circ$  for  $q = 2, +\infty$ , so the infimum in Definition 5.4 can be replaced by a minimum in practice.

The oriented root invariant space  $\text{RIS}^\circ$  and the space of oriented projected invariants  $\text{PIN}^\circ$  can be defined similarly to  $\text{RIS}$  and  $\text{PIN}$  in Definition 5.1 as the doubled cone  $\text{DC}$  and quotient square  $\text{QS}$  with any metrics from Definition 5.4.

**Lemma 5.5 (metric axioms for  $\text{RM}^\circ, \text{PM}^\circ$ )** Any root metric  $\text{RM}^\circ$  and projected metric  $\text{PM}^\circ$  from Definition 5.4 satisfy all metric axioms in (1.1c) on the Lattice Isometry Space  $\text{LIS}^\circ$  and the Lattice Similarity Space  $\text{LSS}^\circ$ , respectively.  $\blacktriangle$

*Proof* Lemma 5.3 implies metric axioms in all cases when involved lattices have the same sign or sign 0. For example, the metrics  $\text{RM}^\circ, \text{PM}^\circ$  vanish only if the lattices  $\Lambda_1, \Lambda_2$  in question have equal invariants  $\text{RI}^\circ, \text{PI}^\circ$ , respectively, so  $\Lambda_1, \Lambda_2$  are isometric or similar by Theorem 4.2 or Corollary 4.6, respectively. The symmetry axiom for any lattices  $\Lambda, \Lambda'$  with opposite signs follows from the symmetry of the sum in Definition 5.4:  $\text{RM}^\circ(\Lambda_1, \Lambda_2) = \min_{\text{sign}(\Lambda_3)=0} (\text{RM}(\Lambda_1, \Lambda_3) + \text{RM}(\Lambda_2, \Lambda_3))$ .

Without loss of generality it suffices to prove the required triangle inequality  $\text{RM}^\circ(\Lambda_1, \Lambda_2) + \text{RM}^\circ(\Lambda_2, \Lambda_3) \geq \text{RM}^\circ(\Lambda_1, \Lambda_3)$  in the following two cases below.

*Case*  $\text{sign}(\Lambda_1) \geq 0$  and  $\text{sign}(\Lambda_2) \geq 0 > \text{sign}(\Lambda_3)$ . Then  $\text{RM}^\circ(\Lambda_1, \Lambda_2) = \text{RM}(\Lambda_1, \Lambda_2)$  is the root metric without minimisation from Definition 5.1. Let  $\Lambda'$  be some achiral lattice minimising  $\text{RM}^\circ(\Lambda_2, \Lambda_3) = \min_{\text{sign}(\Lambda')=0} (\text{RM}(\Lambda_2, \Lambda') + \text{RM}(\Lambda_3, \Lambda'))$ . Then

$$\begin{aligned} & \text{RM}^\circ(\Lambda_1, \Lambda_2) + \text{RM}^\circ(\Lambda_2, \Lambda_3) = \text{RM}(\Lambda_1, \Lambda_2) + \text{RM}(\Lambda_2, \Lambda') + \text{RM}(\Lambda_3, \Lambda') \geq \\ & \geq \text{RM}(\Lambda_1, \Lambda') + \text{RM}(\Lambda_3, \Lambda') \geq \min_{\text{sign}(\Lambda')=0} (\text{RM}(\Lambda_1, \Lambda') + \text{RM}(\Lambda_3, \Lambda')) = \text{RM}^\circ(\Lambda_1, \Lambda_3), \end{aligned}$$

where we used the triangle inequality for the root metric  $\text{RM}$  and  $\Lambda_1, \Lambda', \Lambda_2$ .

*Case*  $\text{sign}(\Lambda_1) \geq 0$  and  $\text{sign}(\Lambda_3) \geq 0 > \text{sign}(\Lambda_2)$ . Then  $\text{RM}^\circ(\Lambda_1, \Lambda_3) = \text{RM}(\Lambda_1, \Lambda_3)$  is the root metric without minimisation from Definition 5.1. Let  $\Lambda', \Lambda''$  be mirror-symmetric lattices minimising  $\text{RM}^\circ(\Lambda_1, \Lambda_2) = \min_{\text{sign}(\Lambda')=0} (\text{RM}(\Lambda_1, \Lambda') + \text{RM}(\Lambda_2, \Lambda'))$  and  $\text{RM}^\circ(\Lambda_2, \Lambda_3) = \min_{\text{sign}(\Lambda'')=0} (\text{RM}(\Lambda_2, \Lambda'') + \text{RM}(\Lambda_3, \Lambda''))$ , respectively. Then

$$\begin{aligned} & \text{RM}^\circ(\Lambda_1, \Lambda_2) + \text{RM}^\circ(\Lambda_2, \Lambda_3) = \text{RM}(\Lambda_1, \Lambda') + \text{RM}(\Lambda_2, \Lambda') + \text{RM}(\Lambda_2, \Lambda'') + \text{RM}(\Lambda_3, \Lambda'') \\ & \geq \text{RM}(\Lambda_1, \Lambda') + \text{RM}(\Lambda', \Lambda'') + \text{RM}(\Lambda_3, \Lambda'') \geq \text{RM}(\Lambda_1, \Lambda_3), \text{ where} \end{aligned}$$

we used the triangle inequality for  $\text{RM}$  and the lattices  $\Lambda_2, \Lambda', \Lambda''$  with non-positive signs, then for the lattices  $\Lambda_1, \Lambda', \Lambda'', \Lambda_3$ , which have only non-negative signs.  $\square$

Lemma 5.6 speeds up computations in the oriented case, see Example 6.8.

**Lemma 5.6 (reversed signs)** *If lattices  $\Lambda_1^\pm, \Lambda_2^\pm \subset \mathbb{R}^2$  have specified signs, then  $\text{RM}^\circ(\Lambda_1^+, \Lambda_2^-) = \text{RM}^\circ(\Lambda_1^-, \Lambda_2^+)$  and  $\text{PM}^\circ(\Lambda_1^+, \Lambda_2^-) = \text{PM}^\circ(\Lambda_1^-, \Lambda_2^+)$ .*  $\blacktriangle$

*Proof* By Definition 5.4, for any base distance  $d$  on  $\mathbb{R}^3$ , when minimising over mirror-symmetric lattices  $\Lambda_3$  with  $\text{sign}(\Lambda_3) = 0$ , the metrics  $\text{RM}^\circ$  are computed for lattices that have one zero sign and one non-zero sign. Hence  $\text{RM}^\circ(\Lambda_1^\pm, \Lambda_3)$  can be replaced by the simpler metric  $\text{RM}(\Lambda_1, \Lambda_3) = d(\text{RI}(\Lambda_1), \text{RI}(\Lambda_3))$  depending only on the unoriented root invariants  $\text{RI}(\Lambda_1)$  and  $\text{RI}(\Lambda_3)$  without a sign. After that the metric  $\text{RM}$  can be lifted back to the lattices  $\Lambda_1^-, \Lambda_3^+$  with reversed signs:

$$\begin{aligned} & \text{RM}^\circ(\Lambda_1^+, \Lambda_2^-) = \min_{\text{sign}(\Lambda_3)=0} (\text{RM}(\Lambda_1^+, \Lambda_3) + \text{RM}(\Lambda_2^-, \Lambda_3)) = \\ & = \min_{\text{sign}(\Lambda_3)=0} (d(\text{RI}(\Lambda_1), \text{RI}(\Lambda_3)) + d(\text{RI}(\Lambda_2), \text{RI}(\Lambda_3))) = \\ & = \min_{\text{sign}(\Lambda_3)=0} (\text{RM}(\Lambda_1^-, \Lambda_3) + \text{RM}(\Lambda_2^+, \Lambda_3)) = \text{RM}^\circ(\Lambda_1^-, \Lambda_2^+). \end{aligned}$$

The proof for the projected metric  $\text{PM}^\circ$  is similar to the above arguments.  $\square$

Lemma 5.7 will help compute  $\text{RM}_q^o, \text{PM}_q^o$  for  $q = 2, +\infty$  in Propositions 5.8, 5.9.

**Lemma 5.7 (maximum sum of moduli)** *For any real numbers  $a, b, c, d \geq 0$ , the maximum sum  $S(x) = \max\{|a - x| + |x - b|, |c - x| + |x - d|\}$  over  $x \geq 0$  has the minimum value  $\text{MS}(a, b, c, d) = \max\{|a - b|, |c - d|, \frac{1}{2}|a + b - c - d|\}$ .  $\blacktriangle$*

*Proof* The maximum sum  $S(x)$  and the formula for  $\text{MS}(a, b, c, d)$  are invariant under permutations  $a \leftrightarrow b, c \leftrightarrow d$  and  $(a, b) \leftrightarrow (c, d)$ . Without loss of generality one can assume that  $a \leq b$  and  $a \leq c \leq d$ . Then Fig. 17 shows the graphs of  $y = |a - x| + |x - b|$ ,  $y = |c - x| + |x - d|$ ,  $y = S(x)$  in green, blue, red, respectively.

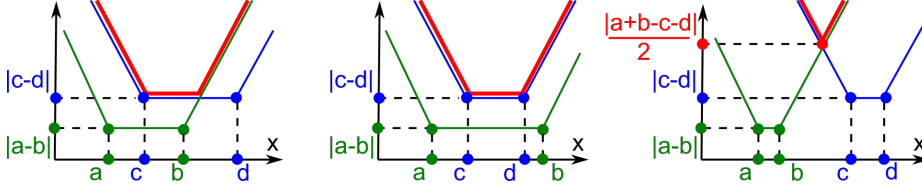


Fig. 17 Lemma 5.7 finds a minimum value of  $S(x)$  for all different positions of  $a, b, c, d$ .

If  $b \geq c$ , then  $a \leq c \leq b \leq d$  or  $a \leq c \leq d \leq b$ , see the first two pictures of Fig. 17. In the first case  $S(x)$  has the minimum value  $\max\{b - a, d - c\}$  for any  $x \in [c, b]$ . In the second case  $S(x)$  has the minimum value  $b - a \geq d - c$  for any  $x \in [a, b]$ . In both cases the minimum value coincides with  $\max\{|a - b|, |c - d|\}$ .

If  $b \leq c$ , then  $a \leq b \leq c \leq d$ , see the last picture of Fig. 17. Then  $S(x) = \max\{2x - a - b, c + d - 2x\}$  has a minimum at  $x$  such that  $2x - a - b = c + d - 2x$ , so  $x = \frac{1}{4}(a + b + c + d)$ . The minimum value is  $\text{MS}(a, b, c, d) = \frac{1}{2}|a + b - c - d| \geq \max\{|a - b|, |c - d|\}$  in this case. The last inequality is reversed in the previous two cases. So  $\text{MS}(a, b, c, d) = \max\{|a - b|, |c - d|, \frac{1}{2}|a + b - c - d|\}$  in all cases.  $\square$

If lattices  $\Lambda_1, \Lambda_2$  have non-opposite signs, so  $\text{sign}(\Lambda_1)\text{sign}(\Lambda_2) \geq 0$ , then the metrics  $\text{RM}_q^o$  and  $\text{PM}_q^o$  from Definition 5.4 coincide with the easily computable unoriented metrics  $\text{RM}_q, \text{PM}_q$  from Definition 5.1. Hence Propositions 5.8 and 5.9 compute  $\text{RM}_q^o(\Lambda_1, \Lambda_2)$  and  $\text{PM}_q^o(\Lambda_1, \Lambda_2)$  only for lattices of opposite signs.

**Proposition 5.8 (root metrics for  $q = 2, +\infty$ )** *Let  $\Lambda_1, \Lambda_2 \subset \mathbb{R}^2$  be lattices of opposite signs with  $\text{RI}(\Lambda_1) = (r_{12}, r_{01}, r_{02})$  and  $\text{RI}(\Lambda_2) = (s_{12}, s_{01}, s_{02})$ . Then*

(a)  $\text{RM}_2^o(\Lambda_1, \Lambda_2)$  is the minimum of the Euclidean distances from the point  $\text{RI}(\Lambda_1)$  to the three points  $(-s_{12}, s_{01}, s_{02})$ ,  $(s_{01}, s_{12}, s_{02})$ , and  $(s_{12}, s_{02}, s_{01})$  in  $\mathbb{R}^3$ .

(b)  $\text{RM}_\infty^o(\Lambda_1, \Lambda_2) = \min\{d_0, d_1, d_2\}$ , where

$$d_0 = \max\{r_{12} + s_{12}, |r_{01} - s_{01}|, |r_{02} - s_{02}|\},$$

$$d_1 = \max\{\text{MS}(r_{12}, r_{01}, s_{12}, s_{01}), |r_{02} - s_{02}|\},$$

$$d_2 = \max\{|r_{12} - s_{12}|, \text{MS}(r_{01}, r_{02}, s_{01}, s_{02})\},$$

see  $\text{MS}(a, b, c, d) = \max\{|a - b|, |c - d|, \frac{1}{2}|a + b - c - d|\}$  in Lemma 5.7.  $\blacktriangle$

*Proof (a)* By Definition 5.4  $\text{RM}^o(\Lambda_1, \Lambda_2)$  is the minimum value of  $\text{RM}(\Lambda_1, \Lambda_3) + \text{RM}(\Lambda_2, \Lambda_3)$  over mirror-symmetric lattices  $\Lambda_3$ . By Lemma 4.7 the root invariant  $\text{RI}(\Lambda_3)$  belongs to one of the boundary sectors of the triangular cone TC. Let  $\text{RI}'$  be the mirror image of  $\text{RI}(\Lambda_2)$  in the boundary sector containing  $\text{RI}(\Lambda_3)$ .

The triangle inequality for the Euclidean distance with  $q = 2$  implies that

$$\text{RM}(\Lambda_1, \Lambda_3) + \text{RM}(\Lambda_2, \Lambda_3) = \|\text{RI}(\Lambda_1) - \text{RI}(\Lambda_3)\|_2 + \|\text{RI}(\Lambda_3) - \text{RI}'\|_2$$

achieves minimum value  $\|\text{RI}(\Lambda_1) - \text{RI}'\|_2$  when the point  $\text{RI}(\Lambda_3)$  is in the straight line between the points  $\text{RI}(\Lambda_1), \text{RI}'$ . The mirror bright2021proof  $\text{RI}'$  of  $\text{RI}(\Lambda_2) = (s_{12}, s_{01}, s_{02})$  in the three boundary sectors  $\{s_{12} = 0\}$ ,  $\{s_{12} = s_{01}\}$ ,  $\{s_{01} = s_{02}\}$  of the cone TC are the points  $(-s_{12}, s_{01}, s_{02})$ ,  $(s_{01}, s_{12}, s_{02})$ ,  $(s_{12}, s_{02}, s_{01})$ , respectively. So  $\text{RM}^o(\Lambda_1, \Lambda_2)$  is the minimum of the Euclidean distances to the points above.

(b) For  $\text{RI}(\Lambda_1) = (r_{12}, r_{01}, r_{02})$  and  $\text{RI}(\Lambda_2) = (s_{12}, s_{01}, s_{02})$ , the required formula  $\text{RM}_\infty^o(\Lambda_1, \Lambda_2) = \min\{d_0, d_1, d_2\}$  will be proved by minimising the total length  $D = \text{RM}_\infty(\Lambda_1, \Lambda_3) + \text{RM}_\infty(\Lambda_2, \Lambda_3)$  of a path from  $\Lambda_1$  to  $\Lambda_2$  via  $\Lambda_3$  whose root invariant  $\text{RI}(\Lambda_3)$  can be in one of the three boundary sectors of TC.

*Horizontal boundary* :  $\text{RI}(\Lambda_3) = (0, t_{01}, t_{02})$  for variables  $0 \leq t_{01} \leq t_{02}$ . Then

$$D = \max\{|r_{12} + s_{12}|, |r_{01} - t_{01}| + |t_{01} - s_{01}|, |r_{02} - t_{02}| + |t_{02} - s_{02}|\}$$

has the minimum  $d_0 = \max\{r_{12} + s_{12}, |r_{01} - s_{01}|, |r_{02} - s_{02}|\}$  for  $t_{01} = \frac{1}{2}(r_{01} + s_{01})$ ,  $t_{02} = \frac{1}{2}(r_{02} + s_{02})$  or any values of  $t_{01}, t_{02}$  close enough to these averages.

*Inclined boundary* :  $\text{RI}(\Lambda_3)$  consists of variables  $t_{12} = t_{01} \leq t_{02}$ . By Lemma 5.7

$$D = \max\{|r_{12} - t_{12}| + |t_{12} - s_{12}|, |r_{01} - t_{12}| + |t_{12} - s_{01}|, |r_{02} - t_{02}| + |t_{02} - s_{02}|\}$$

has the minimum value  $d_1 = \max\{\text{MS}(r_{12}, r_{01}, s_{12}, s_{01}), |r_{02} - s_{02}|\}$ , where  $t_{02}$  can be anywhere between  $r_{02}, s_{02}$ , see the formula of MS in Lemma 5.7.

*Vertical boundary* :  $\text{RI}(\Lambda_3)$  consists of variables  $t_{12} \leq t_{01} = t_{02}$ . By Lemma 5.7

$$D = \max\{|r_{12} - t_{12}| + |t_{12} - s_{12}|, |r_{01} - t_{01}| + |t_{01} - s_{01}|, |r_{02} - t_{01}| + |t_{01} - s_{02}|\}$$

has the minimum value  $d_2 = \max\{|r_{12} - s_{12}|, \text{MS}(r_{01}, r_{02}, s_{01}, s_{02})\}$ , where  $t_{12}$  can be anywhere between  $r_{12}, s_{12}$ . The final distance is  $D = \min\{d_0, d_1, d_2\}$ .  $\square$

**Proposition 5.9 (projected metrics for  $q = 2, +\infty$ )** *Let  $\Lambda_1, \Lambda_2$  be lattices with opposite signs and projected invariants  $\text{PI}(\Lambda_1) = (x_1, y_1)$ ,  $\text{PI}(\Lambda_2) = (x_2, y_2)$ .*

(a)  $\text{PM}_2^o(\Lambda_1, \Lambda_2)$  is the minimum of the Euclidean distances from  $\text{PI}(\Lambda_1) = (x_1, y_1)$  to the three points  $(-x_2, y_2)$ ,  $(x_2, -y_2)$ ,  $(1 - y_2, 1 - x_2)$  in  $\mathbb{R}^2$ .

(b) For  $x_1 \leq x_2$ ,  $\text{PM}_\infty^o(\Lambda_1, \Lambda_2) = \min\{d_x, d_y, d_{xy}\}$  for  $d_x = \max\{x_2 - x_1, y_2 + y_1\}$ ,  $d_y = \max\{x_2 + x_1, |y_2 - y_1|\}$ ,  $d_{xy} = \max\{x_2 - x_1, 1 - x_2 - y_2 + |1 - y_1 - x_2|\}$ .  $\blacktriangle$

*Proof (a)* By Definition 5.4  $\text{PM}^o(\Lambda_1, \Lambda_2)$  is the minimum value of  $\text{PM}(\Lambda_1, \Lambda_3) + \text{PM}(\Lambda_2, \Lambda_3)$  achieved for a mirror-symmetric lattices  $\Lambda_3$ . By Lemma 4.7 the invariant  $\text{PI}(\Lambda_3)$  belongs to one of the sides of the quotient triangle QT. Let  $\text{PI}'$  be the mirror image of  $\text{PI}(\Lambda_2)$  with respect to the side of QT containing  $\text{PI}(\Lambda_3)$ .

The triangle inequality for the Euclidean distance with  $q = 2$  implies that

$$\text{PM}(\Lambda_1, \Lambda_3) + \text{PM}(\Lambda_2, \Lambda_3) = \|\text{PI}(\Lambda_1) - \text{PI}(\Lambda_3)\|_2 + \|\text{PI}(\Lambda_3) - \text{PI}'\|_2$$

achieves minimum value  $\|\text{PI}(\Lambda_1) - \text{PI}'\|_2$  when the point  $\text{PI}(\Lambda_3)$  is in the straight line between the points  $\text{PI}(\Lambda_1), \text{PI}'$  in the plane  $\mathbb{R}^2$  containing the quotient triangle

QT. The mirror bright2021proof PI' of  $\text{PI}(\Lambda_2) = (x_2, y_2)$  in the three sides  $x_2 = 0$ ,  $y_2 = 0$ ,  $x_2 + y_2 = 1$  are the points  $(-x_2, y_2)$ ,  $(x_2, -y_2)$ ,  $(1 - y_2, 1 - x_2)$ , respectively. Hence  $\text{PM}^o(\Lambda_1, \Lambda_2)$  is the minimum of the Euclidean distances to the points above.

(b)  $\text{PM}^o(\Lambda_1, \Lambda_2)$  is the minimum value of  $\text{PM}(\Lambda_1, \Lambda_3) + \text{PM}(\Lambda_2, \Lambda_3)$  over mirror-symmetric lattices  $\Lambda_3$ . The formula  $\text{PM}^o_\infty(\Lambda_1, \Lambda_2) = \min\{d_x, d_y, d_{xy}\}$  will be proved by minimising the Minkowski length  $M_\infty$  of a path from  $\Lambda_1$  to  $\Lambda_2$  via  $\Lambda_3$  whose projected invariant  $\text{PI}(\Lambda_3)$  can be in one of the three sides of the quotient triangle QT. For given  $\text{PI}(\Lambda_1) = (x_1, y_1)$  and  $\text{PI}(\Lambda_2) = (x_2, y_2)$  with  $x_1 \leq x_2$ , we minimise  $D = \text{PM}_\infty(\Lambda_1, \Lambda_3) + \text{PM}_\infty(\Lambda_2, \Lambda_3)$  for each side of QT below.

*Horizontal side* :  $\text{PI}(\Lambda_3) = (x_3, 0)$  for a variable parameter  $x_3 \geq 0$ . For any  $x_3 \in [x_1, x_2]$ , the distance  $D = \max\{(x_3 - x_1) + (x_2 - x_3), y_2 + y_1\}$  equals the simpler function  $d_x = \max\{x_2 - x_1, y_2 + y_1\}$  and can be only larger for any  $x_3 \notin [x_1, x_2]$ .

*Vertical side* :  $\text{PI}(\Lambda_3) = (0, y_3)$  for a variable parameter  $y_3$ . For any  $y_3$  between  $y_1, y_2$ , the distance  $D = \max\{x_1 + x_2, |y_1 - y_3| + |y_3 - y_2|\}$  has the minimum  $d_y = \max\{x_1 + x_2, |y_1 - y_2|\}$  and is larger for any  $y_3$  that is not between  $y_1, y_2$ .

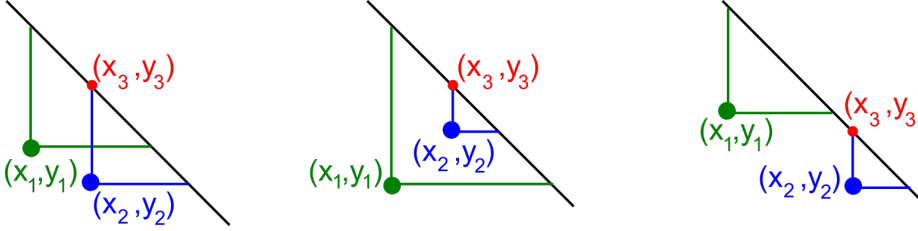


Fig. 18 Relative positions of  $(x_1, y_1), (x_2, y_2)$  for  $x_1 \leq x_2$  in the proof of Proposition 5.9(b).

*Hypotenuse* :  $\text{PI}(\Lambda_3) = (x_3, y_3)$  for variables  $x_3, y_3$  such that  $x_3 + y_3 = 1$ . For  $x_1 \leq x_2$ , we aim to minimise  $D = \max\{|x_1 - x_3| + |x_3 - x_2|, |y_1 - y_3| + |y_3 - y_2|\}$ . Fig. 18 shows all three different cases how we can find an optimal chiral lattice  $\Lambda_3$  with a projected invariant  $\text{PI}(\Lambda_3) = (x_3, y_3)$  for given  $\text{PI}(\Lambda_1) = (x_1, y_1)$  and  $\text{PI}(\Lambda_2) = (x_2, y_2)$ . The sum  $|x_1 - x_3| + |x_3 - x_2|$  has the minimum value  $x_2 - x_1$  for any  $x_3 \in [x_1, x_2]$ . Similarly,  $|y_1 - y_3| + |y_3 - y_2|$  has the minimum value  $|y_1 - y_2|$  for any  $y_3$  between  $y_1, y_2$ . If the point  $(x_3, y_3)$  moves along the hypotenuse so that both  $x_3, y_3$  are outside their minimum ranges above, then  $|x_1 - x_3| + |x_3 - x_2| = |2x_3 - x_1 - x_2|$  increases at the same rate as  $|y_1 - y_3| + |y_3 - y_2| = |2y_3 - y_1 - y_2|$  decreases during this movement because  $x_3 + y_3 = 1$ . Hence  $x_3$  can be chosen as  $x_1$  or  $x_2$  to minimise  $D$ . In the first two pictures of Fig. 18 we choose  $x_3 = x_2$ .

In the last picture of Fig. 18, any  $(x_3, y_3)$  between the triangles with right-angled vertices at  $(x_1, y_1), (x_2, y_2)$  gives the minimum values  $x_2 - x_1$  and  $|y_2 - y_1|$ . Hence  $x_3 = x_2$  always gives the minimum value of the distance

$$d_{xy} = \max\{x_2 - x_1, |y_1 - y_3| + |y_3 - y_2|\} \text{ for } y_3 = 1 - x_2,$$

so  $d_{xy} = \max\{x_2 - x_1, 1 - x_2 - y_2 + |1 - y_1 - x_2|\}$  and  $D = \min\{d_x, d_y, d_{xy}\}$ .  $\square$



## 6 Real-valued chiral distances measure asymmetry of lattices

The classical concept of chirality is a binary property distinguishing mirror bright2021proof of the same object such as a molecule or a periodic crystal. Continuous classifications in Theorem 4.2 and Corollary 4.6 imply that the binary chirality is discontinuous under almost any perturbations similar to other discrete invariants such as symmetry groups. To avoid arbitrary thresholds, it makes more sense to continuously quantify a deviation of a lattice from a higher-symmetry neighbour.

The term *chirality* often refers to 3-dimensional molecules or crystal lattices. One reason is the fact that in  $\mathbb{R}^2$  a reflection with respect to a line  $L$  is realised by the rotation in  $\mathbb{R}^3$  around  $L$  through  $180^\circ$ . However, if our ambient space is only  $\mathbb{R}^2$ , the concepts of isometry and rigid motion differ. For example, Lemma 3.3 described root invariants of all lattices that are related to their mirror bright2021proof by rigid motion. Such lattices can be called *achiral*. We call them mirror-symmetric.

After consulting with crystallographers, Definition 6.1 introduces the real-valued  $G$ -chiral distances of a lattice  $\Lambda \subset \mathbb{R}^2$ . Proposition 7.10 will prove continuity of these functions  $\text{RC}[G] : \text{LIS}(\mathbb{R}^2) \rightarrow \mathbb{R}$  and  $\text{PC}[G] : \text{LSS}(\mathbb{R}^2) \rightarrow \mathbb{R}$ .

Recall that the *crystallographic point group*  $G$  of a lattice  $\Lambda \subset \mathbb{R}^2$  containing the origin  $0$  consists of all symmetry operations that keep  $0$  and map  $\Lambda$  to itself. For example, any such group  $G$  includes the central symmetry with respect to  $0 \in \Lambda \subset \mathbb{R}^2$ . If  $G$  has no other non-trivial symmetries, we get  $G = C_2$  in Schonflies notations. All 2D lattices split into four crystal families by their point groups: oblique ( $C_2$ ), orthorhombic ( $D_2$ ), tetragonal or square ( $D_4$ ) and hexagonal ( $D_6$ ). Orthorhombic lattices split into rectangular and centred rectangular, see Fig. 13.

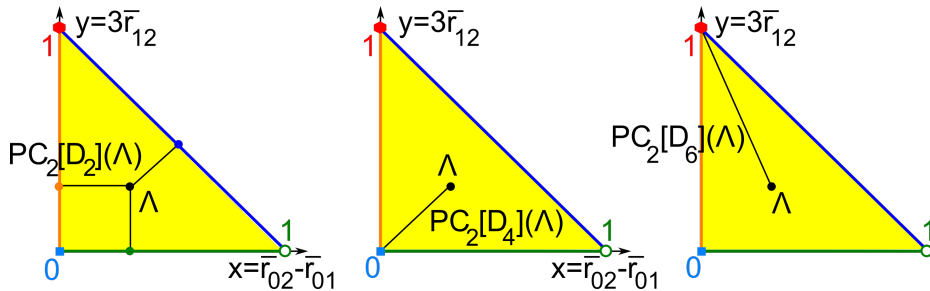


**Fig. 19** **Left:** by Definition 6.1, the projected  $D_2$  chiral distance  $\text{PC}_2[D_2](\Lambda)$  is the minimum Euclidean distance from  $\text{PI}(\Lambda) \in \text{QT}$  to the boundary  $\partial\text{QT}$ . **Middle:**  $\text{PC}_2[D_4](\Lambda)$  is the distance from  $\text{PI}(\Lambda)$  to  $(0,0)$ . **Right:**  $\text{PC}_2[D_6](\Lambda)$  is the distance from  $\text{PI}(\Lambda)$  to  $(0,1)$ .

**Definition 6.1** ( $G$ -chiral distances  $\text{RC}[G]$  and  $\text{PC}[G]$ ) For any crystallographic point group  $G$  in  $\mathbb{R}^2$ , let  $\text{LIS}[G] \subset \text{LIS}(\mathbb{R}^2)$  be the closure of the subspace of all (isometry classes of) lattices that have the crystallographic point group  $G$ . For  $G = D_2$  or  $G = D_4$  or  $G = D_6$ , the root and projected  $G$ -chiral distances are

$$\text{RC}[G](\Lambda) = \min_{\Lambda' \in \text{LIS}[G]} \text{RM}(\Lambda, \Lambda') \geq 0 \text{ and } \text{PC}[G](\Lambda) = \min_{\Lambda' \in \text{LIS}[G]} \text{PM}(\Lambda, \Lambda') \geq 0,$$

where RM, PM are any metrics from Definition 5.1 with a base metric  $d$ . If  $d = M_q$  for  $q \in [1, +\infty]$ , denote the  $G$ -chiral distances by  $\text{RC}_q[G]$  and  $\text{PC}_q[G]$ . ■

Since any lattice  $A$  is symmetric with respect to the origin  $0 \in A$ , the closed subspace  $\text{LIS}[C_2]$  coincides with the 3-dimensional Lattice Isometry Space  $\text{LIS}(\mathbb{R}^2)$ . The 2-dimensional subspace  $\text{LIS}[D_2]$  consists of all mirror-symmetric lattices (rectangular and centred-rectangular) represented by root invariants RI on the boundary  $\partial\text{TC}$  of the triangular cone in Definition 4.4, see Fig. 12. The 1-dimensional subspaces  $\text{LIS}[D_4], \text{LIS}[D_6] \subset \text{LIS}[D_2]$  can be viewed as the blue and orange rays  $\{r_{12} = 0 < r_{01} = r_{02}\}$  and  $\{0 < r_{12} = r_{01} = r_{02}\}$ , respectively.

The  $G$ -chiral distance  $\text{RC}[G]$  in Definition 6.1 measures a distance from  $\text{RI}(A)$  to the root invariant of a closest neighbour in the subspace  $\text{LIS}[G]$ . Any  $\text{RC}[G](A)$  is invariant up to isometry and measures a distance from  $A$  to its nearest neighbour  $A' \in \text{LIS}[G]$ . The signed chiral distances  $\text{sign}(A)\text{RC}(A)$  and  $\text{sign}(A)\text{PC}(A)$  are invariant up to rigid motion. Since  $\text{LIS}[G]$  is a closed subspace within  $\text{LIS}(\mathbb{R}^2)$ , the continuous distances RM, PM achieve their minima if their base distances  $d$  are continuous. If  $\text{LIS}[D_2]$  was defined as an open subspace of only lattices that have the point group  $D_2$  (not  $D_4$  or  $D_6$ ), then  $\text{RC}[G], \text{PC}[G]$  should be defined via infima instead of simpler minima. Indeed, any square or hexagonal lattice  $A$  can be approximated by infinitely many closer and closer orthorhombic lattices  $A'$ , but the expected distance  $\text{RM}(A, A') = 0$  will not be achieved on an open set.

For  $q = 2, +\infty$ , the distances  $\text{RC}_q, \text{PC}_q$  are computed in Propositions 6.5, 6.6.

**Lemma 6.2 (properties of chiral distances)** (a) *A lattice  $A$  is mirror-symmetric if and only if  $\text{RC}[D_2](A) = 0$  or, equivalently,  $\text{PC}[D_2](A) = 0$ .*

(b) *For any crystallographic point group  $G$  in  $\mathbb{R}^2$ , mirror reflections  $A^\pm \subset \mathbb{R}^2$  have equal  $G$ -chiral distances:  $\text{RC}[G](A^+) = \text{RC}[G](A^-)$ ,  $\text{PC}[G](A^+) = \text{PC}[G](A^-)$ .* ▲

*Proof (a)* By Definition 6.1  $\text{RC}[D_2](A) = \min_{\text{sign}(A')=0} \{\text{RM}(A, A')\} = 0$  means that  $\text{RI}(A) = \text{RI}(A')$  for some mirror-symmetric lattice  $A'$  due to Lemma 4.7. Then  $A$  is isometric to  $A'$  by Theorem 4.2 and is mirror-symmetric.

(b) The  $G$ -chiral distances from Definition 6.1 depend only on a root invariant  $\text{RI}(A)$  and projected invariant  $\text{PI}(A)$ , which are the same for mirror  $A^\pm$ . □

**Lemma 6.3 (lower bounds)** (a) *If lattices  $A_1, A_2$  have opposite signs, then  $\text{RM}^\circ(A_1, A_2) \geq \text{RC}[D_2](A_1) + \text{RC}[D_2](A_2)$  and  $\text{PM}^\circ(A_1, A_2) \geq \text{PC}[D_2](A_1) + \text{PC}[D_2](A_2)$ .*

(b) *For the mirror  $A^\pm$  of any lattice  $A$ , the lower bounds in part (a) become equalities:  $\text{RM}^\circ(A^+, A^-) = 2\text{RC}[D_2](A)$  and  $\text{PM}^\circ(A^+, A^-) = 2\text{PC}[D_2](A)$ .* ▲

*Proof (a)* The first lower bound follows from Definitions 6.1 and 5.4, because the minimisations of the root chiral distances are over separate lattices  $A'_1, A'_2$ .

$$\text{RM}^\circ(A_1, A_2) = \min_{\text{sign}(A')=0} (\text{RM}(A_1, A') + \text{RM}(A_2, A')) \geq$$

$$\min_{\text{sign}(A'_1)=0} \text{RM}(A_1, A'_1) + \min_{\text{sign}(A'_2)=0} \text{RM}(A_2, A'_2) = \text{RC}[D_2](A_1) + \text{RC}[D_2](A_2),$$

where the root chiralities are independent of a sign by Lemma 6.2(b). The proof for the projected metric  $\text{PM}^o$  is similar to the above arguments.

(b) If  $A_1 = A_2$ , the sum  $\text{RM}(A_1, A') + \text{RM}(A_2, A')$  in part (a) consists of equal terms. Hence the inequality becomes equality giving the double distance.  $\square$

Lemma 6.4 will help prove Propositions 6.5, 6.6 to explicitly express the chiral distances  $\text{RC}_q[G](A)$ ,  $\text{PC}_q[G](A)$  via the invariants  $\text{RI}(A) \in \text{TC}$  and  $\text{PI}(A) \in \text{QT}$ .

**Lemma 6.4 (maximum modulus)** *For any fixed points  $a, b \in \mathbb{R}$ , the function  $D_\infty(x) = \max\{|a - x|, |x - b|\}$  has the minimum value  $\frac{1}{2}|a - b|$  for  $x = \frac{a + b}{2}$ .  $\blacktriangle$*

*Proof* Without loss of generality assume that  $a \leq b$ . For  $x \in [a, b]$ , the function  $D_\infty(x) = \max\{x - a, b - x\}$  has the minimum value  $\frac{b - a}{2}$  at the mid-point  $x$  of the interval  $[a, b]$  and takes values larger than  $b - a$  for any  $x \notin [a, b]$ .  $\square$

**Proposition 6.5 (chiral distances  $\text{RC}_q[G]$  for  $q = 2, +\infty$ )** *Let a lattice  $A \subset \mathbb{R}^2$  have a root invariant  $\text{RI}(A) = (r_{12}, r_{01}, r_{02})$  with  $0 \leq r_{12} \leq r_{01} \leq r_{02}$ . Then*

$$(6.5a) \quad \text{RC}_2[D_2](A) = \min \left\{ r_{12}, \frac{r_{01} - r_{12}}{\sqrt{2}}, \frac{r_{02} - r_{01}}{\sqrt{2}} \right\};$$

$$\text{RC}_2[D_4](A) = \sqrt{r_{12}^2 + \frac{1}{4}(r_{02} - r_{01})^2};$$

$$\text{RC}_2[D_6](A) = \sqrt{\frac{2}{3}(r_{12}^2 + r_{01}^2 + r_{02}^2 - r_{12}r_{01} - r_{12}r_{02} - r_{01}r_{02})};$$

$$(6.5b) \quad \text{RC}_\infty[D_2](A) = \min \left\{ r_{12}, \frac{r_{01} - r_{12}}{2}, \frac{r_{02} - r_{01}}{2} \right\};$$

$$\text{RC}_\infty[D_4](A) = \min \left\{ r_{12}, \frac{r_{02} - r_{01}}{2} \right\};$$

$$\text{RC}_\infty[D_6](A) = \frac{r_{02} - r_{12}}{2}. \quad \blacktriangle$$

*Proof (a)* The chiral distance  $\text{RC}_2[D_2](A) = \min_{\text{sign}(A')=0} \|\text{RI}(A) - \text{RI}(A')\|_2$  by Definition 6.1 is the minimum Euclidean distance from  $\text{RI}(A)$  to the boundary of TC. This boundary of three triangular sectors consists of root invariants of all mirror-symmetric lattices by Lemma 4.7. Any point  $\text{RI}(A) = (r_{12}, r_{01}, r_{02})$  with  $0 \leq r_{12} \leq r_{01} \leq r_{02}$  has Euclidean distances  $r_{12}$ ,  $\frac{r_{01} - r_{12}}{\sqrt{2}}$ ,  $\frac{r_{02} - r_{01}}{\sqrt{2}}$  to the horizontal boundary  $r_{12} = 0$ , inclined boundary  $r_{12} = r_{01}$ , and the vertical boundary  $r_{01} = r_{02}$ , respectively, see Fig. 14(right). Then  $\text{RC}_2[D_2](A)$  is the minimum of the above Euclidean distances to the three boundary sectors of TC.

$\text{RC}_2[D_4](A)$  is the Euclidean distance from  $\text{RI}(A) = (r_{12}, r_{01}, r_{02})$  to a closest root invariant  $\text{RI}(A') = (0, s, s)$  of a square lattice  $A'$ . The square of  $\|\text{RI}(A) - \text{RI}(A')\|_2$  is  $d_4(s) = r_{12}^2 + (s - r_{01})^2 + (s - r_{02})^2$ . The quadratic function  $d_4(s)$  is minimised when  $0 = d'_4(s) = 2(s - r_{01}) + 2(s - r_{02})$ , so  $s = \frac{1}{2}(r_{01} + r_{02})$ . Then  $d_4(\frac{1}{2}(r_{01} + r_{02})) = r_{12}^2 + \frac{1}{4}(r_{02} - r_{01})^2$  and  $\text{RC}_2[D_4](A) = \sqrt{r_{12}^2 + \frac{1}{4}(r_{02} - r_{01})^2}$ .

$\text{RC}_2[D_6](A)$  is the Euclidean distance from  $\text{RI}(A) = (r_{12}, r_{01}, r_{02})$  to a closest root invariant  $\text{RI}(A') = (s, s, s)$  of a hexagonal lattice  $A'$ . The square of  $\|\text{RI}(A) - \text{RI}(A')\|_2$  is  $d_6(s) = (s - r_{12})^2 + (s - r_{01})^2 + (s - r_{02})^2$ . The quadratic function  $d_6(s)$  is minimised when  $0 = d'_6(s) = 2(s - r_{12}) + 2(s - r_{01}) + 2(s - r_{02})$ , so  $s = \frac{1}{3}(r_{12} + r_{01} + r_{02})$ . Substituting the minimum point  $s$  above, we get

$$\begin{aligned} 9d_6(s) &= (2r_{12} - r_{01} - r_{02})^2 + (2r_{01} - r_{12} - r_{02})^2 + (2r_{02} - r_{12} - r_{01})^2 = \\ &= 6(r_{12}^2 + r_{01}^2 + r_{02}^2) - (4 + 4 - 2)(r_{12}r_{01} + r_{12}r_{02} + r_{01}r_{02}). \end{aligned}$$

Then  $\text{RC}_2[D_6](A) = \sqrt{d_6(s)} = \sqrt{\frac{2}{3}(r_{12}^2 + r_{01}^2 + r_{02}^2 - r_{12}r_{01} - r_{12}r_{02} - r_{01}r_{02})}$ .

(b)  $\text{RC}_\infty[D_2](A) = \min_{\text{sign}(A')=0} \|\text{RI}(A) - \text{RI}(A')\|_\infty$  is minimised over mirror-symmetric

lattices  $A'$  whose root invariants by Lemma 4.7 belong to one of the three boundary sectors of the triangular cone TC. We consider them below one by one.

*Horizontal boundary* :  $\text{RI}(A') = (0, s_{01}, s_{02})$  for  $0 < s_{01} \leq s_{02}$ . Then  $\|\text{RI}(A) - \text{RI}(A')\|_\infty = \|(r_{12}, r_{01}, r_{02}) - (0, s_{01}, s_{02})\|_\infty = \max\{r_{12}, |r_{01} - s_{01}|, |r_{02} - s_{02}|\}$  has the minimum  $r_{12}$  for  $s_{01} = r_{01}$ ,  $s_{02} = r_{02}$  or any  $s_{01}, s_{02}$  close to  $r_{01}, r_{02}$ .

*Inclined boundary* : a variable root invariant  $\text{RI}(A')$  has equal root products  $s_{12} = s_{01}$ . By Lemma 6.4 the  $M_\infty$ -distance  $\|\text{RI}(A) - \text{RI}(A')\|_\infty = \|(r_{12}, r_{01}, r_{02}) - (s_{01}, s_{01}, s_{02})\|_\infty = \max\{|r_{12} - s_{01}|, |r_{01} - s_{01}|, |r_{02} - s_{02}|\}$  has the minimum  $\frac{r_{01} - r_{12}}{2}$  for  $s_{02} = r_{02}$  and  $s_{01}$  at the mid-point of the interval  $[r_{12}, r_{01}]$ .

*Vertical boundary* :  $\text{RI}(A')$  has  $s_{01} = s_{02}$ . By Lemma 6.4  $\|\text{RI}(A) - \text{RI}(A')\|_\infty = \|(r_{12}, r_{01}, r_{02}) - (s_{12}, s_{01}, s_{01})\|_\infty = \max\{|r_{12} - s_{12}|, |r_{01} - s_{01}|, |r_{02} - s_{01}|\}$  has the minimum  $\frac{r_{02} - r_{01}}{2}$  for  $s_{12} = r_{12}$  and  $s_{01}$  at the mid-point of the interval  $[r_{01}, r_{02}]$ . Finally,  $\text{RC}_\infty[D_2](A)$  is the minimum of the three  $A_\infty$  distances.

$\text{RC}_\infty[D_4](A)$  is the distance  $M_\infty$  from  $\text{RI}(A)$  to a closest root invariant  $\text{RI}(A') = (0, s, s)$  of a square lattice  $A'$ . Then  $\|\text{RI}(A) - \text{RI}(A')\|_\infty = \max\{r_{12}, |s - r_{01}|, |s - r_{02}|\}$ . If we ignore  $r_{12}$ , by Lemma 6.4 the minimum of the largest value among the last two is  $\frac{1}{2}(r_{02} - r_{01})$ , so  $\text{RC}_\infty[D_4](A) = \min\{r_{12}, \frac{r_{02} - r_{01}}{2}\}$ .

$\text{RC}_\infty[D_6](A)$  is the distance  $M_\infty$  from  $\text{RI}(A) = (r_{12}, r_{01}, r_{02})$  to a closest root invariant  $\text{RI}(A') = (s, s, s)$  of a hexagonal lattice  $A'$ . Then  $\|\text{RI}(A) - \text{RI}(A')\|_\infty = \max\{|s - r_{12}|, |s - r_{01}|, |s - r_{02}|\}$ . Since  $r_{12} \leq r_{01} \leq r_{02}$ , we could ignore  $|s - r_{01}|$  in the maximum. By Lemma 6.4 the final maximum is  $\frac{r_{02} - r_{01}}{2} = \text{RC}_\infty[D_6](A)$ .  $\square$

When considering lattices up to similarity, the subspace  $\text{LSS}[D_4]$  consists of a single class of all square lattices, which are all equivalent up to isometry and uniform scaling. The subspace  $\text{LSS}[D_6]$  is also a single point representing all hexagonal lattices. Then  $\text{PC}[D_4]$  and  $\text{PC}[D_6]$  are distances to these single points.

**Proposition 6.6 (chiral distances  $\text{PC}_q$  for  $q = 2, +\infty$ )** *Let a lattice  $A$  have a projected invariant  $\text{PI}(A) = (x, y) \in \text{QT}$  so that  $x \in [0, 1]$ ,  $y \in [0, 1]$ ,  $x + y \leq 1$ .*

$$(6.6a) \text{PC}_2[D_2](\Lambda) = \min \left\{ x, y, \frac{1-x-y}{\sqrt{2}} \right\},$$

$$\text{PC}_q[D_4](\Lambda) = (x^q + y^q)^{1/q} \text{ for any } q \in [1, +\infty),$$

$$\text{PC}_q[D_6](\Lambda) = (x^q + (1-y)^q)^{1/q} \text{ for any } q \in [1, +\infty);$$

$$(6.6b) \text{PC}_\infty[D_2](\Lambda) = \min \left\{ x, y, \frac{1-x-y}{2} \right\},$$

$$\text{PC}_\infty[D_4](\Lambda) = x,$$

$$\text{PC}_\infty[D_6](\Lambda) = 1 - y.$$

(6.6c) *The upper bounds  $\text{PC}_2[D_2](\Lambda) \leq \frac{1}{2+\sqrt{2}}$ ,  $\text{PC}_\infty[D_2](\Lambda) \leq \frac{1}{4}$  hold for any  $\Lambda$ , achieved for lattices with  $\text{PI}(\Lambda_2) = (\frac{1}{2+\sqrt{2}}, \frac{1}{2+\sqrt{2}})$ ,  $\text{PI}(\Lambda_\infty) = (\frac{1}{4}, \frac{1}{4})$ , respectively. For  $q \in [1, +\infty]$ , the bound  $\text{PC}_q[D_4](\Lambda) \leq 1$  holds for any  $\Lambda$  and is achieved for any hexagonal lattice. For  $q \in [1, +\infty)$ , the upper bound  $\text{PC}_q[D_6](\Lambda) < 2^{1/q}$  holds for any  $\Lambda$  and is approached but not achieved as  $x \rightarrow 1$ . The bound  $\text{PC}_\infty[D_6](\Lambda) \leq 1$  holds for any  $\Lambda$  and is achieved for any square and rectangular lattice.  $\blacktriangle$*

*Proof (a)* By Definition 6.1  $\text{PC}_2[D_2](\Lambda)$  is the minimum Euclidean distance from  $\text{PI}(\Lambda)$  to the three boundary sides of the quotient triangle QT. These sides consists of projected invariants of all mirror-symmetric lattices by Lemma 4.7. Any point  $\text{PI}(\Lambda) = (x, y) \in \text{QT}$  has distances  $x$ ,  $y$ ,  $\frac{1-x-y}{\sqrt{2}}$  to the vertical side  $x = 0$ , horizontal side  $y = 0$ , and the hypotenuse  $x + y = 1$ , respectively, see Fig. 14 (left). Hence  $\text{PC}_2(\Lambda)$  is the minimum of the above Euclidean distances.

$\text{PC}_q[D_4](\Lambda) = (x^q + y^q)^{1/q}$  is the Minkowski  $M_q$  distance from  $\text{PI}(\Lambda) = (x, y) \in \text{QT}$  to the single-point subspace  $\text{LSS}[D_4] = (0, 0)$  for any  $q \in [1, +\infty)$ .

$\text{PC}_q[D_6](\Lambda) = (x^q + (1-y)^q)^{1/q}$  is the Minkowski  $M_q$  distance from  $\text{PI}(\Lambda) = (x, y) \in \text{QT}$  to the single-point subspace  $\text{LSS}[D_6] = (0, 1)$  for any  $q \in [1, +\infty)$ .

(b)  $\text{PC}_\infty(\Lambda) = \min_{\text{sign}(\Lambda')=0} \|\text{PI}(\Lambda) - \text{PI}(\Lambda')\|_\infty$  is minimised over lattices  $\Lambda'$  whose projected invariant is in one of the three sides of the quotient triangle QT.

*Horizontal side* :  $\text{PI}(\Lambda') = (s, 0)$  for a variable  $s$ . The distance  $\|\text{PI}(\Lambda) - \text{PI}(\Lambda')\|_\infty = \|(x, y) - (s, 0)\|_\infty = \max\{|x-s|, y\}$  has the minimum value  $y$  for  $s = x$ .

*Vertical side* :  $\text{PI}(\Lambda') = (0, t)$  for a variable  $t$ . The distance  $\|\text{PI}(\Lambda) - \text{PI}(\Lambda')\|_\infty = \|(x, y) - (0, t)\|_\infty = \max\{x, |y-t|\}$  has the minimum  $x$  for  $t = y$ .

*Hypotenuse* :  $\text{PI}(\Lambda') = (s, t)$  for variables  $s, t \geq 0$  such that  $s + t = 1$ . To compute the  $M_\infty$  distance from  $(x, y)$  to  $(s, t)$ , first assume that  $s \geq x$ ,  $t \geq y$ . Then  $\|(x, y) - (s, t)\|_\infty = \max\{s-x, t-y\}$  is minimised when  $s-x = t-y$ . Substituting  $t = 1-s$ , we get  $s-x = 1-s-y$ ,  $s = \frac{1+x-y}{2}$ ,  $t = \frac{1-x+y}{2}$ . One can check that  $s+t = 1$  and  $s \geq x$ ,  $t \geq y$  due to  $x+y \leq 1$  as  $(x, y) \in \text{QT}$ . Then  $s-x = t-y = \frac{1-x-y}{2}$ . It remains to show that the minimum  $M = \frac{1-x-y}{2}$  of the distance from  $(x, y)$  to  $(s, t)$  cannot have a smaller value for  $s \leq x$  or  $t \leq y$ .

If  $s \leq x$ , then  $\|(x, y) - (s, t)\|_\infty = \max\{x-s, t-y\} = \max\{x-1+t, t-y\} \leq t-y$ , whose minimum value  $(1-x) - y$  is not less than  $M = \frac{1-x-y}{2}$  as  $x+y \leq 1$ .

If  $t \leq y$ , then  $\|(x, y) - (s, t)\|_\infty = \max\{s-x, y-t\} = \max\{s-x, y-1+s\} \leq s-x$ , whose minimum value  $(1-y) - x$  is not less than  $M = \frac{1-x-y}{2}$  as  $x+y \leq 1$ .

So  $\text{PC}_\infty(A)$  is the minimum of the above three  $M_\infty$  distances.

$\text{PC}_\infty[D_4](A) = x$  is the distance  $M_\infty$  from  $(x, y)$  to  $\text{LSS}[D_4] = (0, 0)$ .

$\text{PC}_\infty[D_6](A) = 1 - y$  is the distance  $M_\infty$  from  $(x, y)$  to  $\text{LSS}[D_6] = (0, 1)$ .

(c) The quotient triangle QT in Fig. 13 (left) is parameterised by  $0 \leq x < 1$  and  $0 \leq y \leq 1$  such that  $x + y \leq 1$ . By Theorem 6.6(a) the distance  $\text{PC}_2[D_2](A) = \min\{x, y, \frac{1-x-y}{\sqrt{2}}\}$  is maximal when  $x = y = \frac{1-x-y}{\sqrt{2}}$ , so  $x = y = \frac{1}{2+\sqrt{2}}$ . By Theorem 6.6(b)  $\text{PC}_\infty[D_2](A) = \min\{x, y, \frac{1-x-y}{2}\}$  is maximal when  $x = y = \frac{1-x-y}{2}$ ,  $x = y = \frac{1}{4}$ . Then  $x^q \leq x$ ,  $y^q \leq y$  and  $(x^q + y^q)^{1/q} \leq (x+y)^{1/q} \leq 1$  for any  $q \in [1, +\infty)$ . Hence the upper bound  $\text{PC}_q[D_4](A) \leq 1$  holds for any  $q \in [1, +\infty]$  and is achieved for any hexagonal lattice with  $\text{PI} = (0, 1)$ . Similarly, the upper bound  $\text{PC}_q[D_6](A) < 2^{1/q}$  holds for any  $q \in [1, +\infty)$  and is approached but not achieved as  $x \rightarrow 1, y = 0$ . The bound  $\text{PC}_\infty[D_6](A) = 1 - y \leq 1$  holds for any  $A$  and is achieved for any square and rectangular lattice with  $y = 0$ .  $\square$

**Example 6.7 (distances  $\text{RC}_q, \text{PC}_q$ )** Table 5 shows the chiral distances computed by Propositions 6.5, 6.6 for the prominent lattices  $\Lambda_2^\pm, \Lambda_\infty^\pm$  in Example 4.10.  $\blacksquare$

**Table 5** Chiral distances  $\text{PC}_q, \text{RC}_q$  for the lattices  $\Lambda_2^\pm, \Lambda_\infty^\pm$  in Fig. 14 and 15, see Example 6.7.

$\Lambda$	$\Lambda_\infty$	$\Lambda_2$	$\Lambda$	$\Lambda_\infty$	$\Lambda_2$
$\text{PI}(\Lambda)$	$(\frac{1}{4}, \frac{1}{4})$	$(\frac{1}{2+\sqrt{2}}, \frac{1}{2+\sqrt{2}})$	$\text{RI}(\Lambda)$	$(1, 4, 7)$	$(2 - \sqrt{2}, 2\sqrt{2} - 1, 5 - \sqrt{2})$
$\text{PC}_2[D_2]$	$\frac{1}{4}$	$\frac{1}{2+\sqrt{2}}$	$\text{RC}_2[D_2]$	1	$2 - \sqrt{2}$
$\text{PC}_2[D_4]$	$\frac{\sqrt{2}}{4}$	$\sqrt{2} - 1$	$\text{RC}_2[D_4]$	$\frac{\sqrt{13}}{2}$	$(2 - \sqrt{2})\frac{\sqrt{13}}{2}$
$\text{PC}_2[D_6]$	$\frac{\sqrt{10}}{4}$	$\sqrt{2} - \sqrt{2}$	$\text{RC}_2[D_6]$	$3\sqrt{2}$	$\sqrt{2(13 - 3\sqrt{2})}$
$\text{PC}_\infty[D_2]$	$\frac{1}{4}$	$\frac{1}{2+\sqrt{2}}$	$\text{RC}_\infty[D_2]$	1	$2 - \sqrt{2}$
$\text{PC}_\infty[D_4]$	$\frac{1}{4}$	$\frac{1}{2+\sqrt{2}}$	$\text{RC}_\infty[D_4]$	1	$2 - \sqrt{2}$
$\text{PC}_\infty[D_6]$	$\frac{3}{4}$	$\frac{1}{\sqrt{2}}$	$\text{RC}_\infty[D_6]$	3	$\frac{3}{2}$

**Example 6.8 (metrics  $\text{RM}_q^\circ, \text{PM}_q^\circ$ )** Table 6 has  $\text{RM}_q^\circ, \text{PM}_q^\circ$  for  $q = 2, +\infty$  and the prominent lattices  $\Lambda_2^\pm, \Lambda_\infty^\pm$ , which were inversely designed in Example 4.10.

If lattices have the same sign, then  $\text{RM}^\circ, \text{PM}^\circ$  coincide with their unoriented versions by Definition 5.4. For example,  $\text{PM}_q^\circ(\Lambda_2^+, \Lambda_\infty^+)$  is the distance  $M_q$  between

the invariants  $\text{PI}(\Lambda_\infty) = (\frac{1}{4}, \frac{1}{4})$  and  $\text{PI}(\Lambda_2) = (\frac{1}{2+\sqrt{2}}, \frac{1}{2+\sqrt{2}}) = (1 - \frac{1}{\sqrt{2}}, 1 - \frac{1}{\sqrt{2}})$ , so  $\text{PM}_\infty^o(\Lambda_2^+, \Lambda_\infty^+) = \frac{3}{4} - \frac{1}{\sqrt{2}} \approx 0.04$  and  $\text{PM}_2^o(\Lambda_2^+, \Lambda_\infty^+) = \frac{3}{4}\sqrt{2} - 1 \approx 0.06$ .

Similarly,  $\text{RM}_q^o(\Lambda_2^+, \Lambda_\infty^+)$  is the  $M_q$  distance between the root invariants  $\text{PI}(\Lambda_\infty) = (1, 4, 7)$  and  $\text{RI}(\Lambda_2) = (2 - \sqrt{2}, 2\sqrt{2} - 1, 5 - \sqrt{2})$ , so  $\text{RM}_\infty^o(\Lambda_2^+, \Lambda_\infty^+) = \max\{\sqrt{2} - 1, 5 - 2\sqrt{2}, 2 + \sqrt{2}\} = 2 + \sqrt{2} \approx 3.41$  and  $\text{RM}_2^o(\Lambda_2^+, \Lambda_\infty^+) = \sqrt{6(7 - 3\sqrt{2})} \approx 4.1$ .

By Lemma 6.3(b) the distance between mirror bright2021proof of the same lattice equals the doubled  $D_2$ -chiral distance. For example,  $\text{PM}_q^o(\Lambda_\infty^+, \Lambda_\infty^-) = 2\text{PC}_q[D_2](\Lambda_\infty) = \frac{1}{2}$  and  $\text{PM}_q^o(\Lambda_2^+, \Lambda_2^-) = 2\text{PC}_q[D_2](\Lambda_2) = \frac{2}{2+\sqrt{2}} = 2 - \sqrt{2} \approx 0.59$  for  $q = 2, +\infty$ .

Lemma 6.3(b) and Table 5 also give  $\text{RM}_q^o(\Lambda_\infty^+, \Lambda_\infty^-) = 2\text{RC}_q[D_2](\Lambda_\infty) = 2$  and  $\text{RM}_q^o(\Lambda_2^+, \Lambda_2^-) = 2\text{RC}_q[D_2](\Lambda_2) = 2(2 - \sqrt{2}) \approx 1.17$  for  $q = 2, +\infty$ .

Lemma 5.6 says that  $\text{RM}^o(\Lambda_2^+, \Lambda_\infty^-) = \text{RM}^o(\Lambda_2^-, \Lambda_\infty^+)$  and  $\text{PM}^o(\Lambda_2^+, \Lambda_\infty^-) = \text{PM}^o(\Lambda_2^-, \Lambda_\infty^+)$ . Using the above properties, it remains to find four distances.

Proposition 5.9(a) finds  $\text{PM}_2^o(\Lambda_2^+, \Lambda_\infty^-)$  as the minimum of the Euclidean distances from  $\text{PI}(\Lambda_2) = (\frac{1}{2+\sqrt{2}}, \frac{1}{2+\sqrt{2}}) = (1 - \frac{1}{\sqrt{2}}, 1 - \frac{1}{\sqrt{2}})$  to the three points  $(-\frac{1}{4}, \frac{1}{4})$ ,  $(-\frac{1}{4}, \frac{1}{4})$ ,  $(\frac{3}{4}, \frac{3}{4})$  obtained from  $\text{PI}(\Lambda_\infty) = (\frac{1}{4}, \frac{1}{4})$  by reflections in the edges of QT. The first two distances equal to  $\frac{\sqrt{25-16\sqrt{2}}}{2\sqrt{2}} \approx 0.54$  are larger than the third.

Given  $\text{PI}(\Lambda_2) = (x_1, y_1) = (1 - \frac{1}{\sqrt{2}}, 1 - \frac{1}{\sqrt{2}})$  and  $\text{PI}(\Lambda_\infty) = (x_2, y_2) = (\frac{1}{4}, \frac{1}{4})$ , Proposition 5.9(b) computes  $\text{PM}_\infty^o(\Lambda_2^+, \Lambda_\infty^-)$  for as the minimum of  $d_x = \max\{x_2 - x_1, y_2 + y_1\} = \frac{5}{4} - \frac{1}{\sqrt{2}}$ ,  $d_y = \max\{x_2 + x_1, |y_2 - y_1|\} = \frac{5}{4} - \frac{1}{\sqrt{2}}$ ,  $d_{xy} = \max\{x_2 - x_1, 1 - x_2 - y_2 + |1 - y_1 - x_2|\} = \frac{1}{4} + \frac{1}{\sqrt{2}}$ , so  $\text{PM}_\infty^o(\Lambda_2^+, \Lambda_\infty^-) = \frac{5}{4} - \frac{1}{\sqrt{2}} \approx 0.54$

Proposition 5.8(a) computes  $\text{RM}_2^o(\Lambda_2^+, \Lambda_\infty^-)$  as the minimum of the Euclidean distances from  $\text{RI}(\Lambda_2) = (2 - \sqrt{2}, 2\sqrt{2} - 1, 5 - \sqrt{2})$  to the three points  $(-1, 4, 7)$ ,  $(4, 1, 7)$ ,  $(1, 7, 4)$  obtained from  $\text{RI}(\Lambda_\infty) = (1, 4, 7)$  by reflections in the boundaries of TC. The first distance is the smallest, so  $\text{RM}_2^o(\Lambda_2^+, \Lambda_\infty^-) = \sqrt{50 - 22\sqrt{2}} \approx 4.3$ .

Given  $\text{RI}(\Lambda_2) = (r_{12}, r_{01}, r_{02}) = (2 - \sqrt{2}, 2\sqrt{2} - 1, 5 - \sqrt{2})$  and  $\text{RI}(\Lambda_\infty) = (s_{12}, s_{01}, s_{02}) = (1, 4, 7)$ , by Proposition 5.8(b)  $\text{RM}_\infty^o(\Lambda_2^+, \Lambda_\infty^-) = \min\{d_0, d_1, d_2\}$ . Using  $\text{MS}(a, b, c, d) = \max\{|a - b|, |c - d|, \frac{1}{2}|a + b - c - d|\}$ , we compute

$$\begin{aligned} d_0 &= \max\{r_{12} + s_{12}, |r_{01} - s_{01}|, |r_{02} - s_{02}|\} \\ &= \max\{3 - \sqrt{2}, 5 - 2\sqrt{2}, 2 + \sqrt{2}\} = 2 + \sqrt{2} \approx 3.4, \end{aligned}$$

$$\begin{aligned} d_1 &= \max\{\text{MS}(r_{12}, r_{01}, s_{12}, s_{01}), |r_{02} - s_{02}|\} = \\ &= \max\{\text{MS}(r_{12}, r_{01}, s_{12}, s_{01}), 2 + \sqrt{2}\} = \\ &= \max\{\text{MS}(2 - \sqrt{2}, 2\sqrt{2} - 1, 1, 4), 2 + \sqrt{2}\} = \\ &= \max\{\max\{3(\sqrt{2} - 1), 3, 2 - \frac{1}{\sqrt{2}}\}, 2 + \sqrt{2}\} = \max\{3, 2 + \sqrt{2}\} = 2 + \sqrt{2}, \end{aligned}$$

$$\begin{aligned} d_2 &= \max\{|r_{12} - s_{12}|, \text{MS}(r_{01}, r_{02}, s_{01}, s_{02})\} = \\ &= \max\{\sqrt{2} - 1, \text{MS}(2\sqrt{2} - 1, 5 - \sqrt{2}, 4, 7)\} = \\ &= \max\{\sqrt{2} - 1, \max\{6 - 3\sqrt{2}, 3, \frac{7-\sqrt{2}}{2}\}\} = 3, \text{ hence } \text{RM}_\infty^o(\Lambda_2^+, \Lambda_\infty^-) = 3. \quad \blacksquare \end{aligned}$$

**Table 6** Metrics  $\text{PM}_q^o$  and  $\text{RM}_q^o$  for the lattices given by their invariants in Table 5, see Fig. 14.

$\text{PM}_2^o$	$\Lambda_\infty^+$	$\Lambda_\infty^-$	$\Lambda_2^+$	$\Lambda_2^-$
$\Lambda_\infty^+$	0	$\frac{1}{2}$	$\frac{3}{4}\sqrt{2} - 1 \approx 0.06$	$\frac{\sqrt{25-16\sqrt{2}}}{2\sqrt{2}} \approx 0.54$
$\Lambda_\infty^-$	$\frac{1}{2}$	0	$\frac{\sqrt{25-16\sqrt{2}}}{2\sqrt{2}} \approx 0.54$	$\frac{3}{4}\sqrt{2} - 1 \approx 0.06$
$\Lambda_2^+$	$\frac{3}{4}\sqrt{2} - 1 \approx 0.06$	$\frac{\sqrt{25-16\sqrt{2}}}{2\sqrt{2}} \approx 0.54$	0	$2 - \sqrt{2} \approx 0.59$
$\Lambda_2^-$	$\frac{\sqrt{25-16\sqrt{2}}}{2\sqrt{2}} \approx 0.54$	$\frac{3}{4}\sqrt{2} - 1 \approx 0.06$	$2 - \sqrt{2} \approx 0.59$	0

$\text{PM}_\infty^o$	$\Lambda_\infty^+$	$\Lambda_\infty^-$	$\Lambda_2^+$	$\Lambda_2^-$
$\Lambda_\infty^+$	0	$\frac{1}{2}$	$\frac{3}{4} - \frac{1}{\sqrt{2}} \approx 0.04$	$\frac{5}{4} - \frac{1}{\sqrt{2}} \approx 0.54$
$\Lambda_\infty^-$	$\frac{1}{2}$	0	$\frac{5}{4} - \frac{1}{\sqrt{2}} \approx 0.54$	$\frac{3}{4} - \frac{1}{\sqrt{2}} \approx 0.04$
$\Lambda_2^+$	$\frac{3}{4} - \frac{1}{\sqrt{2}} \approx 0.04$	$\frac{5}{4} - \frac{1}{\sqrt{2}} \approx 0.54$	0	$2 - \sqrt{2} \approx 0.59$
$\Lambda_2^-$	$\frac{5}{4} - \frac{1}{\sqrt{2}} \approx 0.54$	$\frac{3}{4} - \frac{1}{\sqrt{2}} \approx 0.04$	$2 - \sqrt{2} \approx 0.59$	0

$\text{RM}_2^o$	$\Lambda_\infty^+$	$\Lambda_\infty^-$	$\Lambda_2^+$	$\Lambda_2^-$
$\Lambda_\infty^+$	0	2	$\sqrt{6(7-3\sqrt{2})} \approx 4.1$	$\sqrt{50-22\sqrt{2}}$
$\Lambda_\infty^-$	2	0	$\sqrt{50-22\sqrt{2}} \approx 4.3$	$\sqrt{6(7-3\sqrt{2})}$
$\Lambda_2^+$	$\sqrt{6(7-3\sqrt{2})}$	$\sqrt{50-22\sqrt{2}} \approx 4.3$	0	$2(2-\sqrt{2})$
$\Lambda_2^-$	$\sqrt{50-22\sqrt{2}}$	$\sqrt{6(7-3\sqrt{2})} \approx 4.1$	$2(2-\sqrt{2}) \approx 1.17$	0

$\text{RM}_\infty^o$	$\Lambda_\infty^+$	$\Lambda_\infty^-$	$\Lambda_2^+$	$\Lambda_2^-$
$\Lambda_\infty^+$	0	2	$2 + \sqrt{2} \approx 3.41$	3
$\Lambda_\infty^-$	2	0	3	$2 + \sqrt{2} \approx 3.41$
$\Lambda_2^+$	$2 + \sqrt{2} \approx 3.41$	3	0	$2(2-\sqrt{2}) \approx 1.17$
$\Lambda_2^-$	3	$2 + \sqrt{2} \approx 3.41$	$2(2-\sqrt{2}) \approx 1.17$	0

## 7 Bi-continuity of the map from obtuse superbases to root invariants

Theorems 3.7 and 4.2 established the bijections  $\text{LIS} \rightarrow \text{OSI} \rightarrow \text{RIS}$ ,  $A \mapsto B \rightarrow \text{RI}(B) = \text{RI}(A)$ , mapping any lattice  $A \subset \mathbb{R}^2$  to its (unique up to isometry) obtuse superbase  $B$  and then to the complete invariant  $\text{RI}(A)$ . Hence the Lattice Isometry Space  $\text{LIS}(\mathbb{R}^2)$  having a root metric  $\text{RM}$  can be identified with the Root Invariant Space  $\text{RIS} = (\text{TC}, d)$  having any metric  $d$  on the triangular cone  $\text{TC} \subset \mathbb{R}^3$ .

This section studies continuity of the bijection  $B \mapsto A(B)$ , where an obtuse superbase  $B$  and its lattice  $A(B)$  are considered up to isometry, rigid motion or two types of similarity. To state continuity results, we need metrics on lattices and superbases. Up to each of the four equivalence relations, a lattice  $A$  will be identified with its complete invariant with a relevant metric. For example, up to



isometry, the space  $\text{LIS}(\mathbb{R}^2)$  is represented by root invariants RI with the root metric RM. Now we define natural metrics on obtuse superbases in any  $\mathbb{R}^n$ .

**Definition 7.1 (space OSI of obtuse superbases up to isometry)** (a) Let  $B = \{v_i\}_{i=0}^n$  and  $B' = \{u_i\}_{i=0}^n$  be any obtuse superbases in  $\mathbb{R}^n$ . The Superbase Isometry Metric  $\text{SIM}_\infty(B, B') = \min_{f \in \text{O}(\mathbb{R}^n)} \max_{i=0, \dots, n} |f(u_i) - v_i|$  minimises vector differences over orthogonal maps  $f$  from the group  $\text{O}(\mathbb{R}^n)$ . Let  $\text{OSI}(\mathbb{R}^n)$  denote the space of all obtuse superbases up to isometry with the metric  $\text{SIM}_\infty$ .

(b) Define the space  $\text{OSI}^o(\mathbb{R}^n)$  of obtuse superbases up to rigid motion (orientation-preserving isometry) with the metric  $\text{SIM}_\infty^o(B, B') = \min_{f \in \text{SO}(\mathbb{R}^n)} \max_{i=0, \dots, n} |f(u_i) - v_i|$ .

(c) Define the spaces  $\text{OSS}(\mathbb{R}^n), \text{OSS}^o(\mathbb{R}^n)$  of obtuse superbases up to similarity and orientation-preserving similarity with the Superbase Similarity Metrics  $\text{SSM}_\infty, \text{SSM}_\infty^o$  minimising basis differences over  $\text{O}(\mathbb{R}^n) \times \mathbb{R}_+, \text{SO}(\mathbb{R}^n) \times \mathbb{R}_+$ . ■

Since any continuous function over a compact domain achieves its minimum value and  $\text{SO}(\mathbb{R}^n), \text{O}(\mathbb{R}^n)$  are compact, the minima in Definition 7.1 are achievable.

**Lemma 7.2 (metric axioms for  $\text{SIM}_\infty$ )** The metrics from Definition 7.1 on  $\text{OSI}(\mathbb{R}^n), \text{OSI}^o(\mathbb{R}^n), \text{OSS}(\mathbb{R}^n), \text{OSS}^o(\mathbb{R}^n)$  satisfy all metric axioms in (1.1c). ▲

*Proof* Let  $B_j = \{v_{j0}, \dots, v_{jn}\}$ ,  $j = 1, 2, 3$ , be any obtuse superbases in  $\mathbb{R}^n$ . The first axiom: if  $0 = \text{SIM}_\infty(B_1, B_2) = \min_{f \in \text{O}(\mathbb{R}^n)} \max_{i=0, \dots, n} |f(v_{1i}) - v_{2i}|$ , there is an isometry  $f \in \text{O}(\mathbb{R}^n)$  such that  $f(B_1) = B_2$ . The superbases  $B_1, B_2$  are isometric.

Since any isometry  $f$  preserves Euclidean distance, we get  $|f(v_{1i}) - v_{2i}| = |f^{-1}(f(v_{1i}) - v_{2i})| = |v_{1i} - f^{-1}(v_{2i})|$  and the second axiom:  $\text{SIM}_\infty(B_1, B_2) = \min_{f \in \text{O}(\mathbb{R}^n)} \max_{i=0, \dots, n} |f(v_{1i}) - v_{2i}| = \min_{f^{-1} \in \text{O}(\mathbb{R}^n)} \max_{i=0, \dots, n} |v_{1i} - f^{-1}(v_{2i})| = \text{SIM}_\infty(B_2, B_1)$ .

To prove the triangle inequality in the third axiom for  $\text{SIM}_\infty$ , let  $f, g \in \text{O}(\mathbb{R}^n)$  be rotations that minimise the distances  $\text{SIM}_\infty(B_1, B_2) = \max_{i=0, \dots, n} |f(v_{1i}) - v_{2i}|$  and  $\text{SIM}_\infty(B_2, B_3) = \max_{i=0, \dots, n} |g(v_{2i}) - v_{3i}|$ , respectively. Then we get  $\text{SIM}_\infty(B_1, B_3) \leq \max_{i=0, \dots, n} |g(f(v_{1i})) - v_{3i}| \leq \max_{i=0, \dots, n} |g(f(v_{1i})) - g(v_{2i})| + \max_{i=0, \dots, n} |g(v_{2i}) - v_{3i}| = \max_{i=0, \dots, n} |f(v_{1i}) - v_{2i}| + \text{SIM}_\infty(B_2, B_3) = \text{SIM}_\infty(B_1, B_2) + \text{SIM}_\infty(B_2, B_3)$ . The proof for other spaces is identical after replacing  $\text{O}(\mathbb{R}^n)$  with the relevant groups. □

**Lemma 7.3 (bounds for root products)** Let vectors  $u_1, u_2, v_1, v_2 \in \mathbb{R}^n$  have a maximum length  $l$ , have non-positive scalar products  $u_1 \cdot u_2, v_1 \cdot v_2 \leq 0$ , and be  $\delta$ -close in the Euclidean distance so that  $|u_i - v_i| \leq \delta$  for  $i = 1, 2$ . Then

$$|u_1 \cdot u_2 - v_1 \cdot v_2| \leq 2l\delta \quad \text{and} \quad |\sqrt{-u_1 \cdot u_2} - \sqrt{-v_1 \cdot v_2}| \leq \sqrt{2l\delta}. \quad \blacktriangle$$

*Proof* If  $\sqrt{-u_1 \cdot u_2} + \sqrt{-v_1 \cdot v_2} \leq \sqrt{2l\delta}$ , the difference of square roots is at most  $\sqrt{2l\delta}$ . Assuming that  $\sqrt{-u_1 \cdot u_2} + \sqrt{-v_1 \cdot v_2} \geq \sqrt{2l\delta}$ , it remains to prove that

$$|u_1 \cdot u_2 - v_1 \cdot v_2| = |\sqrt{-u_1 \cdot u_2} - \sqrt{-v_1 \cdot v_2}|(\sqrt{-u_1 \cdot u_2} + \sqrt{-v_1 \cdot v_2}) \leq 2l\delta.$$

We estimate the scalar product  $|u \cdot v| \leq |u| \cdot |v|$  by using Euclidean lengths. Then we apply the triangle inequality for scalars and replace vector lengths by  $l$  as follows:  $|u_1 \cdot u_2 - v_1 \cdot v_2| = |(u_1 - v_1) \cdot u_2 + v_1 \cdot (u_2 - v_2)| \leq |(u_1 - v_1) \cdot u_2| + |v_1 \cdot (u_2 - v_2)| \leq |u_1 - v_1| \cdot |u_2| + |v_1| \cdot |u_2 - v_2| \leq \delta(|u_2| + |v_1|) \leq 2l\delta$  as required.

**Lemma 7.4 (a lower bound of the size)** *If all vectors of an obtuse superbase  $B = \{v_0, v_1, v_2\}$  of a lattice  $\Lambda \subset \mathbb{R}^2$  have a maximum length  $l$ , the size  $\sigma(\Lambda) = r_{12} + r_{01} + r_{02}$  of the lattice  $\Lambda$  has the lower bound  $l \leq \sigma(\Lambda)$ .  $\blacktriangle$*

*Proof* Let  $|v_1| = l$ . Formula 2.7(a) gives  $p_{12} + p_{01} = v_1^2 = l^2$  and  $r_{12} + r_{01} + r_{02} = \sqrt{(r_{12} + r_{01} + r_{02})^2} \geq \sqrt{r_{12}^2 + r_{01}^2 + r_{02}^2} = \sqrt{p_{12} + p_{01} + p_{02}} \geq l$ .  $\square$

For  $q = +\infty$ , both  $2^{1/q}, 3^{1/q}$  are interpreted as their limit 1 when  $q \rightarrow +\infty$ .

**Theorem 7.5 (continuity of  $\text{OSI} \rightarrow \text{LIS} = \text{RIS}$ ) (a)** *Let  $q \in [1, +\infty]$  and lattices  $\Lambda, \Lambda' \subset \mathbb{R}^2$  have obtuse superbases  $B$  and  $B'$  whose vectors have a maximum length  $l$ . If  $\text{SIM}_\infty(B, B') = \delta \geq 0$ , then  $\text{RM}_q(\Lambda, \Lambda') \leq 3^{1/q} \sqrt{2l\delta}$ . Hence the bijection  $\text{OSI}(\mathbb{R}^2) \rightarrow \text{LIS}(\mathbb{R}^2)$  is continuous in the metrics  $\text{SIM}_\infty$  and  $\text{RM}_q$ .*

*(b) In the conditions above, the projected metric satisfies  $\text{PM}_q(\Lambda, \Lambda') \leq 2^{1/q} 3 \sqrt{2\delta/l}$ , so the bijection  $\text{OSS}(\mathbb{R}^2) \rightarrow \text{LSS}(\mathbb{R}^2)$  is continuous in the metrics  $\text{SIM}_\infty, \text{PM}_q$ .*

*(c) In the oriented case, if  $\delta \rightarrow 0$  then  $\text{RM}_q^o(\Lambda, \Lambda') \rightarrow 0$  and  $\text{PM}_q^o(\Lambda, \Lambda') \rightarrow 0$ , so both  $\text{OSI}^o(\mathbb{R}^2) \rightarrow \text{LIS}^o(\mathbb{R}^2)$  and  $\text{OSS}^o(\mathbb{R}^2) \rightarrow \text{LSS}^o(\mathbb{R}^2)$  are continuous.  $\blacktriangle$*

*Proof (a)* One can assume that given obtuse superbases  $B = (v_0, v_1, v_2)$  and  $B' = (u_0, u_1, u_2)$  satisfy  $|u_i - v_i| \leq \delta$  for  $i = 0, 1, 2$  after applying a suitable isometry to  $B'$  by Definition 7.1. Lemma 7.3 implies that the root products  $r_{ij} = \sqrt{-v_i \cdot v_j}$  and  $\sqrt{-u_i \cdot u_j}$  differ by at most  $2l\delta$  for any pair  $(i, j)$  of indices. The  $M_q$ -norm of the vector difference in  $\mathbb{R}^3$  is  $\text{RM}_q(\Lambda, \Lambda') \leq 3^{1/q} \sqrt{2l\delta}$ ,  $q \in [1, +\infty]$ .

*(b)* The coordinates  $x = \bar{r}_{02} - \bar{r}_{01}$  and  $y = 3\bar{r}_{12}$  have an error bound that is at most three times larger than the error for  $\bar{r}_{ij}$ . In Definition 4.5 each  $\bar{r}_{ij}$  is obtained by dividing the root product  $r_{ij}$  by the sizes with the lower bound  $l \leq \sigma = r_{12} + r_{01} + r_{02}$  by Lemma 7.4. The above error bound  $\sqrt{2l\delta}$  for  $r_{ij}$  gives the error bound  $3\sqrt{2\delta/l}$  for  $x, y$ . Then  $\text{PM}_q(\Lambda, \Lambda') \leq 2^{1/q} 3 \sqrt{2\delta/l}$ ,  $q \in [1, +\infty]$ .

*(c)* In the oriented case, if  $\text{sign}(\Lambda) > 0$ , then  $\text{RI}(\Lambda)$  is strictly inside the triangular cone TC. The continuity of RM implies that under any continuous motion of  $\delta$ -close superbases  $B \rightarrow B'$ , if  $\delta$  is sufficiently small, then all intermediate lattices have their unoriented root invariants inside TC, so their signs are positive and  $\text{sign}(\Lambda') > 0$ . Hence  $\text{sign}(\Lambda), \text{sign}(\Lambda')$  coincide or one of them is 0. In all cases by Definition 5.4 the metric  $\text{RM}^o(\Lambda, \Lambda')$  coincides with  $\text{RM}(\Lambda, \Lambda')$  whose convergence to 0 as  $\delta \rightarrow 0$  was proved above. The proof of  $\text{PM}^o(\Lambda, \Lambda') \rightarrow 0$  is similar.  $\square$

Theorem 7.5 is proved for the metrics  $\text{RM}_q, \text{PM}_q$  only to give explicit upper bounds. A similar argument proves continuity for any metrics RM, PM in Definition 5.1 based on a metric  $d(u, v) \rightarrow 0$  when  $u \rightarrow v$  coordinate-wise. All Minkowski norms in  $\mathbb{R}^n$  are topologically equivalent [1] due to the bounds  $\|v\|_q \leq \|v\|_r \leq n^{\frac{1}{q} - \frac{1}{r}} \|v\|_q$  for any  $1 \leq q \leq r$ , hence continuity for one value of  $q$  is enough. Theorem 7.5 implies continuity of  $\text{OSI}^o \rightarrow \text{RIS}^o$ , because closeness of superbases up to rigid motion is a stronger condition than up to isometry.

Example 7.6 illustrates Theorem 7.5 and shows that the root invariant changes continuously for a deformation when a reduced basis changes discontinuously.

**Example 7.6 (continuity of root invariants)** *The obtuse superbase  $v_1 = (1, 0)$ ,  $v_2(t) = (-t, 2)$ ,  $v_0(t) = (t-1, -2)$  continuously deforms for  $t \in [0, 1]$  in Fig. 4. The basis of  $v_1, v_2(t)$  is reduced (non-acute) for  $t \in [0, \frac{1}{2}]$  and at the critical moment  $t = \frac{1}{2}$  changes to its mirror image  $v_1, v_0(t)$ , which remains reduced for  $t \in [\frac{1}{2}, 1]$ . The obtuse superbase of unordered vectors  $\{v_1, v_2(t), v_0(t)\}$  keeps changing continuously because  $v_2(t), v_0(t)$  only swap their places at  $t = \frac{1}{2}$ . The discontinuity of the obtuse superbases in the above deformation emerges at  $t = 1$  when the final superbase of  $(1, 0), (-1, 2), (0, -2)$  becomes a mirror image of the initial superbase of  $(1, 0), (0, 2), (-1, -2)$ , not related by rigid motion, though both (unordered) superbases at  $t = 0, 1$  generate the same lattice with the rectangular cell  $1 \times 2$ .*

The root invariants are  $r_{12} = \sqrt{t}$ ,  $r_{01} = \sqrt{1-t}$ ,  $r_{02} = \sqrt{4-t+t^2}$ . Since  $4-t+t^2 \geq \frac{15}{4} \geq \max\{t, 1-t\}$  for  $t \in [0, 1]$ , the root invariant can be written as

$$\text{RI}(\Lambda(t)) = \begin{cases} (\sqrt{t}, \sqrt{1-t}, \sqrt{4-t+t^2}) & \text{for } t \in [0, \frac{1}{2}], \\ (\sqrt{1-t}, \sqrt{t}, \sqrt{4-t+t^2}) & \text{for } t \in [\frac{1}{2}, 1]. \end{cases}$$

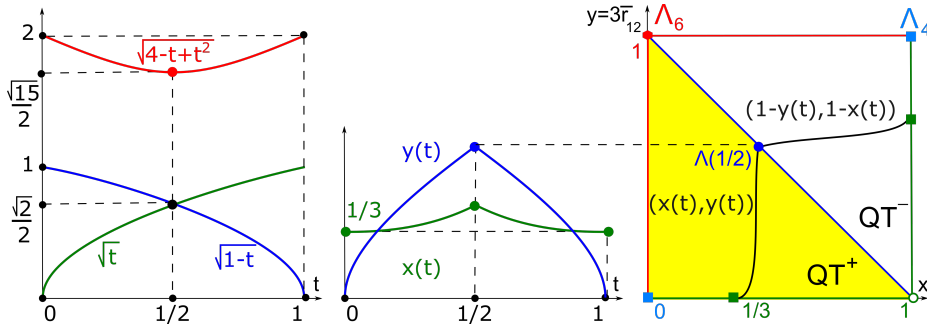


**Fig. 20** **Left:** graphs of root products in  $\text{RI}(\Lambda(t))$ , see Example 7.6. **Middle:** graphs of the components in  $\text{PI}(\Lambda(t))$ . **Right:** the continuous path of  $\text{PI}(\Lambda(t))$  in the quotient square  $QS$ .

By Definition 4.5 the size is  $\sigma(\Lambda(t)) = r_{12} + r_{01} + r_{02} = \sqrt{t} + \sqrt{1-t} + \sqrt{4-t+t^2}$ . The projected invariant is  $\text{PI}(\Lambda(t)) = (x(t), y(t))$ , see Fig. 23. where

$$x(t) = \frac{\sqrt{4-t+t^2} - \max\{\sqrt{t}, \sqrt{1-t}\}}{\sqrt{t} + \sqrt{1-t} + \sqrt{4-t+t^2}}, \quad y(t) = \frac{3 \min\{\sqrt{t}, \sqrt{1-t}\}}{\sqrt{t} + \sqrt{1-t} + \sqrt{4-t+t^2}}.$$

If  $t = 0$  or  $t = 1$ , then  $\text{RI}(\Lambda(t)) = (0, 1, 2)$ ,  $\sigma(\Lambda(t)) = 3$ ,  $\text{PI}(\Lambda(t)) = (\frac{1}{3}, 0)$ . If  $t = \frac{1}{2}$ , then  $\sqrt{t} = \sqrt{1-t} = \frac{\sqrt{2}}{2}$ ,  $\sqrt{4-t+t^2} = \frac{\sqrt{15}}{2}$ ,  $\sigma(\Lambda(\frac{1}{2})) = \sqrt{2} + \frac{\sqrt{15}}{2}$ . So

$$\text{RI}\left(\Lambda\left(\frac{1}{2}\right)\right) = \left(\frac{\sqrt{2}}{2}, \frac{\sqrt{2}}{2}, \frac{\sqrt{15}}{2}\right), \quad \text{PI}\left(\Lambda\left(\frac{1}{2}\right)\right) = \left(\frac{\sqrt{15} - \sqrt{2}}{\sqrt{15} + 2\sqrt{2}}, \frac{3\sqrt{2}}{\sqrt{15} + 2\sqrt{2}}\right).$$

The last point is approximately  $(0.37, 0.63)$  in the diagonal  $x + y = 1$  of  $QS$ . Under the symmetry  $t \leftrightarrow 1-t$ , all the functions above remain invariant and  $\Lambda(t)$  changes its sign. Both paths  $\text{RI}(\Lambda(t))$  and  $\text{PI}(\Lambda(t)) \in QS$  are continuous everywhere, while the obtuse superbasis is discontinuous (up to rigid motion) at  $t = 0, 1$ . ■

Theorem 7.7 below proves the inverse continuity of  $\text{RIS} \rightarrow \text{OSI}$  and a weaker claim in the oriented case saying that we can choose an obtuse superbase  $B'$  of a perturbed lattice arbitrarily close to a given superbase  $B$  of an original lattice.

**Theorem 7.7 (continuity of  $\text{LIS} \rightarrow \text{OSI}$ )** (a) For  $q \in [1, +\infty]$ , let lattices  $\Lambda, \Lambda'$  in  $\mathbb{R}^2$  satisfy  $\text{RM}_q(\Lambda, \Lambda') \leq \delta$ . For any obtuse superbase  $B$  of  $\Lambda$ , there is an obtuse superbase  $B'$  of  $\Lambda'$  such that  $\text{SIM}_\infty(B, B') \leq \text{SIM}_\infty^\circ(B, B') \rightarrow 0$  as  $\delta \rightarrow 0$ .

(b) The bijection  $\text{LIS}(\mathbb{R}^2) \rightarrow \text{OSI}(\mathbb{R}^2)$  is continuous in the metrics  $\text{RM}_q, \text{SIM}_\infty$ .  $\text{LIS}^\circ(\mathbb{R}^2) \rightarrow \text{OSI}^\circ(\mathbb{R}^2)$  is continuous in  $\text{RM}_q^\circ, \text{SIM}_\infty^\circ$  at non-rectangular lattices.

(c) The above conclusions hold for lattices and superbases up to similarity.  $\blacktriangle$

*Proof (a)* The obtuse superbase  $B = (v_0, v_1, v_2)$  of  $\Lambda$  is already given. Let  $B' = (u_0, u_1, u_2)$  be any obtuse superbase of  $\Lambda'$  found from  $\text{RI}(\Lambda')$  by Lemma 4.1.

Up to rigid motion in  $\mathbb{R}^2$ , one can assume that  $\Lambda, \Lambda'$  share the origin and the first vectors  $v_0, u_0$  lie in the positive  $x$ -axis. Let  $r_{ij}, s_{ij}$  be the root products of  $B, B'$ , respectively. Formulae (2.7a) imply that  $v_i^2 = r_{ij}^2 + r_{ik}^2$  and  $u_i^2 = s_{ij}^2 + s_{ik}^2$  for distinct indices  $i, j, k \in \{0, 1, 2\}$ , for example if  $i = 0$  then  $j = 1, k = 2$ .

For any given continuous transformation of root invariants from  $\text{RI}(\Lambda)$  to  $\text{RI}(\Lambda')$ , all root products have a finite upper bound  $M$ , which we use to estimate

$$\begin{aligned} |v_i^2 - u_i^2| &= |(r_{ij}^2 + r_{ik}^2) - (s_{ij}^2 + s_{ik}^2)| \leq |r_{ij}^2 - s_{ij}^2| + |r_{ik}^2 - s_{ik}^2| = \\ &(r_{ij} + s_{ij})|r_{ij} - s_{ij}| + (r_{ik} + s_{ik})|r_{ik} - s_{ik}| \leq (r_{ij} + s_{ij})\delta + (r_{ik} + s_{ik})\delta \leq 4M\delta. \end{aligned}$$

Since at least two continuously changing conorms are strictly positive to guarantee positive lengths of basis vectors by formula (2.7a), all basis vectors reconstructed by Lemma 4.1 have a minimum length  $a > 0$ . Then  $||v_i| - |u_i|| \leq \frac{4M\delta}{|v_i| + |u_i|} \leq \frac{2M}{a}\delta$ . Since the vectors  $v_0, u_0$  lie in the positive horizontal axis, the lengths can be replaced by vectors:  $|v_0 - u_0| \leq \frac{2M}{a}\delta$ , so  $|v_0 - u_0| \rightarrow 0$  as  $\delta \rightarrow 0$ .

If the superbases  $B, B'$  have opposite signs, apply to  $B'$  the reflection with respect the fixed  $x$ -axis. To conclude that  $\text{SIM}_\infty(B, B') \rightarrow 0$ , we show below that the basis vectors  $v_i, u_i$  from both superbases have close angles  $\alpha_i, \beta_i$  measured anticlockwise from the positive  $x$ -axis for  $i = 1, 2$ . To estimate the small difference  $\alpha_i - \beta_i$ , we first express the angles via the root products by Lemma 4.1:

$$\begin{aligned} \alpha_i &= \arccos \frac{v_0 \cdot v_i}{|v_0| \cdot |v_i|} = \arccos \frac{-r_{0i}^2}{\sqrt{r_{01}^2 + r_{02}^2} \sqrt{r_{ij}^2 + r_{ik}^2}}, \\ \beta_i &= \arccos \frac{u_0 \cdot u_i}{|u_0| \cdot |u_i|} = \arccos \frac{-s_{0i}^2}{\sqrt{s_{01}^2 + s_{02}^2} \sqrt{s_{ij}^2 + s_{ik}^2}}, \end{aligned}$$

where  $j \neq k$  differ from  $i = 1, 2$ . If  $\delta \rightarrow 0$ , then  $s_{ij} \rightarrow r_{ij}$  and  $\alpha_i - \beta_i \rightarrow 0$  for all indices because all functions above are continuous for  $|u_j|, |v_j| \geq a, j = 0, 1, 2$ .

We estimate the squared length of the difference by using the scalar product:

$$|v_i - u_i|^2 = v_i^2 + u_i^2 - 2u_i \cdot v_i = (|v_i|^2 - 2|u_i| \cdot |v_i| + |u_i|^2) + 2|u_i| \cdot |v_i| - 2|u_i| \cdot |v_i| \cos(\alpha_i - \beta_i)$$

$$\begin{aligned}
&= (|v_i| - |u_i|)^2 + 2|u_i| \cdot |v_i|(1 - \cos(\alpha_i - \beta_i)) = (|v_i| - |u_i|)^2 + |u_i| \cdot |v_i| 4 \sin^2 \frac{\alpha_i - \beta_i}{2} \leq \\
&\leq (|v_i| - |u_i|)^2 + |u_i| \cdot |v_i| 4 \left( \frac{\alpha_i - \beta_i}{2} \right)^2 = (|v_i| - |u_i|)^2 + |u_i| \cdot |v_i| (\alpha_i - \beta_i)^2,
\end{aligned}$$

where we used that  $|\sin x| \leq |x|$  for  $x \in \mathbb{R}$ . The upper bound  $M$  of root products guarantees a fixed upper bound for the lengths  $|u_i|, |v_i|$ . If  $\delta \rightarrow 0$ , then  $|v_i| - |u_i| \rightarrow 0$  and  $\alpha_i - \beta_i \rightarrow 0$  as proved above, so  $v_i - u_i \rightarrow 0$  and  $\text{SIM}_\infty(B, B') \rightarrow 0$ . Since the metric  $\text{SIM}_\infty$  from Definition 7.1 is minimised over the larger group  $\text{O}(\mathbb{R}^2)$  in comparison with  $\text{SO}(\mathbb{R}^2)$ , we have  $\text{SIM}_\infty(B, B') \leq \text{SIM}_\infty^\circ(B, B') \rightarrow 0$  as  $\delta \rightarrow 0$ .

(b) By Theorem 3.7, the obtuse superbases  $B, B'$  of  $\Lambda, \Lambda'$  are unique up to isometry, also up to rigid motion if  $\Lambda, \Lambda'$  are not rectangular. Since we can start with any obtuse superbase  $B$ , the convergence  $\text{SIM}_\infty^\circ(B, B') \rightarrow 0$  for a unique obtuse superbase  $B'$  proves the continuity of  $\text{LIS}(\mathbb{R}^2) \rightarrow \text{OSI}(\mathbb{R}^2)$ . The continuity of  $\text{LIS}^\circ(\mathbb{R}^2) \rightarrow \text{OSI}^\circ(\mathbb{R}^2)$  similarly follows for all non-rectangular lattices.

(c) To extend part (a) to the similarity equivalence, we use the size  $\sigma = r_{12} + r_{01} + r_{02}$  of the given superbase  $B$  to reconstruct an obtuse superbase  $B'$  of  $\Lambda'$  from  $\text{PI}(\Lambda')$  with the same size  $\sigma$  by Proposition 4.9. By formula (4.9) the given condition  $\text{PM}_q(\Lambda, \Lambda') \rightarrow 0$  implies that  $\text{RM}_q(\Lambda, \Lambda') \rightarrow 0$ , hence part (a) implies the required conclusions for the smaller metrics  $\text{SSM}_\infty \leq \text{SIM}_\infty$  and  $\text{SSM}_\infty^\circ \leq \text{SIM}_\infty^\circ$ . The same argument extends part (b) to the similarity case.  $\square$

Lemma 7.8 proves a non-trivial lower bound needed for Corollary 7.9 later.

**Lemma 7.8 (lower bound for  $\text{SIM}_\infty^\circ$ )** *For any ordered obtuse superbases  $B, B'$  of lattices in  $\mathbb{R}^2$  with coforms  $\text{CF}(B) = (p_{12}, p_{01}, p_{02})$  and  $\text{CF}(B') = (p'_{12}, p'_{01}, p'_{02})$ , let  $\text{CM}_\infty(B, B') = \min_{\zeta \in A_3} \max_{i \neq j} \{|p_{ij} - p'_{\zeta(i)\zeta(j)}|\}$  be minimised over three cyclic permutations  $\zeta \in A_3$  of indices  $0, 1, 2$ . Let  $l$  be a maximum length of all vectors from  $B, B'$ . Then we have the lower bound  $\text{SIM}_\infty^\circ(B, B') \geq \text{CM}_\infty(B, B')/2l$ .  $\blacktriangle$*

*Proof* For the superbase  $B = \{v_0, v_1, v_2\}$ , by Definition 7.1 find an optimal rotation around the origin so that the resulting image  $\{v'_0, v'_1, v'_2\}$  of  $B'$  satisfies  $|u_i - v_i| \leq \text{SIM}_\infty^\circ(B, B')$ ,  $i = 0, 1, 2$ . Lemma 7.3 implies that  $|p_{ij} - p'_{ij}| \leq 2l \cdot \text{SIM}_\infty^\circ(B, B')$  for all distinct  $i, j \in \{0, 1, 2\}$ . The above rotation might have cyclically shifted the coforms of  $B'$ , but  $\text{CM}_\infty(B, B')$  is minimised over cyclic permutations. Then  $\text{CM}_\infty(B, B') \leq \max_{i \neq j} \{|p_{ij} - p'_{ij}|\} \leq 2l \cdot \text{SIM}_\infty^\circ(B, B')$  gives the lower bound.  $\square$

One can prove that the min-max distance in Lemma 7.8 satisfies all metric axioms. Corollary 7.9 shows that Theorem 7.7(b) is the strongest possible continuity in the oriented case. In  $\mathbb{R}^3$ , a similar discontinuity around high-symmetry lattices will be much harder to resolve for continuous invariants even up to isometry [22].

**Corollary 7.9 (partial discontinuity of  $\text{RIS}^\circ \rightarrow \text{OSI}^\circ$ )** *The bijection  $\text{LIS}^\circ \rightarrow \text{OSI}^\circ$  is discontinuous in the metrics  $\text{RM}_\infty, \text{SIM}_\infty^\circ$  at any rectangular lattice.  $\blacktriangle$*

*Proof* For any  $0 \leq 3\delta < a < b$ , start from any rectangular lattice with a unit cell  $a \times b$  and consider the lattices  $\Lambda^\pm(\delta) \subset \mathbb{R}^2$  with the obtuse superbases

$$B^+(\delta) : \quad v_1 = (a, 0) \quad v_2^+(\delta) = (-\delta, b) \quad v_0^+(\delta) = (\delta - a, -b)$$

$$B^-(\delta) : \quad v_1 = (a, 0) \quad v_2^-(\delta) = (\delta - a, b) \quad v_0^-(\delta) = (-\delta, -b)$$

Notice that the vectors in both superbases are ordered anticlockwise around 0. The initial lattice  $\Lambda^\pm(0)$  has two superbases  $v_1 = (a, 0)$ ,  $v_2^\pm(0) = (0, \pm b)$ ,  $v_0 = (-a, \mp b)$  related by reflection, not by rigid motion, see Fig. 1 (right).

Keeping the anticlockwise order above, write the ordered coforms below.

$$\begin{aligned} \text{CF}(B^+(\delta)) \quad & -v_1 \cdot v_2^+ = \delta a & -v_0 \cdot v_1^+ = a^2 - \delta a & -v_0 \cdot v_2^+ = b^2 - \delta a + \delta^2 \\ \text{CF}(B^-(\delta)) \quad & -v_1 \cdot v_2^- = a^2 - \delta a & -v_0 \cdot v_1^- = \delta a & -v_0 \cdot v_2^- = b^2 - \delta a + \delta^2 \end{aligned}$$

The above coforms differ by the transposition of the first two conorms. The maximum difference of all corresponding conorms in  $\text{CF}(B^\pm(\delta))$  is  $a^2 - 2\delta a$ . If we cyclically shift  $\text{CF}(B^-(\delta))$  to the left, the maximum difference becomes  $b^2 - a^2 + \delta^2$ . If we cyclically shift  $\text{CF}(B^-(\delta))$  to the right, the maximum difference becomes  $b^2 - 2\delta a + \delta^2$ . By Lemma 7.8 and  $\delta < \frac{a}{3}$ , the cyclic metric between the coforms is

$$\text{CM}_\infty(B^+(\delta), B^-(\delta)) = \min\{a^2 - 2\delta a, b^2 - a^2 + \delta^2, b^2 - 2\delta a + \delta^2\} \geq \min\{\frac{a^2}{3}, b^2 - a^2\}.$$

Since the vectors of  $B^\pm(\delta)$  have a maximum length  $l \leq \sqrt{a^2 + b^2}$ , we get

$$\text{SIM}_\infty^o(B^+(\delta), B^-(\delta)) \geq \text{CM}_\infty(B^+(\delta), B^-(\delta))/2l \geq \min\{\frac{a^2}{3}, b^2 - a^2\}/2\sqrt{a^2 + b^2}.$$

This lower bound shows that, for any  $0 < \delta < \frac{a}{3}$ , the (unique up to rigid motion) obtuse superbases  $B^\pm(\delta)$  of the lattices  $\Lambda^\pm(\delta)$  are not close in the metric  $\text{SIM}_\infty^o$ .

The lattices  $\Lambda^\pm(\delta)$  have  $\text{RI}(\Lambda^\pm(\delta))$  consisting of  $\sqrt{\delta a}$ ,  $\sqrt{a^2 - \delta a}$ ,  $\sqrt{b^2 - a^2 + \delta^2}$ , which might need to be ordered. Since the lattices  $\Lambda^\pm(\delta)$  are related by reflection, Lemma 6.3(b) computes  $\text{RM}(\Lambda^+(\delta), \Lambda^-(\delta))$  as the double distance  $2\text{RC}[D_2](\Lambda(\delta))$  depending only on the root invariant above without signs. For the Minkowski parameter  $q = +\infty$ , Proposition 6.5(a) computes the required distance as follows:

$$\text{RC}_\infty[D_2](\Lambda(\delta)) = \min\{\delta a, \frac{a^2 - 2\delta a}{2}, \frac{b^2 - 2a^2 + \delta a + \delta^2}{2}\} \leq \delta a \rightarrow 0 \text{ as } \delta \rightarrow 0.$$

Hence the lattices  $\Lambda^\pm(\delta)$  have close root invariants with  $\text{RM}_\infty(\Lambda^+(\delta), \Lambda^-(\delta)) \rightarrow 0$  as  $\delta \rightarrow 0$ , but their obtuse superbases have a constant lower bound for the metric  $\text{SIM}_\infty^o$  independent of  $\delta$ . The discontinuity conclusion holds for all  $q \in [1, +\infty)$ , because all Minkowski distances  $M_q$  are topologically equivalent [1].  $\square$

Corollary 7.9 should be positively interpreted in the sense that we need to study lattices up to rigid motion by their complete oriented root invariants in the continuous space  $\text{LIS}^o(\mathbb{R}^2)$  rather than in terms of reduced bases (or, equivalently, obtuse superbases due to Proposition 3.10b), which are inevitably discontinuous.

Proposition 7.10 shows that all  $G$ -chiral distances  $\text{RC}[G] : \text{LIS}(\mathbb{R}^2) \rightarrow \mathbb{R}$  and  $\text{PC}[G] : \text{LSS}(\mathbb{R}^2) \rightarrow \mathbb{R}$  are continuous in any metrics  $\text{RM}, \text{PM}$  from Definition 5.1.

**Proposition 7.10 (continuous chiral distances)** *For a crystallographic point group  $G$  and lattices  $\Lambda_1, \Lambda_2$  in  $\mathbb{R}^2$ , we have  $|\text{RC}[G](\Lambda_1) - \text{RC}[G](\Lambda_2)| \leq \text{RM}(\Lambda_1, \Lambda_2)$  and  $|\text{PC}[G](\Lambda_1) - \text{PC}[G](\Lambda_2)| \leq \text{PM}(\Lambda_1, \Lambda_2)$  for any metrics  $\text{RM}$  and  $\text{PM}$ .  $\blacktriangle$*

*Proof* In Definition 6.1 let  $A_1, A_2 \in \text{LIS}[G]$  be lattices that minimise  $\text{RC}[G](A_1) = \text{RM}(A_1, A'_1)$  and  $\text{RC}[G](A_2) = \text{RM}(A_2, A'_2)$ . The triangle inequality implies that  $\text{RC}[G](A_1) \leq \text{RM}(A_1, A'_2) \leq \text{RM}(A_1, A_2) + \text{RM}(A_2, A'_2) = \text{RM}(A_1, A_2) + \text{RC}[G](A_2)$  and  $\text{RC}[G](A_1) - \text{RC}[G](A_2) \leq \text{RM}(A_1, A_2)$ . Swapping indices  $1 \leftrightarrow 2$ , we similarly get  $\text{RC}[G](A_2) - \text{RC}[G](A_1) \leq \text{RM}(A_1, A_2)$ . Hence we get the required upper bound  $|\text{RC}[G](A_1) - \text{RC}[G](A_2)| \leq \text{RM}(A_2, A_1)$ . The proof for  $\text{PC}[G]$  is similar.  $\square$

### 8 New mathematical structures on lattices, conclusions, and discussion

This section first connects the recent invariants of more general periodic point sets with the complete invariants of lattices. Then we discuss linear operations, scalar products,  $\text{CAT}(0)$  property of  $\text{LIS}(\mathbb{R}^2)$  and finally describe the future work.

Below we prove that other continuous isometry invariants AMD (average minimum distances) and PDD (pointwise distance distribution) are complete for lattices, though they make sense for general periodic and finite point sets [41,40]. Other isometry invariants such as persistent homology turned out to be weaker than expected, see generic families of sets that have identical persistence in [33].

**Definition 8.1 (RSD invariant)** For any lattice  $A \subset \mathbb{R}^n$ , both AMD and PDD invariants reduce to the sequence of distances  $(d_1, d_1, d_2, d_2, d_3, d_3, \dots)$  from the origin  $0 \in A$  to its  $k$ -th nearest neighbour in  $A$  for  $k \geq 1$ . Since any  $A$  is symmetric with respect to  $0$ , define the Reduced Sequence of Distances  $\text{RSD}(A) = (d_1, d_2, d_3, \dots)$  containing one distance from each pair of equal distances above.  $\blacksquare$

In 1938 Delone reduced  $\text{RSD}(A)$  even further and considered only distinct increasing distances [16, p. 163]. He proved that the resulting weaker invariant (of only the first four distinct distances) is complete for all lattices  $A \subset \mathbb{R}^2$  except the two lattices  $A_6, A$  in Fig. 21, which are distinguished by the stronger RSD:

$$\text{RSD}(A_6) = (1, 1, 1, \sqrt{3}, \sqrt{3}, \sqrt{3}, 2, 2, 2, \sqrt{7}, \sqrt{7}, \sqrt{7}, \sqrt{7}, \sqrt{7}, \sqrt{7}, \sqrt{7}, 3, 3, 3, \dots),$$

$$\text{RSD}(A) = (1, \sqrt{3}, 2, 2, 2, \sqrt{7}, \sqrt{7}, 3, \dots).$$

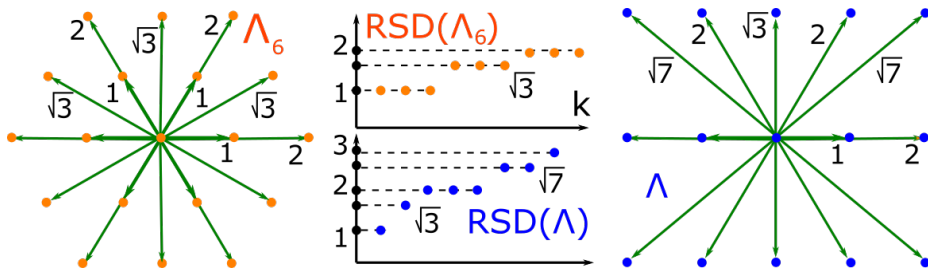


**Fig. 21** Left and Right: first neighbours of the origin  $0$  in the hexagonal lattice  $A_6$  and rectangular lattice  $A$  with unit cell  $1 \times \sqrt{3}$ . Middle:  $\text{RSD}(A_6)$  and  $\text{RSD}(A)$ , see Definition 8.1.

Any quadratic form  $Q(x, y)$  is uniquely determined (up to a linear change of variables) by the sets of its values with the only exception of  $Q_6 = x^2 + xy + y^2$  and  $Q = x^2 + 3y^2$  corresponding to the lattices in Fig. 21, see references in [39].

For any lattice  $\Lambda \subset \mathbb{R}^n$ , the ‘halved’ sequence RSD contains the same information as AMD and PDD. We conjecture that PDD is complete for all finite and periodic points sets in  $\mathbb{R}^2$ . Proposition 8.2 means completeness for lattices in  $\mathbb{R}^2$ .

For any lattice  $\Lambda \subset \mathbb{R}^n$ ,  $\text{RSD}(\Lambda)$  can be represented as the *theta series*  $\Theta_\Lambda(q) = \sum_{v \in \Lambda} q^{|v|^2} = 1 + 2 \sum_{k \geq 1} q^{\text{RSD}_k^2(\Lambda)}$ ,  $q \in \mathbb{C}$ . Lecture 2 in [12, p. 45] mentions that  $\Theta_{\Lambda(q)}$  determines the shape of any lattice  $\Lambda \subset \mathbb{R}^2$ , which is proved below via  $\text{RSD}(\Lambda)$ .

**Proposition 8.2 (RSD completeness)** *Any lattices  $\Lambda, \Lambda' \subset \mathbb{R}^2$  are isometric if and only if  $\text{RSD}(\Lambda) = \text{RSD}(\Lambda')$ .*  $\blacktriangle$

*Proof* The lengths  $|v_1| \leq |v_2| \leq |v_0|$  of shortest Voronoi vectors from Fig. 3 are not necessarily the first three distances in RSD. For example, if  $\Lambda$  has the basis  $v_1 = (1, 0)$ ,  $v_2 = (0, 3)$ , then  $\text{RSD}(\Lambda) = (1, 2, 3, \dots)$ , where  $2 = 2|v_1| \neq |v_2| = 3$ . We will extract  $|v_1| \leq |v_2| \leq |v_0|$  from  $\text{RSD}(\Lambda)$ , which proves completeness.

For any integer  $k > 1$ , the shortest Voronoi vector  $v_1 \in \Lambda$  of length  $d_1 = |v_1|$  generates a single integer multiple  $kv_1 \in \Lambda$  of length  $kd_1$ , which can be removed from  $\text{RSD}(\Lambda)$ . The second shortest Voronoi vector  $v_2 \in \Lambda$  may accidentally have the same length  $|v_2| = d_1$ . If not, the next distance  $d_2$  in the resulting sequence equals  $|v_2|$  as in  $\text{RSD}(\Lambda) = \{1, \sqrt{3}, \dots\}$  for the lattice  $\Lambda$  in Fig. 21 (right). If yes, we recognise the repeated value of  $d_1$  as  $d_2 = |v_2|$  and do not confuse  $d_2$  with any multiple  $kd_1$  for  $k > 1$ . For example, if  $\Lambda$  has the basis  $v_1 = (1, 0)$ ,  $v_2 = (0, 2)$ , then  $\text{RSD}(\Lambda) = \{1, 2, 2, \dots\}$ , where one distance 2 is  $2d_1$ , another distance 2 is  $d_2$ , so we remove only one distance  $2 = 2d_1$ . Again for any  $k > 1$ , we remove one multiple  $kd_2$  and find the next distance  $d_3$  equal to the length of the third shortest Voronoi vector  $v_0 = -v_1 - v_2$  as in Fig. 3. Since  $(v_1^2, v_2^2, v_0^2) = (d_1^2, d_2^2, d_3^2)$  is a complete invariant by Theorem 4.2 and Lemma 4.3, then so is  $\text{RSD}(\Lambda)$ .  $\square$

The invariant  $\text{RSD}(\Lambda)$  can be made complete for lattices up to rigid motion by adding  $\text{sign}(\Lambda)$  and up to similarity after dividing all distances by the first  $d_1$ .

Now Remark 8.3 summarises a wide range of rich mathematical structures that can be considered on the lattice spaces in addition to continuous metrics.

**Remark 8.3 (linear structure, scalar product on lattices)** *Since the triangular cone TC in Fig. 12 is convex, we can consider any convex linear combination of root invariants  $t\text{RI}(\Lambda_1) + (1-t)\text{RI}(\Lambda_2) \in \text{TC}$ ,  $t \in [0, 1]$ . The resulting root invariant determines (an isometry class of) the new lattice that can be denoted by  $t\Lambda_1 + (1-t)\Lambda_2$ . The average of the square and hexagonal lattices with  $\text{RI}(\Lambda_4) = (0, 1, 1)$ ,  $\text{RI}(\Lambda_6) = (1, 1, 1)$  has  $\text{RI} = (\frac{1}{2}, 1, 1)$ . The new lattice  $\frac{1}{2}(\Lambda_4 + \Lambda_6)$  is centred rectangular and has the basis  $v_1 = (\sqrt{\frac{3}{2}}, 0)$  and  $v_2 = (-\frac{1}{9}\sqrt{\frac{3}{2}}, \frac{4}{9}\sqrt{\frac{15}{2}})$ . We can define similar sums in  $\text{LSS}(\mathbb{R}^2)$  due to the convexity of the triangle QT.*

*The usual scalar product of vectors in  $\mathbb{R}^3$  defines the positive product of root invariants:  $\text{RI}(\Lambda_4) \cdot \text{RI}(\Lambda_6) = (0, 1, 1) \cdot (1, 1, 1) = 2$ . The lattice spaces  $\text{LIS}^\circ(\mathbb{R}^2)$  and  $\text{LSS}^\circ(\mathbb{R}^2)$  up to rigid motion and orientation-preserving similarity are geodesic metric spaces, even CAT(0) spaces and flat manifolds (locally Euclidean).*  $\blacksquare$

In conclusion, Problem 1.1 was resolved by the new invariants RI, RI $^\circ$ , PI, PI $^\circ$  classifying all 2D lattices up to four equivalences, see a summary in Table 7.



- (1.1a) Invariants : Definitions 3.1 and 3.4, Lemma 3.6 and Lemma 3.8(a).
- (1.1b) Completeness of invariants : Theorem 4.2 and Corollary 4.6.
- (1.1c) Continuous metrics : Definitions 5.1 and 5.4, Theorems 7.5 and 7.7.
- (1.1d) Computability of metrics : Propositions 5.8,5.9 with Examples 5.2, 6.7.
- (1.1e) Inverse design : Lemma 4.1 and Proposition 4.9 with Example 4.10.

**Table 7** A summary of classifications of all lattices  $A \subset \mathbb{R}^2$  up to four equivalence relations.

equivalence	complete invariant	configuration space	continuous metric	visual results
any	root invariant	$\text{LIS}(\mathbb{R}^2) \leftrightarrow \text{TC}$	root metric	Theorem 4.2
isometry	$\text{RI}(A)$	triangular cone	RM	Fig. 12 (left)
rigid	oriented	$\text{LIS}^\circ(\mathbb{R}^2) \leftrightarrow \text{DC}$	oriented	Theorem 4.2
motion	invariant $\text{RI}^\circ(A)$	doubled cone	metric $\text{RM}^\circ$	Fig. 14 (right)
any	projected	$\text{LSS}(\mathbb{R}^2) \leftrightarrow \text{QT}$	projected	Corollary 4.6
similarity	invariant $\text{PI}(A)$	quotient triangle	metric PM	Fig. 13 (left)
orientation-	oriented	$\text{LSS}^\circ(\mathbb{R}^2) \leftrightarrow \text{QS}$	oriented	Corollary 4.6
preserving	projected	quotient	projected	Fig. 13 (right)
similarity	invariant $\text{PI}^\circ(A)$	square	metric $\text{PM}^\circ$	Fig. 15

The key contributions are the easily computable metrics in Definitions 5.1,5.4, which led to continuous real-valued deviations of lattices from their higher symmetry neighbours. The chiral distances in Definition 6.1 continuously extend the classical binary chirality and have explicit formulae in Propositions 6.5,6.6.

The discontinuity of basis reduction in [41, Theorem 15] was proved with a simple metric on bases without isometry. When we consider obtuse superbases up to isometry, the continuity holds in Theorem 7.7 up to isometry for all lattices and up to rigid motion for non-rectangular lattices. For rigid motion, when orientation is preserved, Corollary 7.9 proves discontinuity at any rectangular lattice in  $\mathbb{R}^2$ .

It was important to clarify the above discontinuity of bases in Corollary 7.9 since the 3-dimensional case is much harder to resolve even up to isometry [22].

**Applications.** The structures in Remark 8.3 help treat lattices as vectors in a meaningful way (independent of a basis), for example, as inputs or outputs in machine learning algorithms. The paper [11] visualises for the first time millions of 2D lattices extracted from real crystals in the Cambridge Structural Database (CSD), see the Python code at [https://github.com/MattB-242/Lattice\\_Invariance](https://github.com/MattB-242/Lattice_Invariance). Patterns of symmetries for densest packings in  $\mathbb{R}^2$  were found in [35] based on a new optimisation in [36]. It will be interesting to compare the distribution of these real lattices with the uniform distribution of 2D lattices defined by the Haar measure [25] on the fundamental domain of the action of  $\text{SL}(\mathbb{R}^2)$  on the upper half-plane.

Lattice invariants can be used as a first ultra-fast step to find (near-)duplicates of a potential new material in all existing experimental datasets. In the next step, more advanced distance-based invariants of general periodic point sets detected five pairs of isometric duplicates in the CSD [40]. In each pair, one atom was replaced with a different one, which seems physically impossible without perturbing distances to neighbours. As a result, five journals are investigating the integrity of the underlying publications. The same invariants PDD (Pointwise Distance Distributions) were used for real materials applications in [43,38]. The underlying Earth Mover’s Distance on PDDs was used to map the discrete space of chemical 125,627 chemical compositions from the Inorganic Crystal Structure Database.

In summary, this paper essentially contributed to the foundations of Geometric Data Science (GDS), which studies geometry on moduli spaces of data objects up to important equivalences. The first achievement of GDS is the *Crystal Isometry Principle* [40] saying that all real periodic crystals can be uniquely parameterised by complete isometry invariants of periodic point sets. The second achievement of GDS is a continuous parameterisation of finite point sets under isometry [24,23].

The future work [22,10] extends the isometry classification of Theorem 4.2 to  $\mathbb{R}^3$ . The author thanks all reviewers for their valuable time and helpful suggestions, also Peter Bubenik, Nikolai Dolbilin, Marjorie Senechal, Jens Marklof, Andy Cooper, Olga Anosova, Matt Bright, Dan Widdowson for fruitful discussions.

**Acknowledgements** This research was supported by the £3.5M EPSRC grant ‘Application-driven Topological Data Analysis’ (2018-2023), the Royal Academy of Engineering Fellowship ‘Data Science for Next Generation Engineering of Solid Crystalline Materials’ (2021-2023), and the EPSRC New Horizons grant ‘Inverse design of periodic crystals’ (2022-2024).

## References

1. Relations between norms (2021). URL [https://en.wikipedia.org/wiki/Lp\\_space#Relations\\_between\\_p-norms](https://en.wikipedia.org/wiki/Lp_space#Relations_between_p-norms)
2. Ajtai, M.: The shortest vector problem in L2 is NP-hard for randomized reductions. In: Proceedings of Symposium on Theory of Computing, pp. 10–19 (1998)
3. Andrews, L., Bernstein, H., Pelletier, G.: A perturbation stable cell comparison technique. *Acta Crystallographica Section A* **36**(2), 248–252 (1980)
4. Anosova, O., Kurlin, V.: Introduction to periodic geometry and topology. arXiv:2103.02749 (2021)
5. Anosova, O., Kurlin, V.: An isometry classification of periodic point sets. In: Proceedings of Discrete Geometry and Mathematical Morphology, pp. 229–241 (2021)
6. Anosova, O., Kurlin, V.: Density functions of periodic sequences (2022)
7. Aroyo, M.I., Perez-Mato, J., Orobengoa, D., Tasci, E., de la Flor, G., Kirov, A.: Crystallography online: Bilbao crystallographic server. *Bulg. Chem. Commun* **43**(2), 183–197 (2011)
8. Aroyo, M.I., Wondratschek, H.: *International Tables for Crystallography*. Wiley Online Library (2013)
9. B.N.Delone, Padurov, N., Aleksandrov, A.: *Mathematical foundations of structural analysis of crystals* (1934)
10. Bright, M., Cooper, A.I., Kurlin, V.: Welcome to a continuous world of 3-dimensional lattices. arxiv:2109.11538
11. Bright, M.J., Cooper, A.I., Kurlin, V.A.: Geographic-style maps for 2-dimensional lattices. *Acta Crystallographica Section A* (2023)
12. Conway, J., Sloane, N.: *Sphere packings, lattices and groups*, vol. 290. Springer Science & Business Media (2013)

13. Conway, J.H., Sloane, N.J.: Low-dimensional lattices. vi. voronoi reduction of three-dimensional lattices. *Proceedings of the Royal Society A* **436**(1896), 55–68 (1992)
14. De Lagrange, J.L.: *Recherches d'arithmétique*. *Nouveaux Mémoires de l'Académie de Berlin* (1773)
15. Delone, B., Galiulin, R., Shtogrin, M.: On the Bravais types of lattices. *Journal of Soviet Mathematics* **4**(1), 79–156 (1975)
16. Delone, B.N.: Geometry of positive quadratic forms. part ii (in russian). *Uspekhi Matematicheskikh Nauk* (4), 102–164 (1938)
17. Edelsbrunner, H., Heiss, T., Kurlin, V., Smith, P., Wintraecken, M.: The density fingerprint of a periodic point set. In: *Proceedings of SoCG*, pp. 32:1–32:16 (2021)
18. Engel, P., Michel, L., Sénéchal, M.: Lattice geometry. *Tech. Rep. IHES-P-2004-45* (2004)
19. Gruber, B.: Reduced cells based on extremal principles. *Acta Cryst A* **45**(1), 123–131 (1989)
20. Jones, G.A., Singerman, D.: *Complex functions: an algebraic and geometric viewpoint*. Cambridge University press (1987)
21. Jost, J.: *Compact Riemann surfaces: an introduction to contemporary mathematics*. Springer Science & Business Media (2013)
22. Kurlin, V.: A complete isometry classification of 3-dimensional lattices. arxiv:2201.10543
23. Kurlin, V.: Computable complete invariants for finite clouds of unlabeled points. arxiv:2207.08502 (2022)
24. Kurlin, V.: Exactly computable and continuous metrics on isometry classes of finite and 1-periodic sequences. arXiv:2205.04388 (2022)
25. Marklof, J.: The low-density limit of the lorentz gas: periodic, aperiodic and random. *Proceedings of ICM* (arXiv:1404.3293) (2014)
26. Minkowski, H.: Ueber die positiven quadratischen formen und über kettenbruchähnliche algorithmen. *Journal für die reine und angewandte Mathematik (Crelles Journal)* (107), 278–297 (1891)
27. Mosca, M., Kurlin, V.: Voronoi-based similarity distances between arbitrary crystal lattices. *Crystal Research and Technology* **55**(5), 1900197 (2020)
28. Nguyen, P.Q., Vallée, B.: *The LLL algorithm*. Springer (2010)
29. Niggli, P.: *Krystallographische und strukturtheoretische Grundbegriffe*, vol. 1. Akademische verlagsgesellschaft mbh (1928)
30. Petitjean, M.: Chirality and symmetry measures: A transdisciplinary review. *Entropy* **5**(3), 271–312 (2003)
31. Selling, E.: Ueber die binären und ternären quadratischen formen. *Journal für die reine und angewandte Mathematik* **77**, 143–229 (1874)
32. Senechal, M.: *Quasicrystals and geometry*. CUP Archive (1996)
33. Smith, P., Kurlin, V.: Families of point sets with identical 1d persistence. arxiv:2202.00577 (2022)
34. Smith, P., Kurlin, V.: A practical algorithm for degree- $k$  voronoi domains of three-dimensional periodic point sets. In: *Proc. Int. Symposium on Visual Computing* (2022)
35. Torda, M., Goulermas, J.Y., Kurlin, V.A., Day, G.M.: Densest plane group packings of regular polygons. *Physical Review E* (arXiv:2207.08959) (2022)
36. Torda, M., Goulermas, J.Y., Púček, R., Kurlin, V.A.: Entropic trust region for densest crystallographic symmetry group packings. arXiv:2202.11959 (2022)
37. Voronoi, G.: Nouvelles applications des paramètres continus à la théorie des formes quadratiques. *J. Reine Angew. Math* (133), 97–178 (1908)
38. Vriza, A., Sovago, I., Widdowson, D., Wood, P., Kurlin, V., Dyer, M.: Molecular set transformer: Attending to the co-crystals in the cambridge structural database. *Digital Discovery* (2022). DOI 10.1039/D2DD00068G
39. Watson, G.: Determination of a binary quadratic form by its values at integer points: Acknowledgement. *Mathematika* **27**(2), 188–188 (1980)
40. Widdowson, D., Kurlin, V.: Resolving the data ambiguity for periodic crystals. *Advances in Neural Information Processing Systems (Proceedings of NeurIPS 2022)* **35** (2022)
41. Widdowson, D., Mosca, M., Pulido, A., Kurlin, V., Cooper, A.: Average minimum distances of periodic point sets. *MATCH Communications in Mathematical and in Computer Chemistry* **87**, 529–559 (2022)
42. Zhilinskii, B.: Introduction to lattice geometry through group action. *EDP sciences* (2016)
43. Zhu, Q., Johal, J., Widdowson, D., Pang, Z., Li, B., Kane, C.M., Kurlin, V., Day, G., Little, M., Cooper, A.I.: Analogy powered by prediction and structural invariants: Computationally-led discovery of a mesoporous hydrogen-bonded organic cage crystal. *J American Chemical Society* **144**, 9893–9901 (2022)

**A Appendix A: examples and proofs of past results by Conway-Sloane**

To make the paper self-contained, the appendix includes detailed proofs of past results whose outlines in Delone [15], Conway, Sloane [13] contained a few typos.

Fig. 22 shows the deformation of  $\Lambda(t)$  generated by  $v_1 = (1, 0)$ ,  $v_2(t) = (-t, -1)$  for  $t \in [0, 1]$ . The square lattice  $\Lambda(0)$  deforms to  $\Lambda(\frac{1}{2})$  in Fig. 22 (bottom middle), where the reduced (non-acute) basis  $v_1, v_2(t) = (-t, -1)$  becomes non-reduced at  $t = \frac{1}{2}$  and is replaced by the new reduced basis  $v_1, v'_2(t) = (t - 1, 1)$  for  $t \in (\frac{1}{2}, 1]$ .

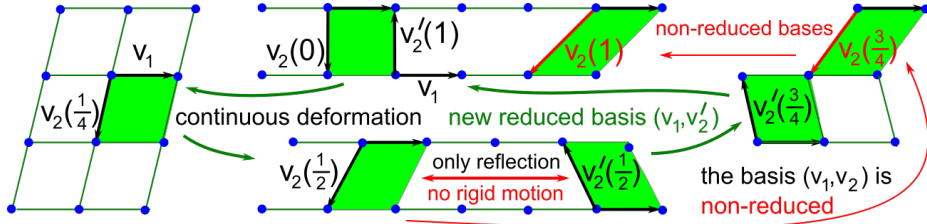


**Fig. 22** The basis  $v_1 = (1, 0)$ ,  $v_2(t) = (-t, -1)$  is reduced only for  $t \in [0, \frac{1}{2}]$  and at  $t = \frac{1}{2}$  discontinuously changes to another reduced basis  $v_1 = (1, 0)$ ,  $v'_2(t) = (t - 1, 1)$  for  $t \in (\frac{1}{2}, 1]$ .

Example A.1 illustrates Theorem 7.5 and shows that the root invariant changes continuously for a deformation while a reduced basis changes discontinuously.

**Example A.1** In Fig. 22, the superbase  $v_1 = (1, 0)$ ,  $v_2(t) = (-t, -1)$ ,  $v_0 = (t - 1, 1)$  of the lattice  $\Lambda(t)$  remains obtuse for  $t \in [0, 1]$  and is unique up to rigid motion by Theorem 3.7. Then  $r_{12} = \sqrt{t}$ ,  $r_{01} = \sqrt{1 - t}$ ,  $r_{02} = \sqrt{1 - t + t^2}$ . Since  $1 - t + t^2 \geq \max\{t, 1 - t\}$  for  $t \in [0, 1]$ , the root invariant can be written as

$$RI(\Lambda(t)) = \begin{cases} (\sqrt{t}, \sqrt{1-t}, \sqrt{1-t+t^2}) \text{ for } t \in [0, \frac{1}{2}], \\ (\sqrt{1-t}, \sqrt{t}, \sqrt{1-t+t^2}) \text{ for } t \in [\frac{1}{2}, 1]. \end{cases}$$

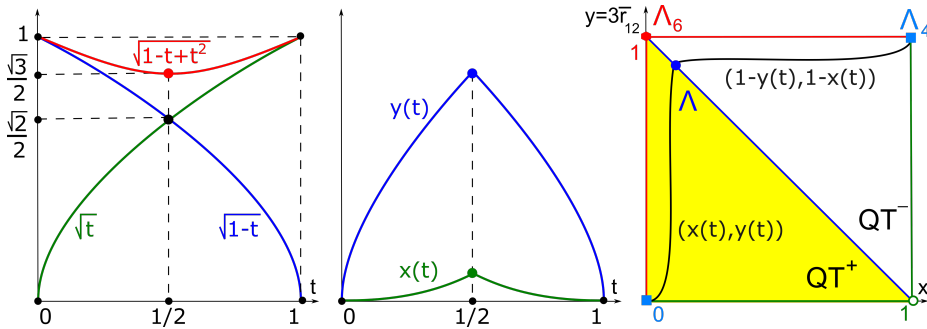


**Fig. 23** Left: graphs of root products in  $RI(\Lambda(t))$ , see Example A.1. Middle: graphs of the components in  $PI(\Lambda(t))$ . Right: the continuous path of  $PI(\Lambda(t))$  in the quotient square  $QS$ .

By Definition 4.5 the size is  $\sigma(\Lambda(t)) = r_{12} + r_{01} + r_{02} = \sqrt{t} + \sqrt{1-t} + \sqrt{1-t+t^2}$ . The projected invariant is  $\text{PI}(\Lambda(t)) = (x(t), y(t))$ , see Fig. 23. where

$$x(t) = \frac{\sqrt{1-t+t^2} - \max\{\sqrt{t}, \sqrt{1-t}\}}{\sqrt{t} + \sqrt{1-t} + \sqrt{1-t+t^2}}, \quad y(t) = \frac{3 \min\{\sqrt{t}, \sqrt{1-t}\}}{\sqrt{t} + \sqrt{1-t} + \sqrt{1-t+t^2}}.$$

If  $t = \frac{1}{2}$ , then  $\sqrt{t} = \sqrt{1-t} = \frac{\sqrt{2}}{2}$ ,  $\sqrt{1-t+t^2} = \frac{\sqrt{3}}{2}$ ,  $\sigma(\Lambda(\frac{1}{2})) = \sqrt{2} + \frac{\sqrt{3}}{2}$ . So

$$\text{RI}\left(\Lambda\left(\frac{1}{2}\right)\right) = \left(\frac{\sqrt{2}}{2}, \frac{\sqrt{2}}{2}, \frac{\sqrt{3}}{2}\right), \quad \text{PI}\left(\Lambda\left(\frac{1}{2}\right)\right) = \left(\frac{\sqrt{3}-\sqrt{2}}{\sqrt{3}+2\sqrt{2}}, \frac{3\sqrt{2}}{\sqrt{3}+2\sqrt{2}}\right).$$

The last point is approximately (0.07, 0.93) in the diagonal  $x + y = 1$  of QS. Under the symmetry  $t \leftrightarrow 1 - t$ , all the functions above invariant and  $\Lambda(t)$  changes its sign. The paths  $\text{RI}(\Lambda(t))$  and  $\text{PI}(\Lambda(t)) \in \text{QS}$  are continuous everywhere, while the reduced basis  $v_1, v_2(t)$  is discontinuous up to rigid motion at  $t = \frac{1}{2}$ .

The obtuse superbase  $\{v_1, v_2(t), v_0(t)\}$  remains continuous for  $t \in [0, 1]$ . For  $t = 0, 1$ , the superbases are related by rotation through  $90^\circ$ . There is no such a rotation for the strictly rectangular lattice in Fig. 4 and Example 7.6. ■

Lemma A.2 (probably due to Voronoi) was mentioned in [15, section 2.3].

**Lemma A.2 (lattices  $\leftrightarrow$  Voronoi domains)** Lattices  $\Lambda, \Lambda' \subset \mathbb{R}^n$  are related by an isometry  $f$  if and only if Voronoi domains  $V(\Lambda), V(\Lambda')$  are related by  $f$ . ▲

*Proof* Since any isometry  $f$  preserves distances and the Voronoi domain is defined in terms of distances, if  $f$  maps a lattice  $\Lambda$  to  $\Lambda'$ , then  $f$  restricts to an isometry of Voronoi domains:  $V(\Lambda) \rightarrow V(\Lambda')$ . Conversely, the whole space  $\mathbb{R}^n$  is covered by the lattice translates  $V(\Lambda) + \Lambda = \{V(\Lambda) + v \mid v \in \Lambda\}$ , which have disjoint interiors. Hence any isometry  $f : V(\Lambda) \rightarrow V(\Lambda')$  gives rise to an isometry of  $\mathbb{R}^n$ . □

*Proof (of Lemma 2.5)* We prove the second part for strict Voronoi vectors with all strict inequalities. The first part follows by making all inequalities non-strict.

Assume that  $v \in \Lambda$  is a Voronoi vector of a lattice  $\Lambda \subset \mathbb{R}^2$  but there is a shorter vector  $w \in v + 2\Lambda$ . Then the point  $\frac{1}{2}v$  is closer to  $\frac{1}{2}(v+w) \in \Lambda$  than to  $v$ , because  $\frac{1}{2}|w| < \frac{1}{2}|v|$ , which contradicts the assumption that  $v$  is a Voronoi vector.

Conversely, let  $v$  be a shortest vector in its  $2\Lambda$ -class. If  $v$  is not a Voronoi vector, there is another vector  $w \in \Lambda$  whose bisector hyperspace separates  $\frac{1}{2}v$  from 0. Then  $\frac{1}{2}v \cdot w > \frac{1}{2}|w|^2$ ,  $|v^2| > |v - 2w|^2$ , so  $v - 2w$  is shorter than  $v$ . □

**Lemma A.3** For any basis  $v_1, \dots, v_n$  in  $\mathbb{R}^n$ , let  $p_{ij} = -v_i \cdot v_j$  be the conorms of a superbase  $v_0, v_1, \dots, v_n$  with  $v_0 = -\sum_{i=1}^n v_i$ . The squared norm  $v^2$  of any vector

$$v = \sum_{i=1}^n c_i v_i \text{ equals } N(v) = \sum_{i=1}^n c_i^2 p_{0i} + \sum_{1 \leq i < j \leq n} (c_i - c_j)^2 p_{ij}. \text{ If we decompose } v = \sum_{i=0}^n c_i v_i \text{ over the full superbase, then } N(v) = \sum_{0 \leq i < j \leq n} (c_i - c_j)^2 p_{ij}. \quad \blacktriangle$$

*Proof* In the right hand side of the required formula, we substitute the conorms in terms of scalar products of basis vectors as follows:  $p_{ij} = -v_i \cdot v_j$  for  $i, j \in \{1, \dots, n\}$ . Then  $p_{0i} = -v_0 \cdot v_i = v_i \cdot \sum_{j=1}^n v_j = v_i^2 + \sum_{j \neq i}^n v_i \cdot v_j$  and  $\sum_{i=1}^n c_i^2 p_{0i} + \sum_{1 \leq i < j \leq n} (c_i - c_j)^2 p_{ij} = \sum_{i=1}^n c_i^2 (v_i^2 + \sum_{j \neq i}^n v_i \cdot v_j) - \sum_{1 \leq i < j \leq n} (c_i^2 - 2c_i c_j + c_j^2) v_i \cdot v_j$

$$= \sum_{i=1}^n c_i^2 v_i^2 + \sum_{i=1}^n c_i^2 \sum_{j \neq i}^n v_i \cdot v_j - \sum_{1 \leq i < j \leq n} (c_i^2 + c_j^2) (v_i \cdot v_j) + \sum_{1 \leq i < j \leq n} 2c_i c_j (v_i \cdot v_j) =$$

$$= \sum_{i=1}^n c_i^2 v_i^2 + 2 \sum_{1 \leq i < j \leq n} c_i c_j (v_i \cdot v_j) = \left( \sum_{i=1}^n c_i v_i \right)^2 = N(v)$$

as required. The last formula for  $n + 1$  vectors follows by replacing  $c_i$  with  $c_i - c_0$  for  $i = 1, \dots, n$ .  $\square$

*Proof (of Lemma 2.8)* By Lemma 2.5 Voronoi vectors have smallest squared norms  $N(v)$  in their  $2\Lambda$ -classes. The  $2\Lambda$ -class of any vector  $v = \sum_{i=0}^n c_i v_i \in \Lambda$  with  $c_i \in \mathbb{Z}$  remains invariant if any coefficient  $c_i$  keeps its parity modulo 2. Within the  $2\Lambda$ -class, the squared norm  $N(v) = \sum_{0 \leq i < j \leq n} (c_i - c_j)^2 p_{ij}$  computed in Lemma A.3 is minimal if all even  $c_i$  are replaced by 0 and all odd  $c_i$  are replaced by 1. The resulting shortest vectors with coefficients 0, 1 are all  $2^n - 1$  symmetric pairs of partial sums  $\pm v_S$  for a proper subset  $S \subset \{0, 1, \dots, n\}$ . If all conorms  $p_{ij} > 0$ , to guarantee a minimum value of  $N(v)$ , every difference  $|c_i - c_j|$  should be 0 or 1, hence there are no other Voronoi vectors apart from the partial sums above.  $\square$

*Proof (of Theorem 2.9 for  $n = 2$ )* For any lattice  $\Lambda \subset \mathbb{R}^2$ , permuting vectors of a superbase  $B = (v_0, v_1, v_2)$  allows us to order the conorms:  $p_{12} \leq p_{01} \leq p_{02}$ . Our aim is to reduce  $B$  so that all  $p_{ij} \geq 0$ . Assuming that  $p_{12} = -v_1 \cdot v_2 = -\varepsilon < 0$ , we change the superbase:  $u_1 = -v_1$ ,  $u_2 = v_2$ ,  $u_0 = v_1 - v_2$  so that  $u_0 + u_1 + u_2 = 0$ .

Two vonorms remain the same:  $u_1^2 = v_1^2$ ,  $u_2^2 = v_2^2$ . The third vonorm decreases by  $4\varepsilon > 0$  as follows:  $u_0^2 = (v_1 - v_2)^2 = (v_1 + v_2)^2 - 4v_1 v_2 = v_0^2 - 4\varepsilon$ . One conorm changes its sign:  $q_{12} = -u_1 \cdot u_2 = -p_{12} = \varepsilon > 0$ . The two other conorms decrease:

$$q_{01} = -u_0 \cdot u_1 = -(v_1 - v_2) \cdot (-v_1) = -(-v_1 - v_2)v_1 - 2v_1 \cdot v_2 = p_{01} - 2\varepsilon,$$

$$q_{02} = -u_0 \cdot u_2 = -(v_1 - v_2) \cdot v_2 = -(-v_1 - v_2)v_2 - 2v_1 \cdot v_2 = p_{02} - 2\varepsilon.$$

If one of the new conorms becomes negative, we apply the above reduction again.

To prove that all conorms eventually become non-negative, note that every reduction can make superbase vectors only shorter, but not shorter than a minimum distance between points of  $\Lambda$ . The angle between  $v_i, v_j$  can have only finitely many values when lengths of  $v_i, v_j$  are bounded. Then the scalar product  $\varepsilon = v_i \cdot v_j > 0$  cannot converge to 0. Since every reduction makes one superbase vectors shorter by a positive constant, the reductions will finish in finitely many steps.  $\square$